FHWA/TPF Research Project
Accelerated Implementation of Intelligent Compaction Technology for Embankment Subgrade Soils, Aggregate Base, and Asphalt Pavement Materials

HMA IC Demonstration
IH 39, Mosinee, Wisconsin
Final Report

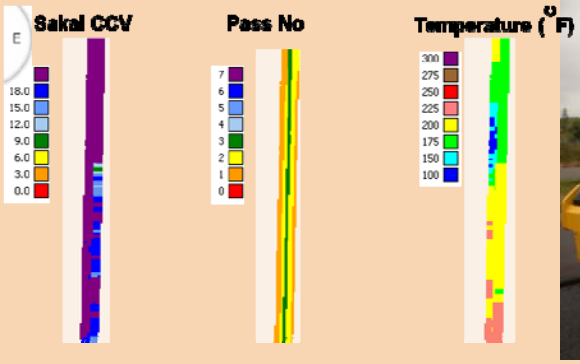

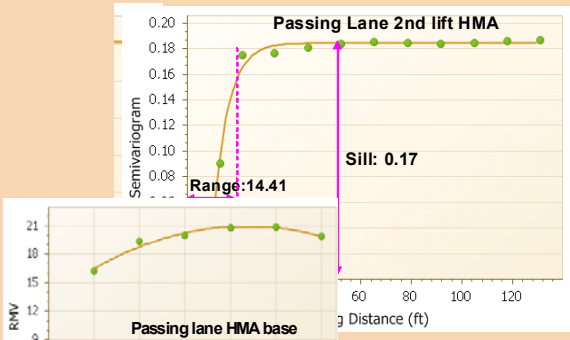

1. Report No. FHWA-IF-07-___	2. Government Accession No. N/A	3 Recipient Catalog No. N/A	
4. Title and Subtitle Accelerated Implementation Of Intelligent Compaction Technology for Embankment Subgrade Soils, Aggregate Base, And Asphalt Pavement Materials - Final Report for the WisDOT HMA IC Demonstration		5. Report Date June 2010 6. Performing Organization Code N/A	
7. Author(s) George Chang and Qinwu Xu of the Transtec Group Inc.; Bob Horan of Asphalt Institute; and Larry Michael of LLM Asphalt Technology Consultant.		8. Performing Organization Report No. N/A	
9. Performing Organization Name and Address The Transtec Group, Inc. 6111 Balcones Drive Austin TX 78731		10. Work Unit No. (TRAIS) N/A 11. Contract or Grant No. DTFH61-07-C-R0032	
12. Sponsoring Agency Name and Address Federal Highway Administration Office of Pavement Technology, HIPT-10 1200 New Jersey Avenue, SE Washington, DC 20590		13. Type of Report and Period Covered Final report (draft) 14. Sponsoring Agency Code N/A	
15. Supplementary Notes Contracting Officer's Technical Representative: Victor (Lee) Gallivan			
16. Abstract Intelligent compaction (IC) is an emerging technology, and for some applications it is mature enough for implementation in field compaction of pavement materials. The intent of this project is to realize the blueprint in the FHWA IC strategic plan. This study was initiated under the Transportation Pooled Fund (TPF) Solicitation No. 954, which includes 12 participating state department of transportation (DOTs): Georgia, Wisconsin, Kansas, Maryland, Wisconsin, Mississippi, North Dakota, Mississippi, Pennsylvania, Texas, Virginia, and Wisconsin. This document is the final report for the WisDOT HMA IC field demonstration.			
17. Key words Compaction, intelligent compaction, roller, asphalt, HMA overlay, pavement performance.		18. Distribution Statement No restrictions. This document is available to the public through the National Technical Information Service, Springfield, Virginia 22161	
19. Security Classif. (of this report) Unclassified	20. Security Classif. (of this page) Unclassified	21. No. of Pages	22. Price

Form DOT F 1700.7 (8-72) Reproduction of completed page authorized (art. 5/94)

SI* (MODERN METRIC) CONVERSION FACTORS

APPROXIMATE CONVERSIONS TO SI UNITS

Symbol	When You Know	Multiply By	To Find	Symbol
		LENGTH		
in	inches	25.4	millimeters	mm
ft	feet	0.305	meters	m
yd	yards	0.914	meters	m
mi	miles	1.61	kilometers	km
		AREA		
in^2	square inches	645.2	square millimeters	mm^2
ft^2	square feet	0.093	square meters	m^2
yd^2	square yard	0.836	square meters	m^2
ac	acres	0.405	hectares	ha
mi^2	square miles	2.59	square kilometers	km^2
		VOLUME		
fl oz	fluid ounces	29.57	milliliters	mL
gal	gallons	3.785	liters	L
ft^3	cubic feet	0.028	cubic meters	m^3
yd^3	cubic yards	0.765	cubic meters	m^3
	NOTE: volumes greater than 1000 L shall be shown in m^3			
		MASS		
oz	ounces	28.35	grams	g
lb	pounds	0.454	kilograms	kg
T	short tons (2000 lb)	0.907	megagrams (or "metric ton")	Mg (or "t")
		TEMPERATURE (exact degrees)		
^oF	Fahrenheit	5 (F-32)/9 or (F-32)/1.8	Celsius	^oC
		ILLUMINATION		
fc	foot-candles	10.76	lux	lx
fl	foot-Lamberts	3.426	$candela/m^2$	cd/m^2
		FORCE and PRESSURE or STRESS		
lbf	poundforce	4.45	newtons	N
lbf/in^2	poundforce per square inch	6.89	kilopascals	kPa

APPROXIMATE CONVERSIONS FROM SI UNITS

Symbol	When You Know	Multiply By	To Find	Symbol
		LENGTH		
mm	millimeters	0.039	inches	in
m	meters	3.28	feet	ft
m	meters	1.09	yards	yd
km	kilometers	0.621	miles	mi
		AREA		
mm^2	square millimeters	0.0016	square inches	in^2
m^2	square meters	10.764	square feet	ft^2
m^2	square meters	1.195	square yards	yd^2
ha	hectares	2.47	acres	ac
km^2	square kilometers	0.386	square miles	mi^2
		VOLUME		
mL	milliliters	0.034	fluid ounces	fl oz
L	liters	0.264	gallons	gal
m^3	cubic meters	35.314	cubic feet	ft^3
m^3	cubic meters	1.307	cubic yards	yd^3
		MASS		
g	grams	0.035	ounces	oz
kg	kilograms	2.202	pounds	lb
Mg (or "t")	megagrams (or "metric ton")	1.103	short tons (2000 lb)	T
		TEMPERATURE (exact degrees)		
^oC	Celsius	1.8C+32	Fahrenheit	^oF
		ILLUMINATION		
lx	lux	0.0929	foot-candles	fc
cd/m^2	$candela/m^2$	0.2919	foot-Lamberts	fl
		FORCE and PRESSURE or STRESS		
N	newtons	0.225	poundforce	lbf
kPa	kilopascals	0.145	poundforce per square inch	lbf/in^2

*SI is the symbol for the International System of Units. Appropriate rounding should be made to comply with Section 4 of ASTM E380.
(Revised March 2003)

TABLE OF CONTENTS

LIST OF TABLES

LIST OF FIGURES

LIST OF MAIN ACRONYMS OR TERMS

LIST OF SYMBOLS

$A_{0.5\Omega}$, $A_{0.5\Omega}$, $A_{0.5\Omega}$	Acceleration at sub-harmonic frequency
A_{Ω}	Acceleration at fundamental frequency
$A_{2\Omega}$	Acceleration at second order harmonic frequency
$A_{3\Omega}$	Acceleration at higher order harmonic frequency
RMV	Roller Measurement Value
CCV	Compaction Control Value for Sakai roller
W	Machine weight

A	Vibration amplitude
v	Roller speed
f	Vibration frequency
d	Diameter of the FWD plate
E	Elastic modulus of LWD measurement
E*	Complex modulus of HMA mixture
$\gamma(h)$	Semivariogram
R	Semivariogram range
C	Semivariogram sill
C_0	Semivariogram nugget

Executive Summary

This report describes the FHWA/TPF intelligent compaction (IC) demonstration for hot mix asphalt (HMA) materials in Mosinee, WI, in May 2010.

The goals of this demonstration project that were successfully achieved include:

1. Demonstration of HMA IC technologies to WisDOT personnel, contractors, etc.;
2. Develop an experienced and knowledgeable IC expertise base within WisDOT,
3. Assisting WisDOT in the development of IC quality control (QC) specifications for the HMA pavement materials, and
4. Identification and prioritization of improvements and further research for IC equipment and data analysis.

Goal number 1 was accomplished by demonstrating the abilities of the IC system such as: tracking roller passes, HMA surface temperatures, and roller measurement values (RMV).

Goal number 2 was achieved by building the IC knowledge base including field data and lessons learned from this demonstration and past demonstrations. Valuable information was collected from this demonstration and served as solid proof for the IC technologies.

Goal number 3 was achieved, albeit still a work in progress, by training WisDOT staff, paving contractors, and etc. on the IC technologies via this field demonstration and an Open House activity. The research team will continue provide support to WisDOT on the development of IC QC specifications during this project period.

Goal number 4 was achieved by compiling a "wish list" or recommendation for the IC roller vendors to further improve their systems for widespread use of the IC technologies. Data of IC system was also reviewed and potential problems are identified for future research and engineering practices.

Unique Features

- It is the first IC demo project to pave HMA courses on the rubblized and crack-and-seat PCC base;
- It is the first IC demo to use IC rollers "from the ground-up", including mapping the rubblized and crack-and-seat PCC base, compaction of the HMA base/intermediate/surface courses;
- It is the first IC demo to perform FWD and LWD tests on all pavement layers: rubblized and crack-and-seat PCC base, compaction of the HMA base/intermediate/surface courses; and
- It is the first IC demo to use IC rollers from the same manufacturer for both the breakdown/intermediate and finishing compactions.

Major Findings

One of the repeated evidence of immediate benefits is improvement of rolling patterns.

New Findings:

- Double-drum IC rollers can be used to map the rubblized and crack-and-seat PCC bases prior to the paving of HMA layer;
- IC mapping of the rubblized and crack-and-seat PCC bases and soil shoulder was shown to be crucial in identifying the pavement conditions prior to the paving of the HMA layer (see CCV maps below);

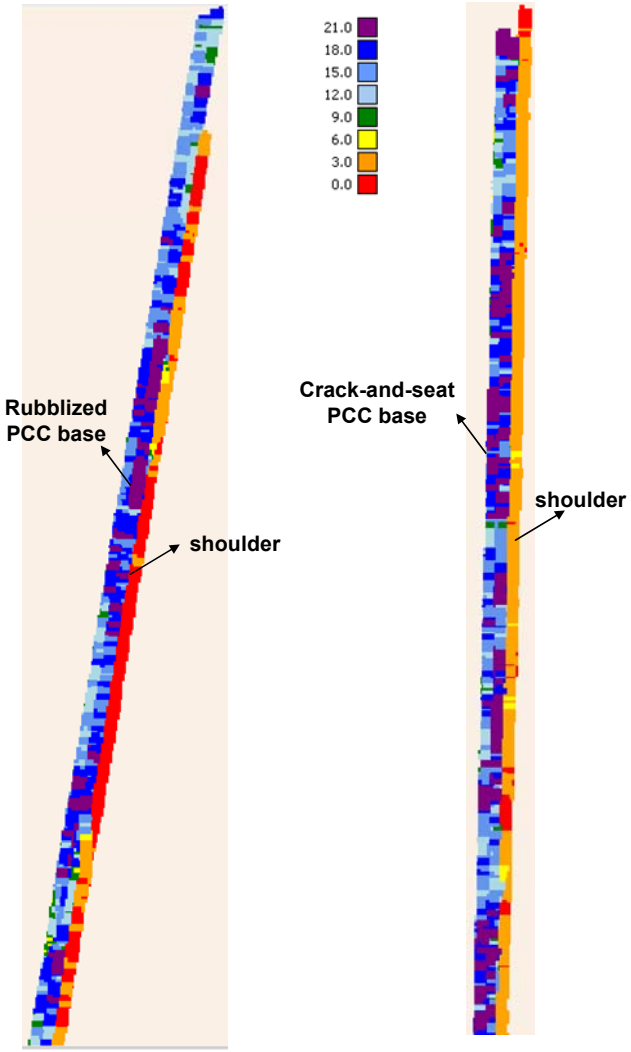

- Night paving has been successfully implemented with the assistance of IC technology;
- LWD measurements (deflection and moduli) and NG density have relatively good linear correlation with the roller measurement value (RMV) for some test beds, and HMA temperature has significant effect on the correlation result (see examples below, RMV vs. LWD on the left, and RMV vs. NG density on the right);

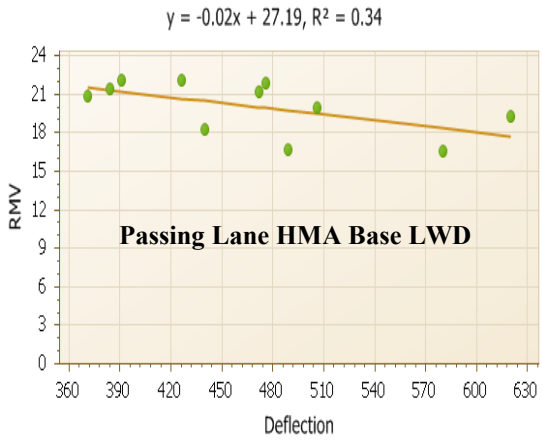

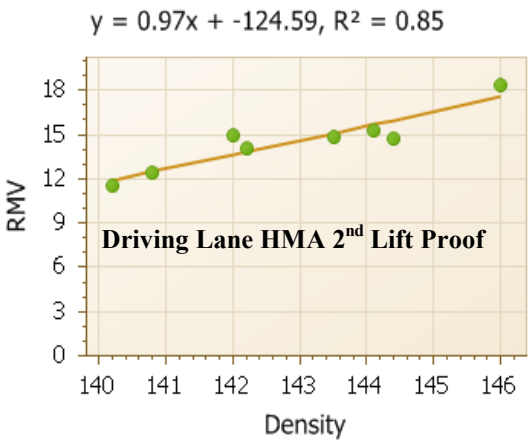

- Generally compaction uniformity increases from the "ground up": i.e., from PCC base to the HMA base and then the 2nd lift HMA course, as indicated in the semi-variogram analysis (see below, semi-variograms for HMA base course and the second lift, intermediate course);

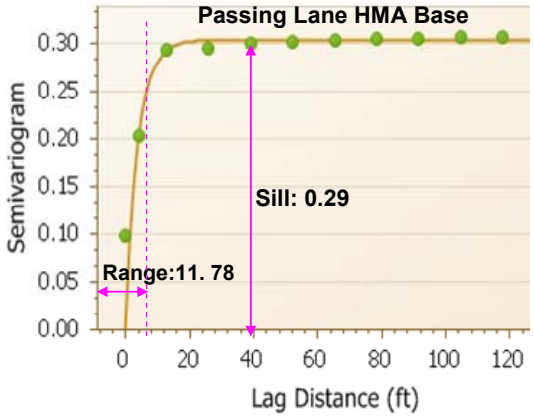

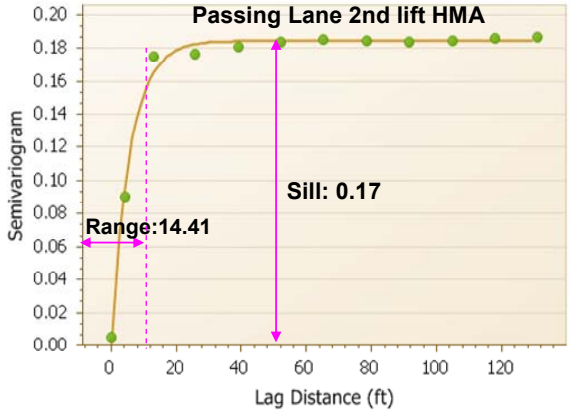

- Optimum roller passes can be determined by the "compaction curves" that help avoiding the over compaction or under compaction. (see below examples of compaction curves that indicate optimum passes as 4)

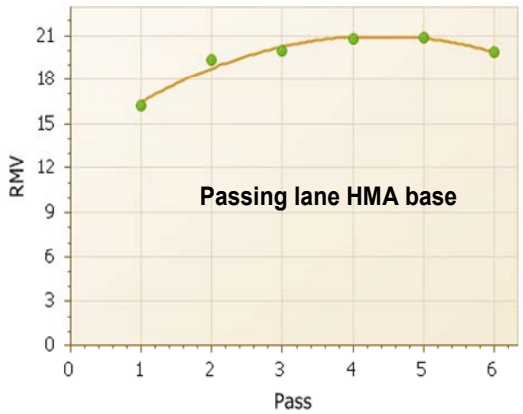

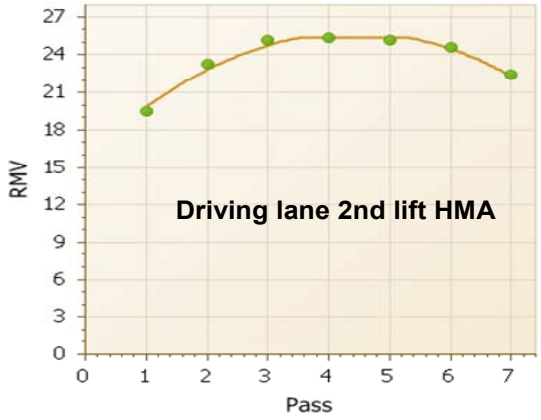

Confirming Past Findings:

- The IC roller can track the roller pass numbers, roller speeds, HMA surface temperatures, and the RMVs, which provides important metrics for the compaction quality;
- With the real-time information of IC roller passes, HMA surface temperatures and RMVs displayed on the screen, the roller operator can adjust rolling patterns to improve the compaction quality.

Recommendations

- Validation of the IC Global Positioning System (GPS) setup prior to the compaction operation using a survey grade GPS hand-held unit is crucial to providing precise and correct measurements. The process should require IC rollers moving forward and backward to validation locations.
- To correlate in-situ tests with IC data properly, in-situ test locations must be established using a hand-held GPS "rover" unit that is tied into the project base station and offers survey grade accuracy.
- It is highly recommended to perform IC measurements (mapping) of the underlying layers prior to the paving of upper layers in order to identify possible weak spots and facilitate the interpretation of the measurements on the asphalt surface layers.
- Long term pavement performance monitoring is recommended in order to identify performance trends that may relate to RMV values.
- Temperature correction for the RMV of HMA material is recommended with developing models.
- Indicators of undesirable IC measurement conditions (such as bouncing, sudden start/stop, loss of real-time kinematic GPS, etc.) are strongly recommended to be stored in order to filter out invalid IC data..
- Standardization is strongly recommended to accelerate the implementation IC for State agencies. The recommended items include: a standard IC data storage format, an independent viewing/analysis software tool, and detailed data collection plan (include any in-situ/lab test results). The research team is currently developing guidelines for IC data collection, storage requirements, data processing, and a prototype of an independent software tool.
- Further investigation on a global scale (e.g., segment-by-segment analysis of entire paved sections) is recommended to provide guidance of usage of IC mapping data on existing pavement layer with subsequent IC measurements during HMA paving. This would include: setting a target RMV value from test trip data based on the onsite support condition and asphalt job mix formula.

Acknowledgement

This demonstration would not have been possible without the help of all the parties involved in this project. The primary parties that were involved with planning and conducting the demonstration projects were the ICPF project team, WisDOT, the Sakai roller vendor, and the paving contractors. The ICPF project team for this demonstration included Dr. George Chang, Qinwu Xu, Bob Horan, Larry Michael, and Victor (Lee) Gallivan. Mr. Gallivan is the contracting officer's technical representative; Mr. Horan was the main coordinator of this demonstration; Dr. Chang was main contact for the ICPF project team, and Mr. Bob Arndofer was the main contact for WisDOT.

The authors would like to acknowledge the following individuals for their contribution to this demonstration:

- WISDOT: Bob Arndofer , Barry Paye, Craig Vils, Bob Schiro, Mike Malaney, Mark Steidl, David Kircher, Robin Stafford, Jeff Hess, Frank Alfaro, Jeff Michalski, and Tim Hansley.
- Sakai: Todd Mansell;
- Trimble: Adam Patrow (Fabco) and Bruce Hanes;
- TopCon: Tom Walrath (Position Solution) and Brian Lingobardo;
- Mathy: Ervin Dukatz and Matt Eslinger;

Introduction

This is the report for the hot mixture asphalt (HMA) intelligent compaction (IC) field demonstration conducted in May 2010 for the Wisconsin State Department of Transportation (WISDOT). This was an IC demonstration under the Transportation Pooled Fund (TPF) study "Accelerated Implementation of Intelligent Compaction Technology for Subbase, Base, and Asphalt Pavement Materials." Key attributes for this field demonstration included on-site training of WisDOT and contractor personnel, comparison of IC roller technologies to traditional compaction equipment and practices, correlating IC roller measurements to in-situ spot test measurements, mapping the rubblized and crack-and-seat PCC base to understand the influence of underlying layer support, selecting the appropriate machine operation parameters (e.g., speed, amplitude, frequency, etc.), and managing and analyzing the IC and in-situ test data.

The specific goals of this demonstration project were to:

- Demonstration of Hot Mix Asphalt (HMA) IC technologies to WISDOT personnel, contractors, etc.;
- Develop an experienced and knowledgeable IC expertise base within WISDOT;
- Assisting WISDOT in the development of IC quality control (QC) specifications for the HMA pavement materials, and
- Identification and prioritization of needed improvements and further research for IC equipment and data analysis.

The objectives of this demonstration project were short-term goals for introducing HMA IC technology to WISDOT and contractors who may not have prior experience with IC technology. The project was intended to demonstrate the benefits of IC for improving the compaction process and quality by achieving more uniform density and modulus of the HMA material and providing roller operators (and superintendents) better feedback tools to make right decisions, and ultimately real-time quality control.

The demonstration site and material of interest were selected by WISDOT. The field IC demonstration was performed from May 11 to 13, 2010 on IH 39, Mosinee, WI.

This report includes:

- Description of the test site;
- Description of IC rollers;
- Description of in-situ test devices;
- Details of field demonstration activities and data analysis;
- Open house activities; and
- Summary and recommendations.

Description of the Test Site

The test site is located on the South Bound (SB) of IH 39 at the junction of IH 39 and 153, Mosinee, WI (Figure 1). The length of the project is about 5 miles with two lanes in the SB direction. The existing pavement is HMA on top of PCC slabs. During the demonstration, the existing HMA layer was milled and removed, then the PCC slab was rubblized or cracked-and-seated, before paving a 25mm HMA base followed by a 19mm second lift HMA intermediate layer and then a 12.5-mm HMA surface.

Figure 1. Location of the test site (the red star area).

Description of IC Rollers

Two Sakai tandem drum IC rollers were used for the HMA IC demonstration.

Both IC rollers are equipped with a global position system (GPS), a roller response measurement system, and a document system. The detailed features of the Sakai IC rollers are described in the following sections.

Sakai Tandem IC Roller

Overall System Description

The Sakai SW880 and SW990 tandem IC rollers are shown in Figure 2 and Figure 3, respectively. The features of these two rollers are described in Table 1.

Figure 2. Sakai SW880 Tandem IC Roller.

Figure 3. Sakai SW990 Tandem IC Roller.

Table 1. Features of the Sakai SW880 and SW990 Tandem IC Rollers.

Manufacturer/ Vendor	Sakai America	Sakai America
Model Name	Exact Compact System (ECS)	Exact Compact System (ECS)
Model Number	SW880	SW990
Drum Width	79”	84”
Machine Weight (W)	29,560 lbs (~ 14 tons)	30,800 lbs (~ 15 tons)
Amplitude Settings (A)	0.013”, 0.025” (0.33 to 0.64 mm)	0.013”, 0.026” (0.33 to 0.66 mm)
Frequency Settings (f)	High amp. 2500 or 3000 vpm Low amp. 2500, 3000, or 4000 vpm	High amp. 2500 or 3000 vpm Low amp. 2500, 3000, or 4000 vpm
Auto-Feedback	No	No
Measurement System	CCV with temperature and passes mapping	CCV with temperature and passes mapping
Measurement Value	Compaction control value (Sakai CCV)	Compaction control value (Sakai CCV)
Measurement Unit	Unitless	Unitless
GPS Capability	Yes (RTK)	Yes (RTK)
Temperature Measurement	Infra-red sensor at front	Infra-red sensor at front
Documentation System	Compaction Information System (CIS)	Compaction Information System (CIS)

The Sakai Compaction Information System (CIS) is the IC hardware and software that map roller passes, temperature, and stiffness of the compacted surface. CIS can be installed on Sakai single drum vibratory soil rollers or double drum asphalt rollers with or without the continuous compaction value (CCV) sensor. The Real Time Kinematic (RTK) Global Position Systems (GPS) provided by Trimble Navigation Limited and the Topcon Positioning Systems were used for Sakai SW880 and SW990 roller, respectively, to obtain the precise roller position for recording the roller pass data as well as data from the CCV sensor, as shown in Figure 4.

Figure 4. RTK GPS receiver and antenna on a Sakai roller

Figure 5 shows a view of the Sakai IC system installed on the roller where the monitor on the left displays the IC color coded maps. The monitor is portable and has good visibility in bright daylight it also has a reduced brightness "Night" mode. The Exact Compact display and IPF controls are located on the standard roller dash panel with the other instruments and controls for the roller. Exact Compact is a standard feature on Sakai SW880 and SW990 roller models.

Figure 5. Sakai Compaction Information System (CIS) display at the operator station.

The schematic of the Sakai IC system (for both soil and HMA) can be best demonstrated by the diagram shown in Figure 6. The basis of this system is the IC roller (equipped with CCV measurement system, temperature sensors, and GPS radio/receiver) and a GPS with radio base station. All measurements are consolidated to the CIS display. IC data can then be transferred to PCs via USB ports for further reporting/documentation and integration with CAD systems.

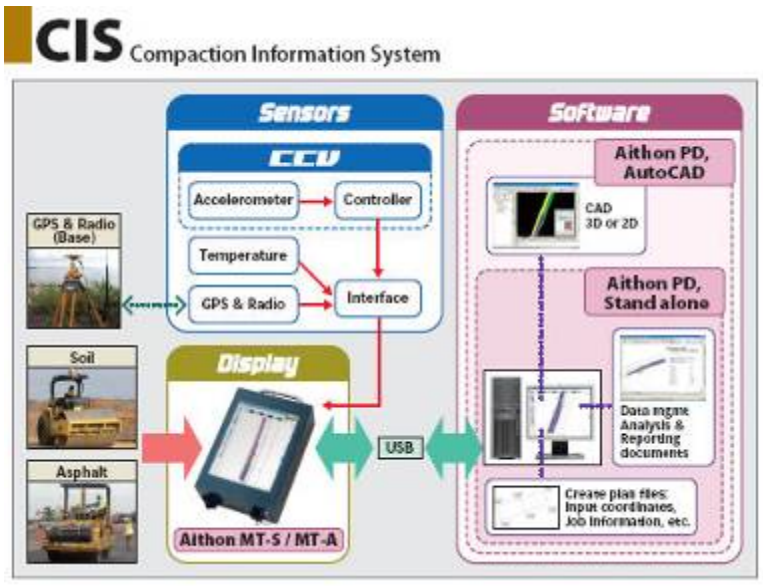

(Courtesy of Sakai)

Figure 6. The Sakai IC system.

Measurement Value

The Sakai Compaction control value (CCV) is a unitless vibratory-based technology which makes use of an accelerometer mounted to the roller drum to create a record of machine-ground interaction. Its value represents the stiffness of the compacted pavement layers underneath. The concept behind the CCV is that as the ground stiffness increases, the roller drum starts to enter into a "jumping" motion which results in vibration accelerations at various frequency components, as illustrated in Figure 7. The CCV is calculated by using the acceleration data from first sub-harmonic (0.5Ω), fundamental (Ω), and higher-order harmonics (1.5Ω, 2Ω, 2.5Ω, 3Ω) as presented in Eq. 1. The vibration acceleration signal from the accelerometer is transformed through the Fast Fourier Transform (FFT) method and then filtered through band pass filters to detect the acceleration amplitude spectrum (Nohse and Kitano, 2002; Scherocman et al., 2007).

$$CCV = \left[\frac{A_{0.5\Omega} + A_{1.5\Omega} + A_{2\Omega} + A_{2.5\Omega} + A_{3\Omega}}{A_{0.5\Omega} + A_{\Omega}} \right] \times 100 \qquad (1)$$

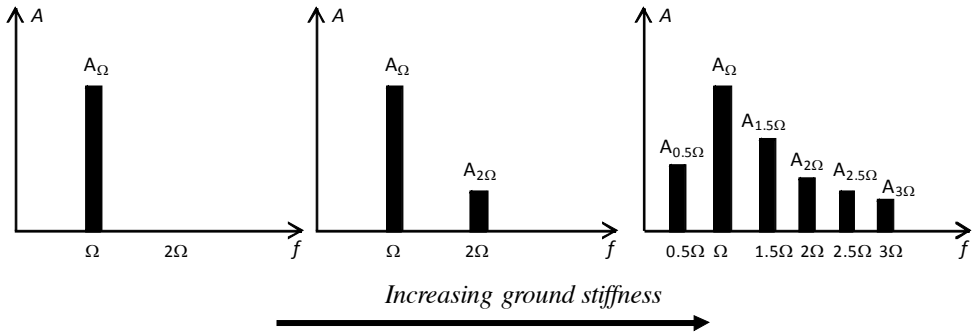

(Modified from the Sakai manual)

Figure 7. Sakai CCV - Changes in amplitude spectrum with increasing ground stiffness.

Feedback Control

NA

Documentation System

The Sakai IC documentation system is called Compaction Information System. The system makes use of field software—Aithon MT-R, and an office version—Aithon PD-R software.

Prior to the compaction operation, a plan file that delineates the pavement edges can be loaded to the Sakai CIS system in order to be overlaid with the color-coded map. The plan file can be generated using the Aithon MT-R software provided that the GPS locations of the paved edges are known. The IC measurements by the Sakai system are stored in a proprietary binary file format (with file name extension, GPS). To replay the compaction data, one would need to load both the plan file and the IC data file using the Aithon MT-R software. The Aithon MT-R software can also generate "construction result" files in ASCII format (with a file name extension, PLN) that can be imported to AUTOCAD 2007/8 using a macro by Sakai. A 0.3 m by 0.3 m (1ft by 1ft) mesh often is used to present the data and display in graphics.

Figure 8, Figure 9, and Figure 10 show screenshots of the Sakai Aithon MT-A software that can be viewed by the roller operator in real time during the compaction process in order to track roller passes, CCV, and surface temperatures, respectively. The purpose of this graphical display is to provide an easy way to understand system for eliminating the common problem of not getting uniform coverage of the desired number of passes.

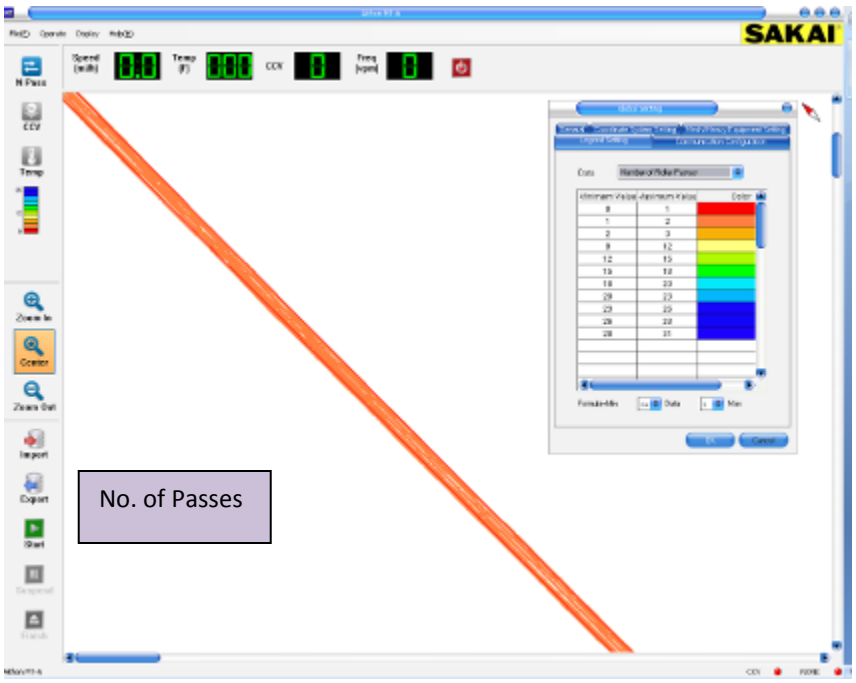

Figure 8. Sakai Aithon MT-R software output for number of rollers passes.

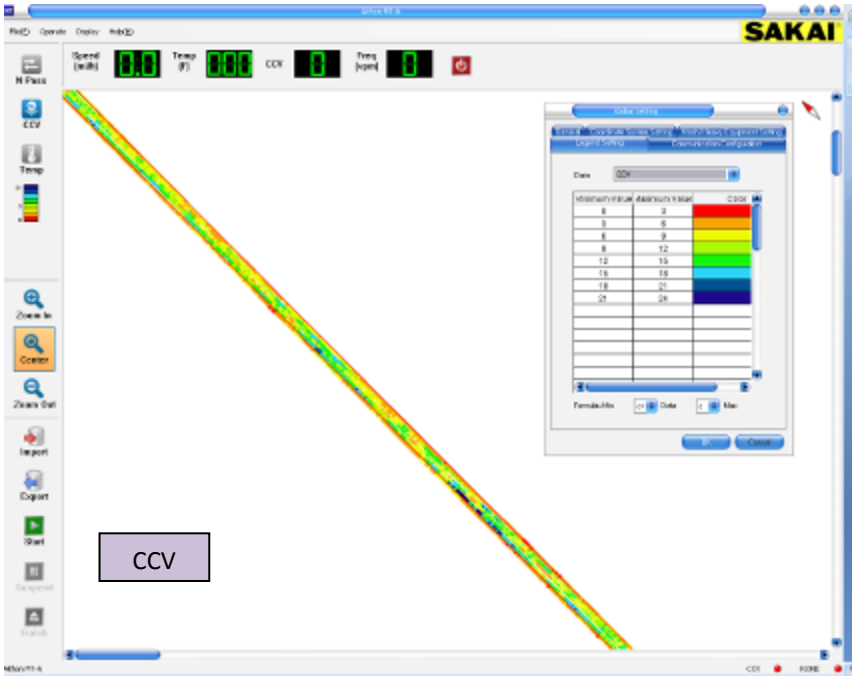

Figure 9. Sakai Aithon MT-R software output for CCV.

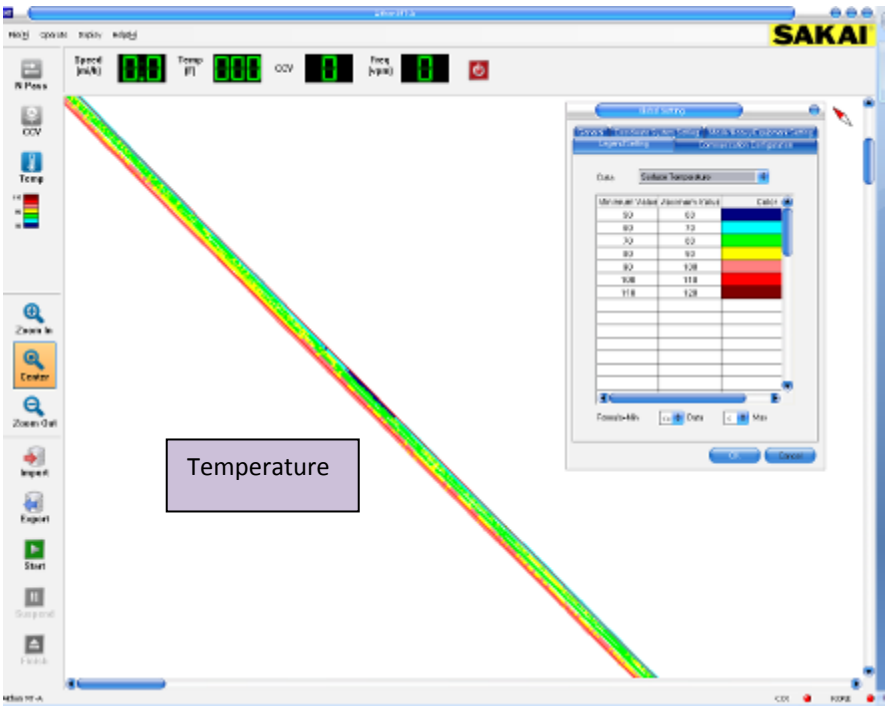

Figure 10. Sakai Aithon MT-R software output for surface temperatures.

GPS System

The Trimble and TopCon GPS systems were used for the Sakai SW880 and SW990 rollers, respectively.

Trimble GPS

- A Trimble GPS receiver and a radio were mounted on the Sakai SW880 machine.
- A Trimble GPS base station was setup to provide RTK correction signals.
- A hand-held Trimble GPS rover was used for in-situ point measurements.

TopCon GPS

- A TopCon GPS receiver and a radio were mounted on the Sakai SW990 machine.
- A TopCon GPS base station was setup to provide RTK correction signals.
- A hand-held TopCon GPS rover was used for in-situ point measurements.

Description of In-situ Testing Methods

Various in-situ testing methods were employed in this study to evaluate the in-situ pavement physical and mechanical properties:

- Nuclear gauge (NG) to determine in-situ HMA densities,
- Laboratory test on HMA core samples to determine the bulk densities;
- Mobil laboratory test on HMA at the mix plant to determine the complex modulus E*;
- FWD with a 300-mm diameter plate to measure the deflections for back-calculating elastic modulus (E_{FWD}) of each layer;
- LWD test on each pavement layer to measure the deflection and moduli;
- FLIR Thermal Imaging to measure the HMA surface temperature.

The above tests were conducted by the research team, Mathy Construction, and the WisDOT personnel. For each discrete in-situ test location, the GPS location was recorded.

Nuclear Density Gauge (NG)

The nuclear density gauge (NG) was used to measure the densities of HMA materials, as shown in Figure 11. The nuclear density gauge measures the in-place material density based on the gamma radiation. NG usually contain a small gamma source (about 10 mCi) such as Cesium-137 on the end of a retractable rod (University of Washington website, see reference).

The device consists of a hander, a retractable rod, the frame, a shielding, a source, and a Geiger-Mueller detector as shown in Figure 12. The source emits gamma rays that interact with electrons in the HMA pavement through absorption, Compton scattering, and the photoelectric effect. The detector (situated in the gauge opposite from the handle) counts gamma rays that reach it from the source. Then, the received number of gamma rays by the detector is correlated to the density of HMA materials (see Figure 12).

Figure 11. Nuclear density gauge.

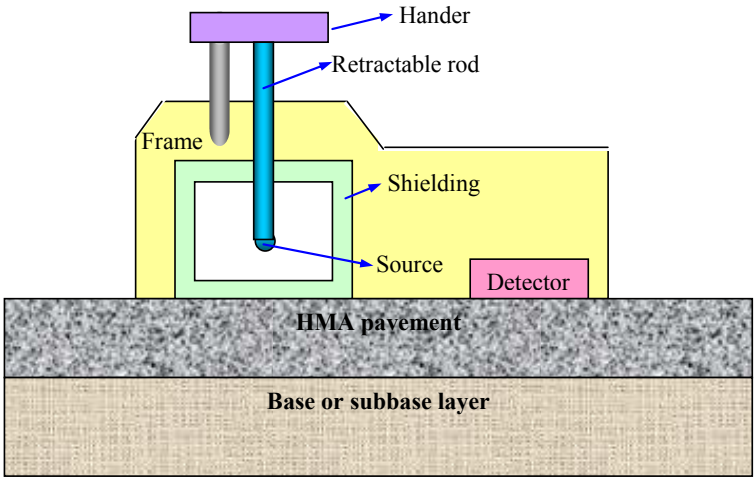

Figure 12. Nuclear density gauge mechanism.

FWD Tests

The FWD test data were collected using a KUAB 2m-FWD (see Figure 13). The test was performed on the rubblized and crack-and-seat PCC bases, HMA base, and the HMA intermediate layer (2nd lift). Four test strips were designed for FWD test: 2 on the passing lane and 2 on the driving lane. Each test strip has 11 or 25 test spots with a distance interval of 100 ft between two spots. The test settings were as follows:

- Platen Size: 5.9" radius (rigid plate)
- Geophone positions: -12, 0, 12, 18, 24, 36, 48 inches (7 sensors)
- Drops/Loads: 2 drops targeting 9,000 and 13,000 lbs
- Field program: KUAB 2m-FWD.
- File format: KUAB *.fwd.

Figure 13. In-situ FWD testing on the rubblized PCC base.

LWD Tests

The LWD data were collected using a Dynatest LWD device (see Figure 14). The electronics are interfaced to a handheld PDA via a wireless Bluetooth connection to record and store data. The test settings were as follows:

- Drop weight: 10 kg;
- Drop height: adjustable;

- Plate diameter *d*: 300 mm.

The data for each loading drop includes the center peaking loading and deflection, and that with time histories. The moduli of pavement layer E can be back-calculated by using the Dynatest LWD software program.

Figure 14. Dynatest LWD.

HMA IC Demonstration

Demonstration Activities

The demonstration activities include mapping of rubblized and crack-and-seat PCC bases, compaction of HMA base, HMA intermediate layer (2nd lift), and HMA surface course.

The Sakai SW990 double-drum IC rollers were used as the break-down or intermediate roller, and the SW880 is used as finishing roller. A Caterpillar roller was used as the intermediate or finishing roller for this demonstration. In-situ tests including the NG density, FWD and LWD measurements. The bulk density of HMA core samples was measured, and the complex modulus E* of HMA mixture at the plant was also tested using the FHWA asphalt mobile lab.

Figure 15 presents the experimental plan. IC compaction and in-situ tests were conducted on two sections of the IH 39 SB highway: section 1 before the bridge and section 2 after the bridge. Existing HMA surface was milled and removed, and then PCC slab/base was rubblized at section 1, while cracked-and-seated at section 2. Each section consists of both the passing lane and the driving lane. Six test beds were designated for the IC compaction or mapping, including 3 test beds for the passing lane (TB01M for mapping rubblized and crack-and-seat PCC bases, TB01B for compacting HMA base, TB01C for compacting HMA 2nd lift), and another 3 test beds for the driving lane (TB02M for mapping rubblized and crack-and-seat PCC bases, TB02B for compacting HMA base, TB02C for compacting HMA 2nd lift).

For the in-situ tests, three test strips were designated on the passing lane: test strip 1, 2, and 4 with ID numbers of TB1 to TB10, TB20 to TB45, and F4-1 to F4-11, respectively, and another two test strips were designated on the driving lane: test strip 5 and 6 with ID numbers of TB5-1 to TB5-11 and F6-1 to F6-11, respectively. LWD tests were also performed at another two special test spots, FS-1 and FS-2, to check the structural capacity per request of the contractor.

These test beds are described in Table 2. Test schedule and IC machine settings are summarized in Table 3.

Figure 15. Experimental design IC compaction and in-situ tests.

Table 2. Test bed description for HMA IC.

TB	Material/Layer	Locations
01M	Rubblized and crack-and-seat PCC base mapping	IH 39 SB, passing lane and soil shoulder
01B	HMA base	IH 39 SB, passing lane
01C	2nd lift HMA intermediate layer	IH 39 SB, passing lane
02M	Rubblized and crack-and-seat PCC base mapping	IH 39 SB, driving lane
02B	HMA base	IH 39 SB, driving lane
02C	2nd lift HMA intermediate layer	IH 39 SB, driving lane

Table 3. Test Settings for HMA IC.

TB	Date	Machine(s)	Passes	Settings	In-situ Test Measurements
01M	05/10	Sakai SW880 (mapping)	1	Low amp, 3000 vpm,3 kmh	FWD, LWD
01B-I	05/10	Sakai SW990 (breakdown or intermediate)	2-3	Low amp, 3000/4000 vpm,3 kmh	LWD, NG, Cores
01B-II	05/10	Sakai SW880 (finishing)	1 vib 1 static	0.3-mm, 4000 vpm,3 kmh	FWD
01C-I	05/10-11	Sakai SW990 (breakdown)	2-3	0.3-mm, 3000 vpm,3 kmh	
01C-II	05/10-11	Sakai SW880 (finishing)	1	0.3-mm, 3000vpm, 3 kmh 0.3-mm, 3000/4000 vpm, 3 kmh	FWD, NG
02M	05/12	Sakai SW880 (mapping)	1	Low amp, 3000 vpm,3 kmh	FWD, LWD
02B-I	05/12	Sakai SW990 (intermediate)	3	Low amp, 3000/4000 vpm,3 kmh	LWD, NG, Cores
02B-II	05/12	Sakai SW880 (finishing)	1 vib 1 static	Low amp, 3000 vpm,3 kmh	FWD, NG
02C-I	05/12-13	Sakai SW990 (breakdown)	3	Low amp, 4000 vpm,3 kmh	NG
02C-II	05/12-13	Sakai SW880 (finishing)	1	Low amp, 3000/4000 vpm,3 kmh	FWD, LWD, NG

Two GPS base stations (TopCon and Trimble) were setup on this project (see Figure 16 for the TopCon base station). Communication was established between the GPS base station and the RTK receivers on the IC rollers as well as handheld GPS rover. The UTM 16 North zone was used as the grid reference during GPS calibration.

Figure 16. A TopCon GPS base station.

Analysis Approaches

Viewing of IC Data and Maps

The Sakai AthonMT® software was used to export data from the measured IC data files. The IC Viewer program developed by the Transtec Group (see Figure 17) are used to view, process the exported IC data (roller pass, surface temperature, RMV, etc.) and perform data analysis including the statistical/geostatistical analysis, correlation study, and compaction curves, etc.

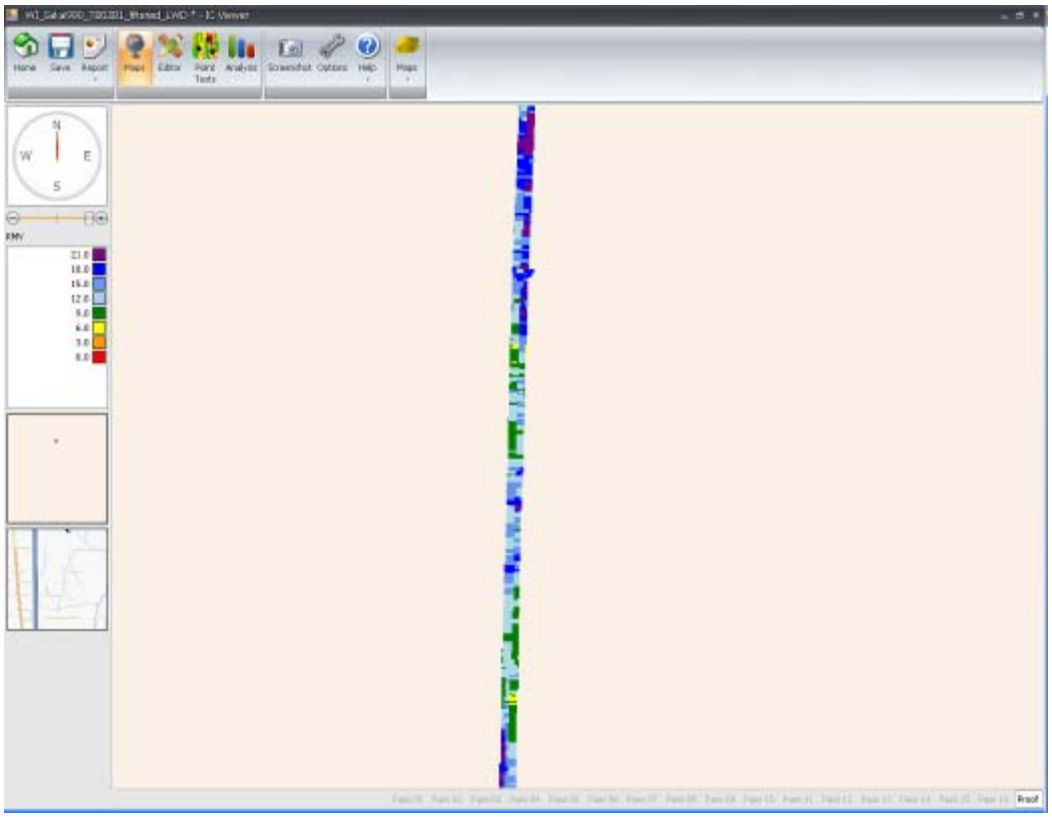

Figure 17. Interface of the IC Viewer.

Statistics Evaluation of Compaction Quality and Uniformity

The basic statistics including the mean value, standard deviation of IC data are analyzed using the IC viewer software.

Geostatistics is used for analysis of the compaction uniformity using the IC viewer software. Spatially referenced IC measurement values provide an opportunity to quantify "uniformity" of compacted fill materials. This topic is slowly gaining popularity among the pavement engineering community. Vennapusa and White (2009b) demonstrated the use of semi-variogram analysis in combination with conventional statistical analysis to effectively address the issue of uniformity in quality assurance during earthwork construction.

A semi-variogram is a plot of the average squared differences between data values as a function of separation distance, and is a common tool used in geostatistical studies to describe spatial variation. A typical semi-variogram plot is presented in Figure 18. The semi-variogram $\gamma(h)$ is defined as one-half of the average squared differences between data values that are separated at a distance h (Isaaks and Srivastava 1989). If this calculation is repeated for many different values of h (as the sample data will support) the result can be graphically presented as experimental semi-variogram shown as circles in Figure 18. More details on experimental semi-variogram calculation procedure are available elsewhere in the literature (e.g., Clark and Harper 2002, Isaaks and Srivastava 1989).

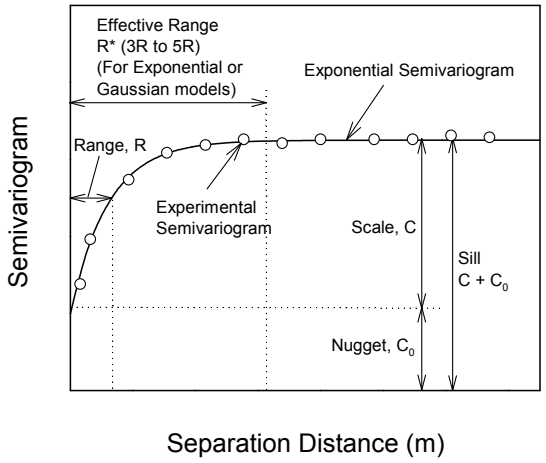

Range: As the separation distance between pairs increase, the corresponding semivariogram value will also generally increase. Eventually, however, an increase in the distance no longer causes a corresponding increase in the semivariogram, i.e., where the semivariogram reaches a plateau. The distance at which the semivariogram reaches this plateau is called as range. Longer range values suggest greater spatial continuity or relatively larger (more spatially coherent) "hot spots".

Sill: The plateau that the semivariogram reaches at the range is called the sill. A semivariogram generally has a sill that is approximately equal to the variance of the data.

Nugget: Though the value of the semivariogram at h = 0 is strictly zero, several factors, such as sampling error and very short scale variability, may cause sample values separated by extremely short distances to be quite dissimilar. This causes a discontinuity at the origin of the semivariogram and is described as nugget effect. (Isaaks and Srivastava, 1989)

Figure 18. Description of a typical experimental and exponential semi-variogram and its parameters

To obtain an algebraic expression for the relationship between separation distance and experimental semi-variogram, a theoretical model is fit to the data. Some commonly used models include linear, spherical, exponential, and Gaussian models. Previous work by White et al. (2007a), White et al. (2007b), Vennapusa and White (2009b), and results from Texas field investigation conducted as part of this project showed that an exponential model generally fits well for IC measurement data.

An exponential semi-variogram is illustrated in Figure 18 as solid line. Three important features to construct a theoretical semi-variogram include: sill ($C+C_0$), range (R), and nugget (C_0). These parameters are briefly described in Figure 18. Arithmetic expressions and detailed descriptions of theoretical models can be found elsewhere in the literature (e.g., Clark and Harper 2002, Isaaks and Srivastava 1989). For the results presented in this section, the sill, range, and nugget values during theoretical model fitting were determined by checking the models for "goodness" using the modified Cressie goodness fit method (see Clark and Harper 2002) and cross-validation process (see Isaaks and Srivastava 1989). From a theoretical semi-variogram model, a low "sill" and longer "range of influence" represent best conditions for uniformity, while the opposite represents an increasingly non-uniform condition.

In this project the IC Viewer program is used to produce semi-variograms of IC data. Different models, e.g. the exponential and Gaussian models (see Figure 19), were used to fit the semi-variogam in order to obtain the semi-variogram parameters (e.g. range, sill, scale, and nugget.).

Exponential Model
Cressie (1991, p. 61)

$$\gamma(h) = C\left[1 - e^{-h}\right]$$

Gaussian Model
Pannatier (1996, p. 50)

$$\gamma(h) = C\left[1 - e^{-h^2}\right]$$

Figure 19. Semi-variogram models

Correlation of IC Data and In-Situ Measurements

The IC data are correlated with the in-situ measurements: including FWD deflections and back-calculated modulus, in-situ non-nuclear density gauge measurements and laboratory bulk densities of cored samples.

Results Analysis and Discussion

IC Results

TB 01M – Mapping Rubblized PCC Base, Crack-and-Seat, and Soil Shoulder

On May 10, 2010, the existing HMA surface on the IH 39 SB passing lane was milled and removed. Consequently, the PCC slabs were rubblized in Section 1 (before the bridge intersecting highway 153), and it was cracked-and-seat in Section 2 (after the bridge intersecting highway 153). The Sakai SW880 double-drum IC roller was used to "map" the rubblized or cracked-and-seat PCC base with one roller pass. The Sakai machine settings were as follows: frequency of 3000 vpm, low amplitude, and speed of 3 mph.

Figure 20 and Figure 21 illustrate the milling of existing HMA, PCC rubblization, Sakai IC mapping, FWD/LWD tests, and GPS measurements.

Figure 22 and Figure 23 display the mapping results of Sakai CCV (roller measurement value) and roller pass number for the rubblized and crack-and-seat PCC, respectively. CCV at the shoulder are relatively lower than that of the rubblized base, which indicates lower stiffness at the shoulder area. Most areas of the mapping zone have one roller pass. However, some areas have 2 or 3 pass number, which is due to the overlapping of roller passes.

Figure 24 and Figure 25 summarize the statistical histograms of Sakai CCV and vibration frequency for the rubblized PCC base/soil shoulder and crack-and-seat PCC/soil shoulder, respectively. The mean CCV for the soil shoulder, the rubblized PCC and crack-and-seat PCC are 4.5, 15, and 16, respectively.

Test bed 01M (5/10/2010)

Description

This test bed consists of mapping the existing soil and rubblized PCC base layer on the IH 39 SB passing lane. The surface HMA was milled and removed, then the PCC base was rubblized or crack-and-seat. The Sakai SW880 double-drum IC roller was used to map the both the existing soil and rubblized PCC surfaces. The purpose is to evaluate the condition of the existing support prior to the asphalt construction.

Figure 20. Milling of existing HMA and Rubblization of PCC base (TB 01M).

Test bed 01M (5/10/2010)

Sakai SW880 Machine setting:

Vibration frequency was 2800 vpm; the low amplitude was used; the speed was set about 3 mph; only the front drum was vibrated.

Figure 21. Sakai IC mapping and in-situ testing (TB 01M)

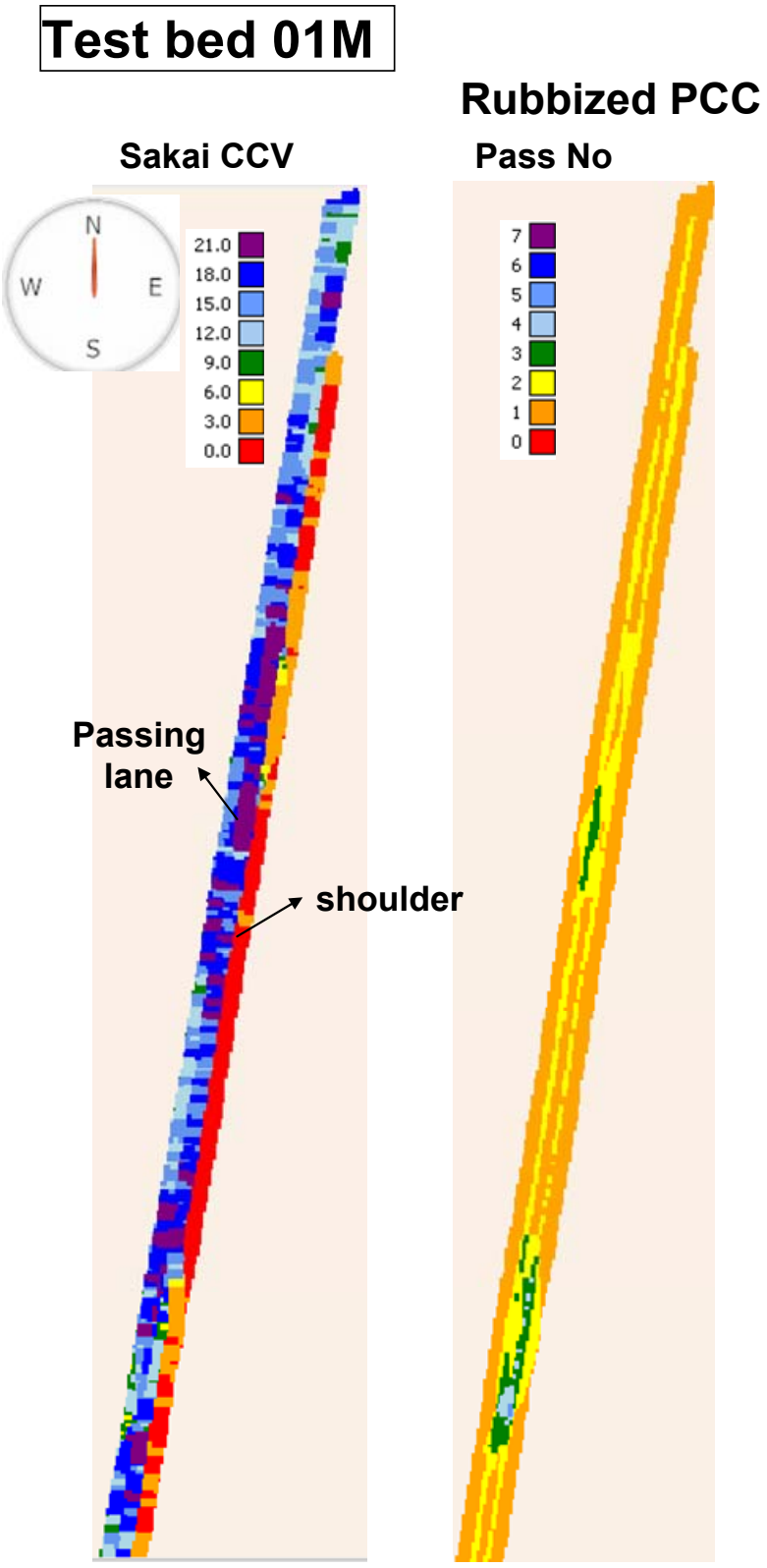

Figure 22. Sakai CCV and pass counts of rubblized PCC base and soil shoulder (TB 01M).

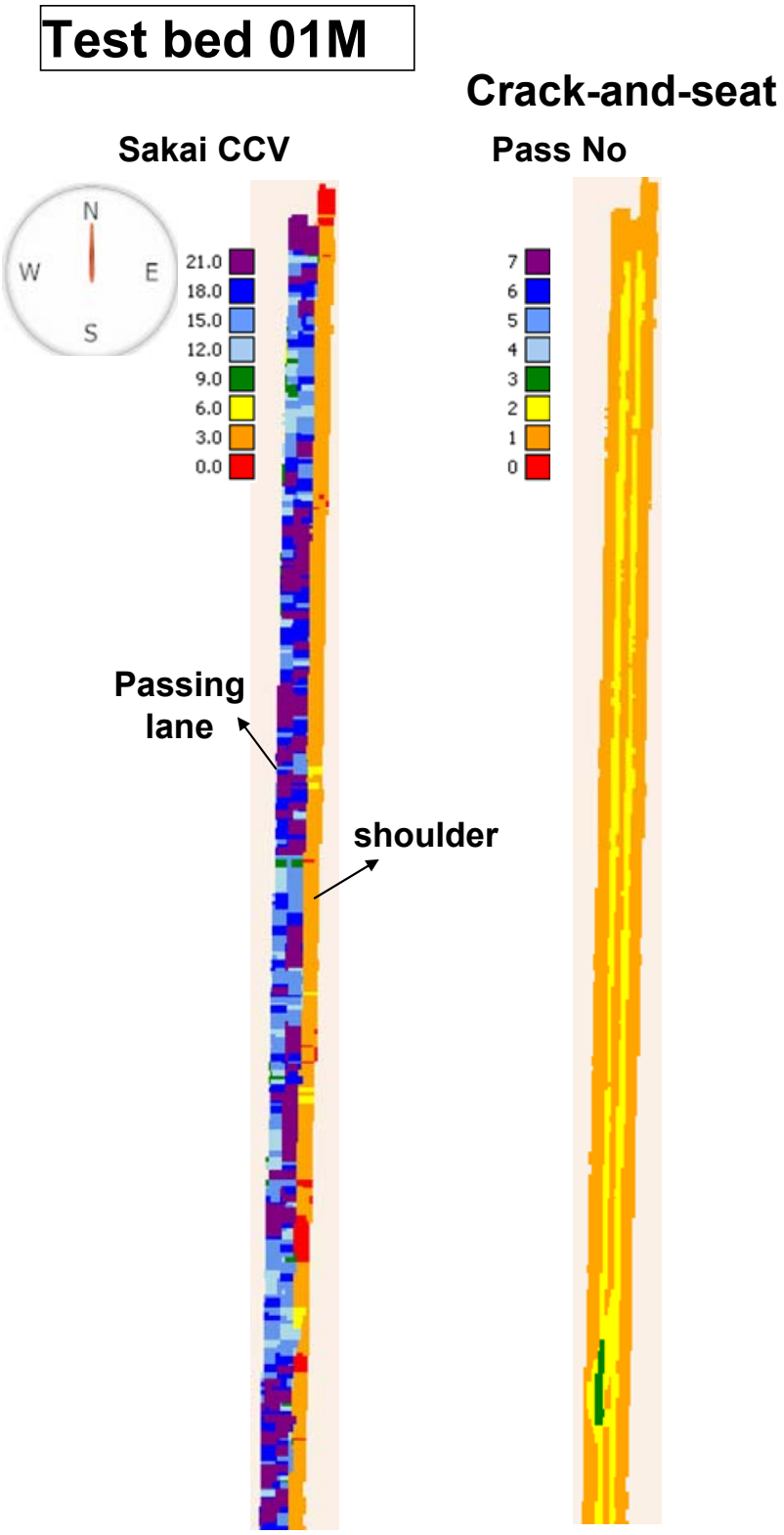

Figure 23. Sakai CCV and pass counts of crack-&-seat PCC base and soil shoulder (TB 01M).

Test bed 01M

Rubblized PCC base and soil shoulder mapping

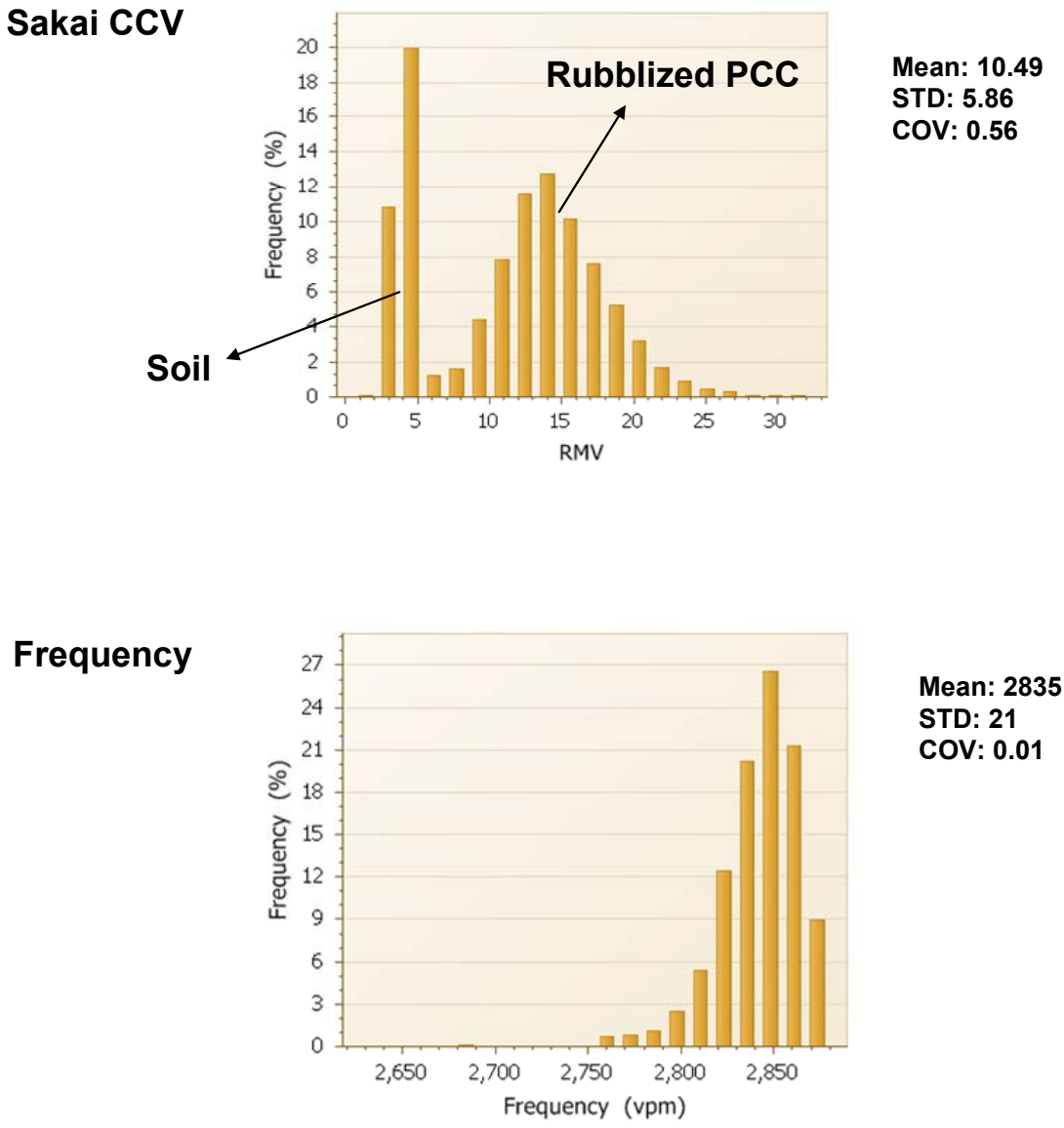

Figure 24. Histograms of Sakai CCV and vibration frequency for rubblized PCC base and soil shoulder (TB 01M).

Test bed 01M

Crack-and-seat and soil shoulder mapping

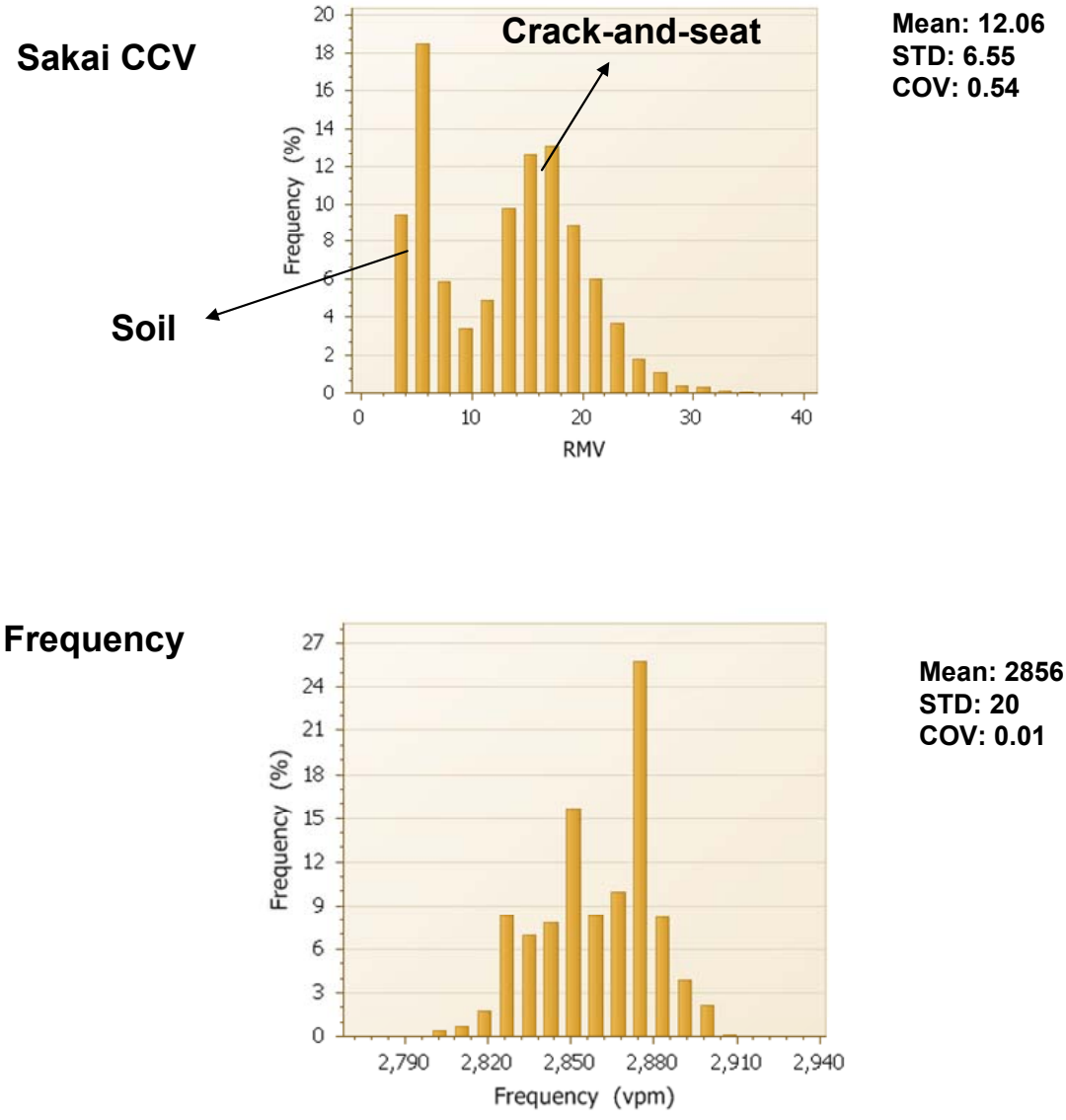

Figure 25. Histograms of Sakai CCV and vibration frequency for crack-&-seat PCC base and soil shoulder (TB 01M).

TB 01B – HMA Base on the Passing Lane

This test bed consists of paving/compacting a HMA base course on top of the rubblized and crack-and-seat PCC bases using the Sakai double-drum IC roller. The Sakai SW990 was used as the breakdown then switched to as an intermediate roller with 3 passes, and the Sakai SW880 was used as the finishing roller with 1-2 passes for the later portion of the paving. The Sakai machine settings were as follows: frequency of 3000 vpm for SW990 intermediate compaction, and 4000 vpm for SW990 breakdown and SW880 finishing compactions; low amplitude; and speed of 3 mph.

Figure 26 summarize the test location, roller machines and compaction parameters (frequency, amplitude, and speed), and the in-situ tests. Figure 27 and Figure 28 present the maps of Sakai CCV, roller pass number, and HMA surface temperature of TB01B resulted from the SW990 breakdown and SW880 finishing compaction, respectively. Results show that more roller passes were performed at the center of the paving lane, and some areas of it were overlapped with higher roller pass numbers (e.g. 4-6 for the SW990 breakdown compaction). Accordingly, those areas with higher pass numbers result in higher CCVs.

Figure 29 to Figure 32 show the statistical histograms of the Sakai CCV, HMA surface temperature, and frequency resulted from the SW990 breakdown/intermediate and SW880 finishing compaction for section 1 and 2, respectively. Obviously HMA remained a higher temperature during the breakdown compaction (mean of 197.3^{o}F) than that during the finishing compaction (mean of 122.2 ^{o}F). The mean values of CCVs resulted from the breakdown and finishing compaction are 17.9 and 12.9, respectively. These CCVs are higher than that of the PCC base due to the improved stiffness of pavement system after paving a stiffer HMA base layer on the top of PCC base.

Figure 33 and Figure 34 display the semi-variograms of the HMA base under the Sakai SW990 breakdown/intermediate and SW880 finishing roller compaction, respectively. Results show that for the SW990 breakdown compaction, section 2 has a larger range yet lower sill value than section 1, indicating its better uniformity. For Section 1, the SW880 finishing compaction results in a higher uniformity than the breakdown compaction with a higher range while lower sill value.

Figure 35 presents the compaction curve of the HMA base layer under the SW990 breakdown compaction. It shows that the CCV increases first and then decreases with increasing pass number, and the optimal CCV is achieved at the roller pass number of 4.

Test bed 01B (5/10/2010)

Description

This test bed consists of compacting the HMA base layer on the rubblized PCC base on the IH 39 SB passing lane. Sakai SW990 double-drum IC roller was used as breakdown roller and Sakai SW880 was used as intermediate roller. The in-situ FWD, LWD, and NG density measurements were performed.

Sakai Machine Setting:
Vibration frequency was 4000 and 3000 vpm; the low amplitude was used; the speed was set about 3 mph.

Figure 26. Paving/Compaction and in-situ test of the HMA base course (TB 01B).

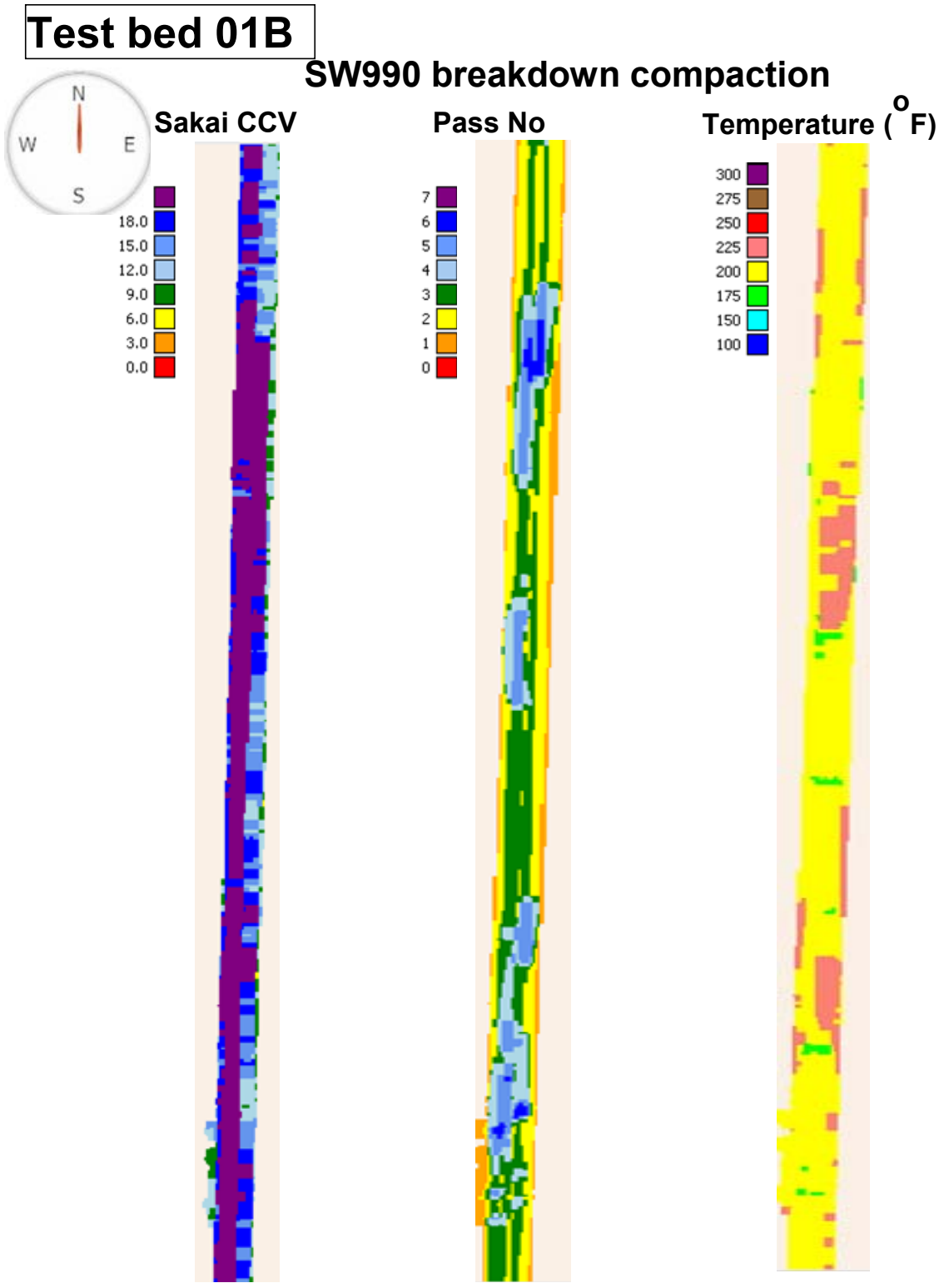

Figure 27. Sakai SW990 CCV, pass number, and surface temperatures for the breakdown/intermediate compaction of the HMA base course (TB 01B).

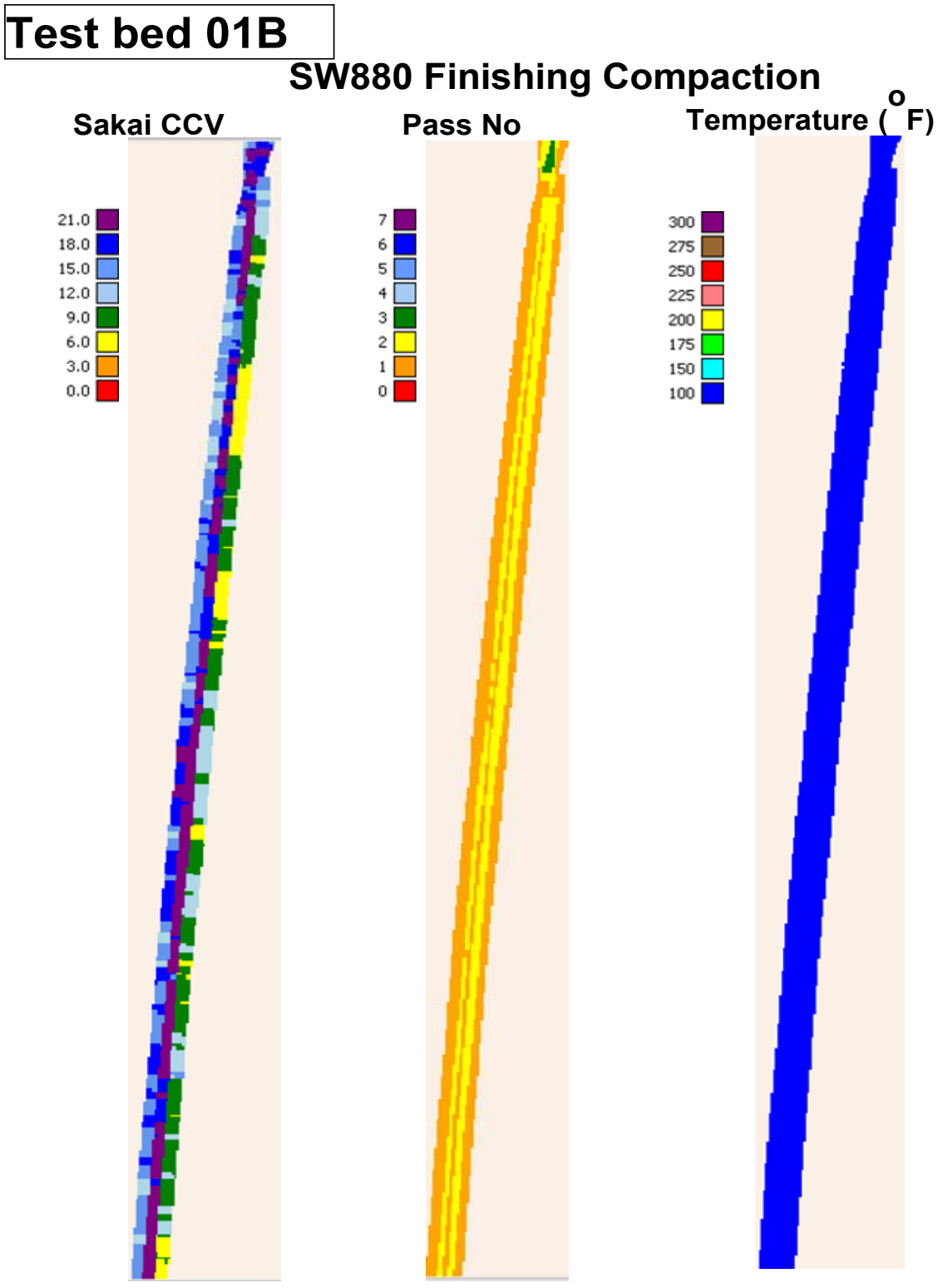

Figure 28. Sakai SW880 CCV, pass number, and surface temperatures for the finishing compaction of the HMA base course. (TB 01B)

TB01B_Section 1

SW990 breakdown compaction

Sakai CCV

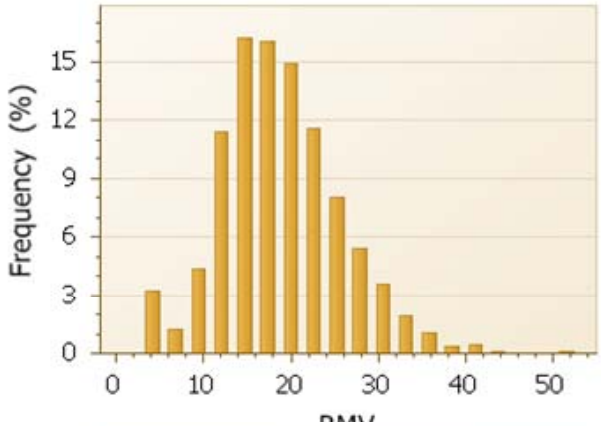

Mean: 17.49
STD: 6.87
COV: 0.39

Temperature

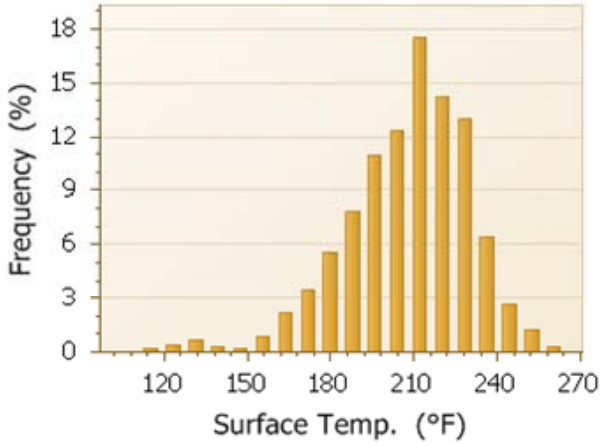

Mean: 200.3
STD: 22.10
COV: 0.11

Frequency

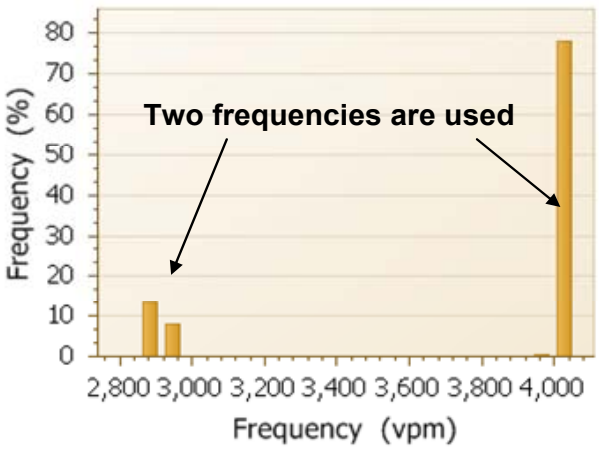

Mean: 3767
STD: 466
COV: 0.12

Figure 29. Sakai SW990 CCV, surface temperatures, and frequency histograms for the breakdown/intermediate compaction of the HMA base course (TB01B - Section 1).

TB01B_Section 2

SW990 breakdown compaction

Sakai CCV

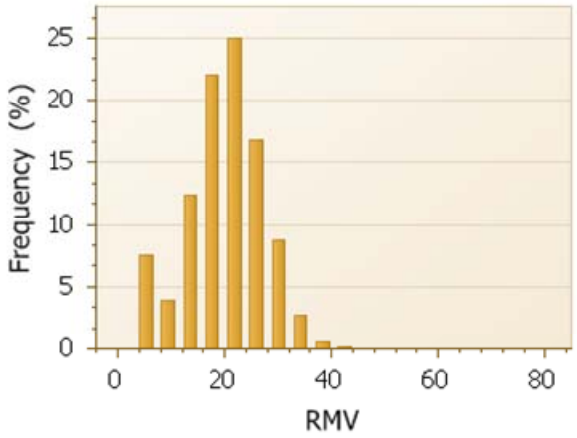

Mean: 18.03
STD: 7.18
COV: 0.40

Temperature

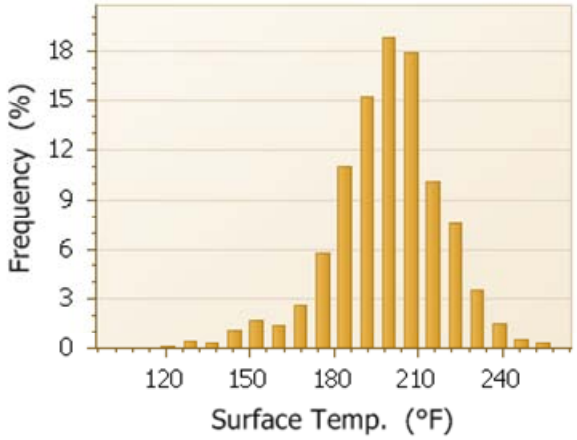

Mean: 194.9
STD: 19.56
COV: 0.10

Frequency

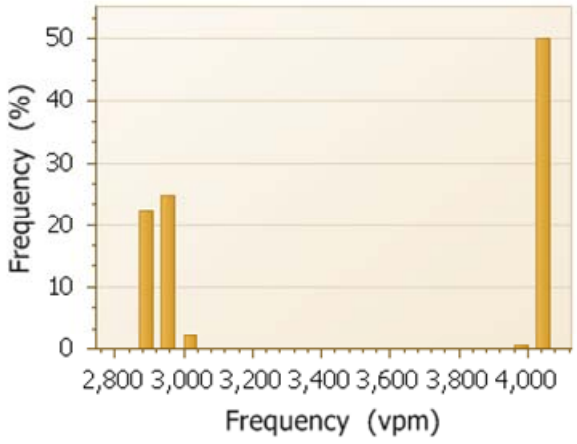

Mean: 3479
STD: 575
COV: 0.17

Figure 30. Sakai SW990 CCV, surface temperatures, and frequency histograms for the breakdown/intermediate compaction of the HMA base course (TB01B - Section 2).

TB01B_Section 1

Sakai CCV

SW880 finishing compaction section 1

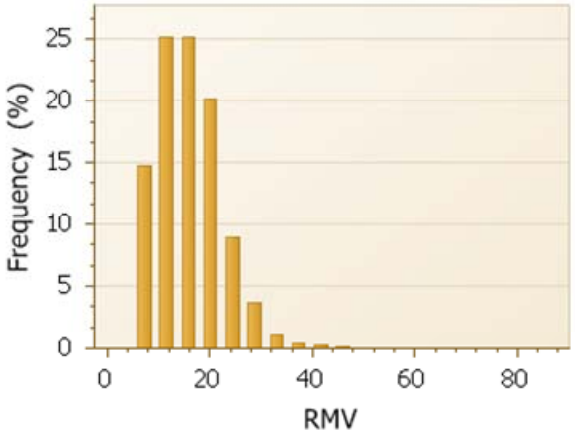

Mean: 13.88
STD: 6. 28
COV: 0.45

Temperature

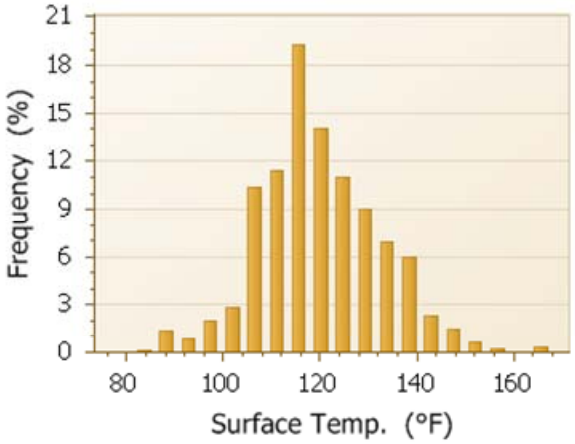

Mean: 117.5
STD: 12.45
COV: 0.11

Frequency

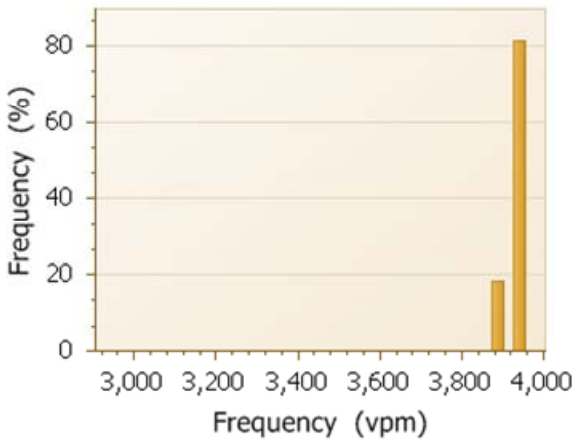

Mean: 3904
STD: 20
COV: 0.01

Figure 31. Sakai SW880 CCV, surface temperatures, and frequency histograms for the finishing compaction of the HMA base course (TB01B - Section 1).

TB01B_Section 2

SW880 finishing compaction section 2

Sakai CCV

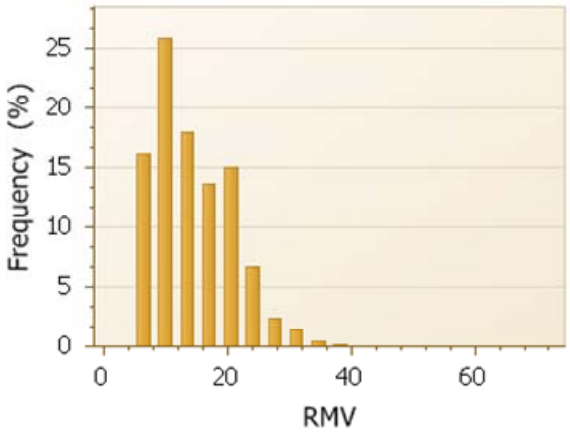

Mean: 12.63
STD: 6.46
COV: 0.51

Temperature

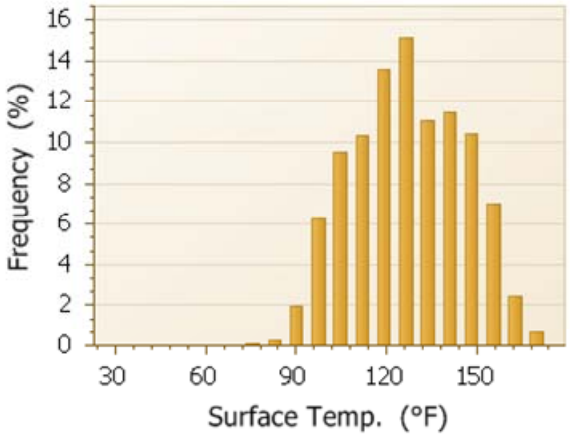

Mean: 123.5
STD: 18.39
COV: 0.15

Frequency

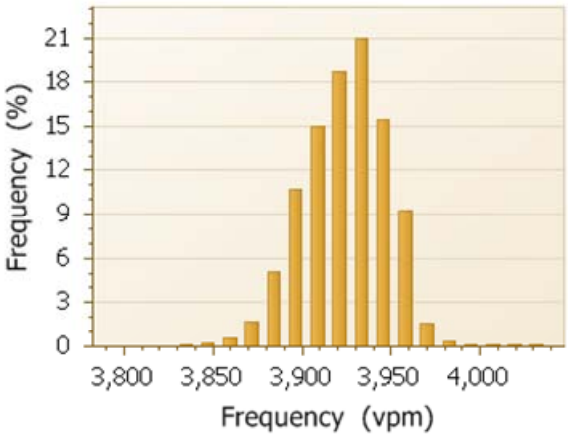

Mean: 3918
STD: 23
COV: 0.01

Figure 32. Sakai SW880 CCV, surface temperatures, and frequency histograms for the finishing compaction of the HMA base course (TB01B - Section 2).

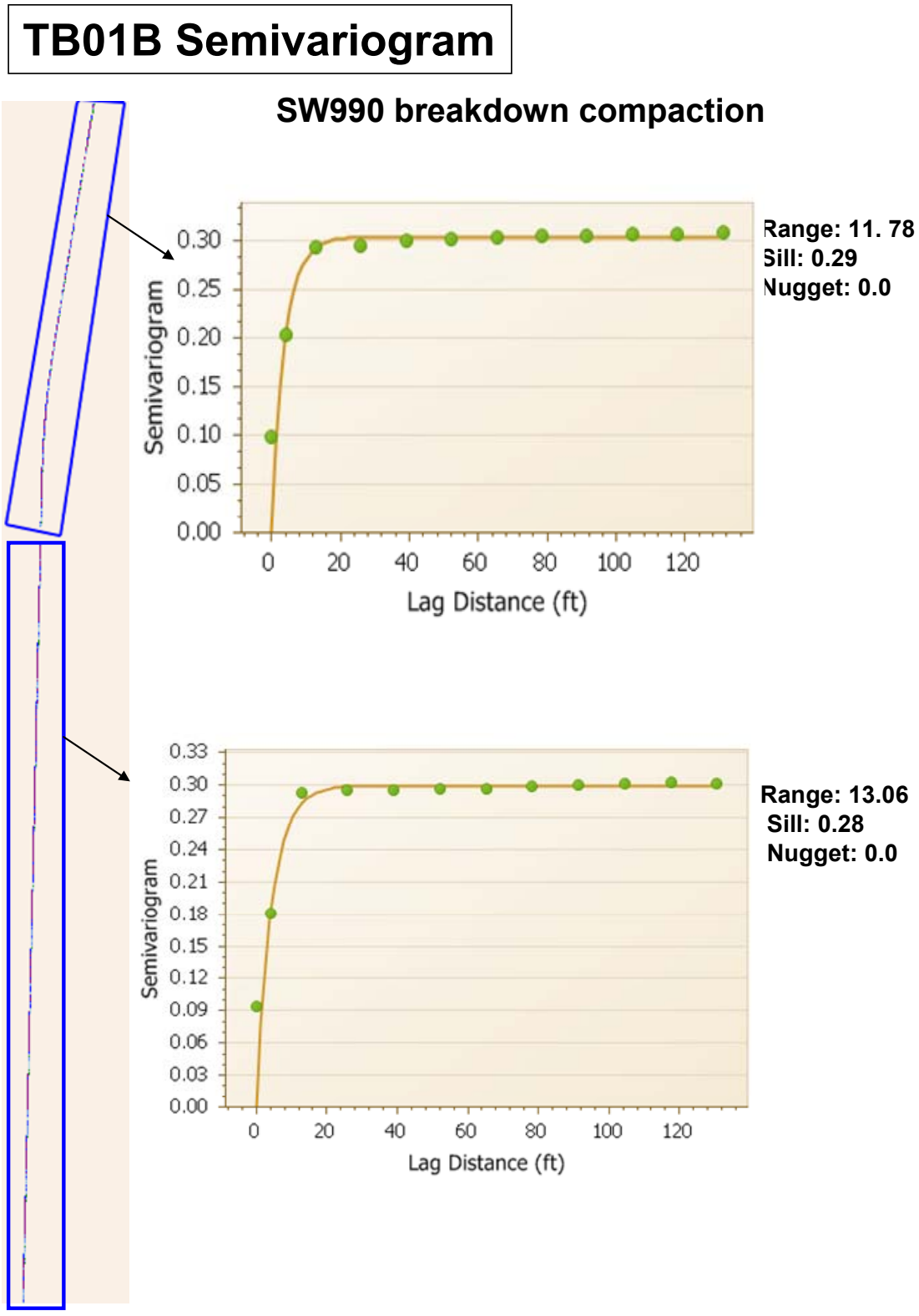

Figure 33. Semivariogram for the Sakai SW990 breakdown/intermediate compaction of the HMA base course. (TB 01B)

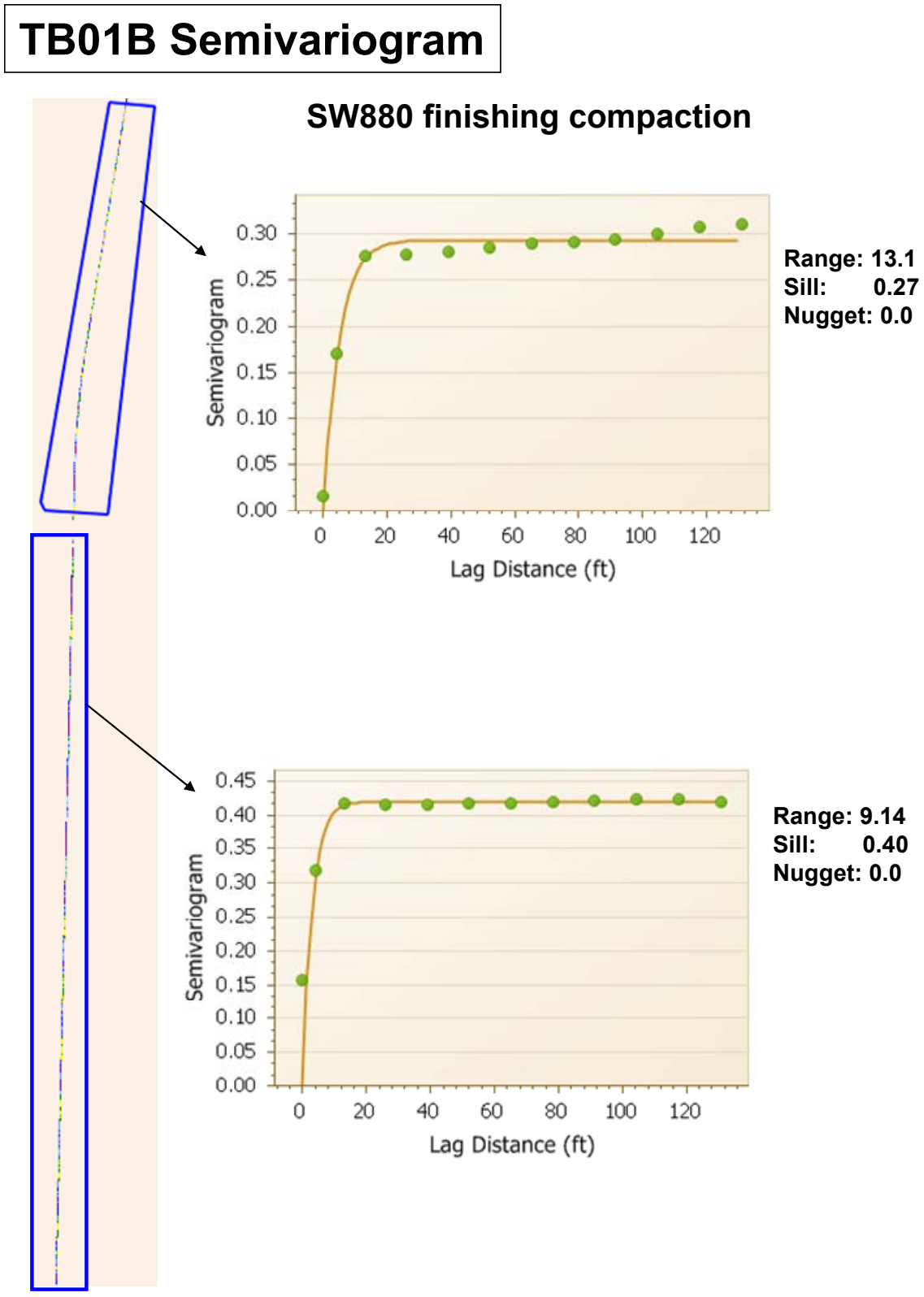

Figure 34. Semivariogram for the Sakai SW880 finishing compaction of the HMA base course. (TB 01B).

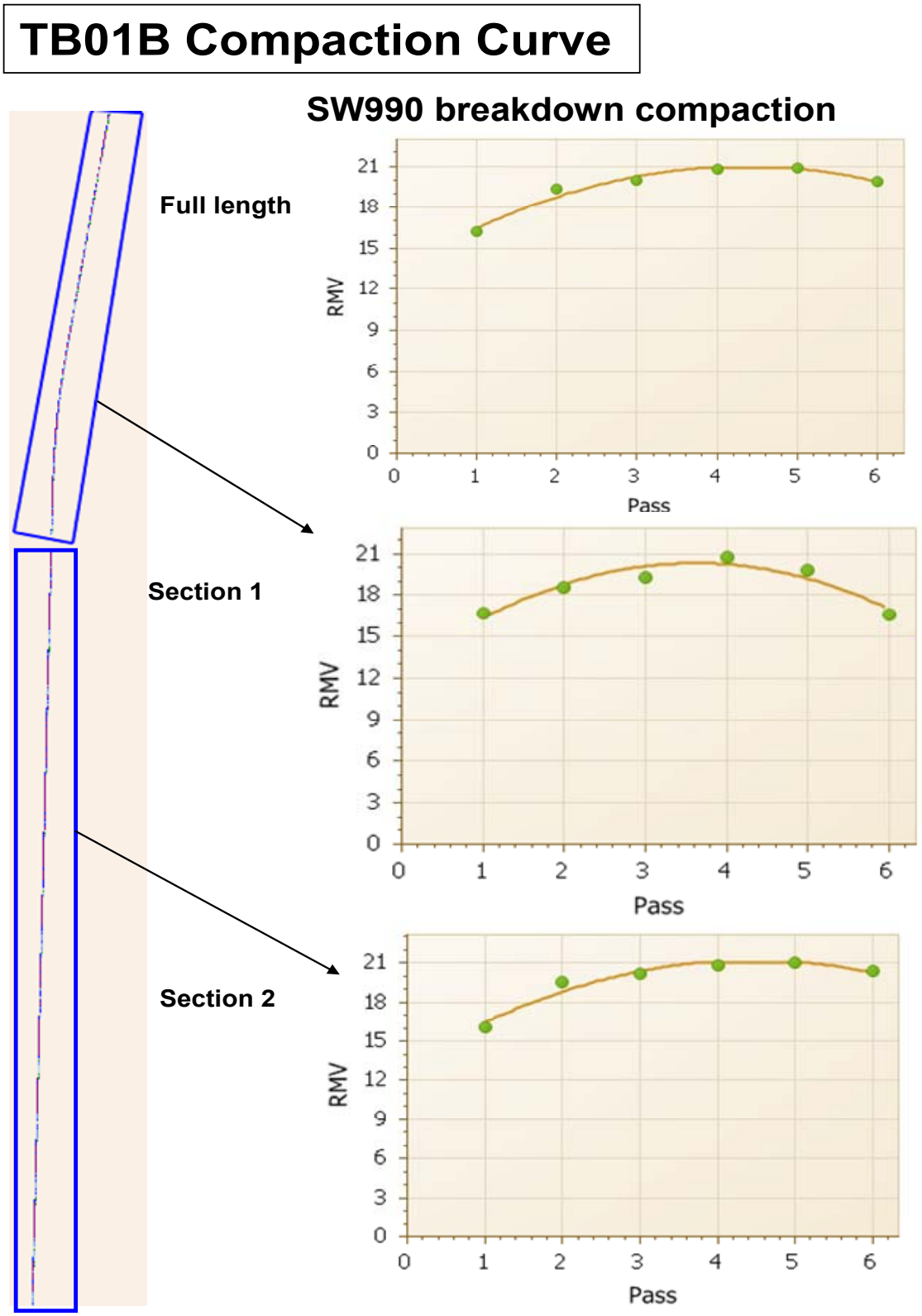

Figure 35. Compaction curve for Sakai SW990 breakdown/intermediate compaction of the HMA base course (TB 01B).

TB 01C – HMA Intermediate Layer on the Passing Lane

This test bed consists of paving the 2nd lift of HMA or intermediate layer on the newly paved HMA base using the Sakai double-drum IC rollers from May 10 to 11. Night paving was successfully implemented. The Sakai SW990 was used as the breakdown roller with 2-3 passes, and the Sakai SW880 was used as the finishing roller with 1-2 passes. The Sakai machine settings were as follows: frequency of 4000 vpm; low amplitude; and speed of 3 mph.

Figure 36 summarizes the test location, roller machines and compaction parameters (frequency, amplitude, and speed), and the in-situ tests. Night paving has been successfully implemented with the help of CIS system to identify the roller location and pass number.

Figure 39 and Figure 40 present the maps of Sakai CCV, roller pass number, and HMA surface temperature of TB01C resulted from the SW990 breakdown and SW880 finishing compaction, respectively. These results show that the CCVs at the shoulder portion (right side) are lower than that at the pavement lane portion (left side), which could be due to the lower roller passes as well as the weaker support on the shoulder portion.

Figure 41 and Figure 42 show the histograms of the Sakai CCV, HMA surface temperature, and frequency resulted from the SW990 breakdown and SW880 finishing compaction, respectively. Obviously HMA remained a higher temperature during the SW990 breakdown compaction (mean value of 196.2°F) than that during the SW880 finishing compaction (mean of 117.0 °F). The mean values of CCVs resulted from the breakdown and finishing compaction are 20.37 and 15.2, respectively. These CCVs are higher than that of the HMA base layer (CCVs of 17.9 and 12.9 for breakdown and finishing compaction on HMA base, respectively). This result illustrates that the HMA intermediate layer has further improved the stiffness of the pavement system.

Figure 43 and Figure 44 display the semi-variograms of the HMA 2nd lift under the Sakai SW990 breakdown and SW880 finishing compaction, respectively. Results show that for the SW990 breakdown compaction section 2 has a larger range yet lower sill value than section 1, indicating its better uniformity. This result is consistent with that for the HMA base, which might illustrate that a better compaction uniformity of the underlying layer would help achieve a better uniformity of the upper layer.

Figure 45 present the compaction curves of the HMA 2nd lift under the SW990 breakdown compaction. It shows that the CCV continuously increases with increasing the roller pass number till 5. However, the trend of compaction curve for section 2 shows that CCV will possibly decrease from pass number of 6 thought the maximum pass number of 5 was performed. This compaction pattern is somehow different than that of the HMA base layer as discussed previously, which would be due to their different material compositions and pavement structures.

Test bed 01C (5/10/2010)

Description

This test bed consists of paving the 19-mm 2nd lift HMA intermediate layer on the newly paved HMA base on the IH 39 SB passing lane. Sakai SW990 and SW880 double-drum IC rollers were used as breakdown and finishing roller, respectively. The in-situ FWD, LWD, and NG density measurements were performed.

Sakai Machine Setting:

Vibration frequency was 4000 vpm; the low amplitude was used; the speed was set about 3 mph.

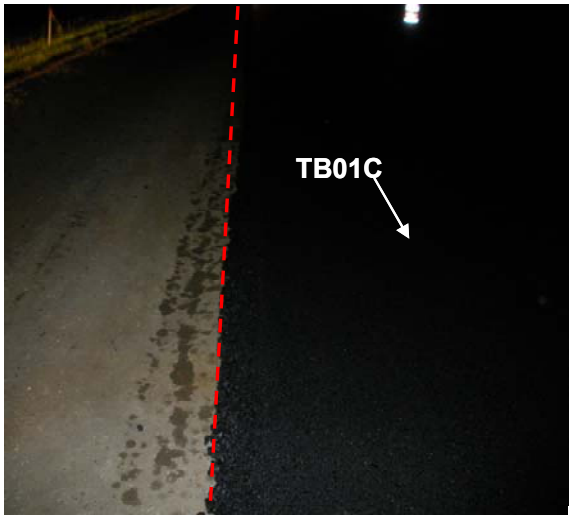

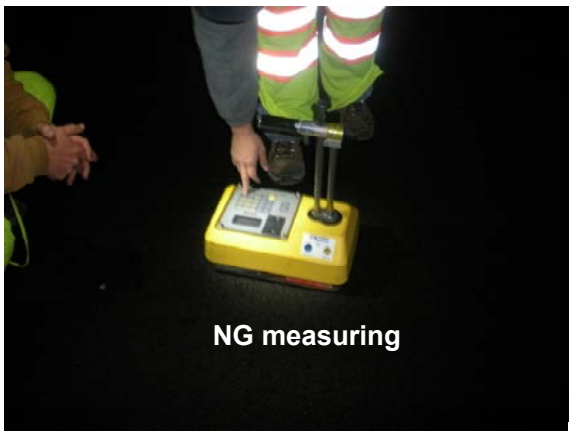

Figure 36. Compacting HMA intermediate layer on the newly paved HMA base (TB 01C).

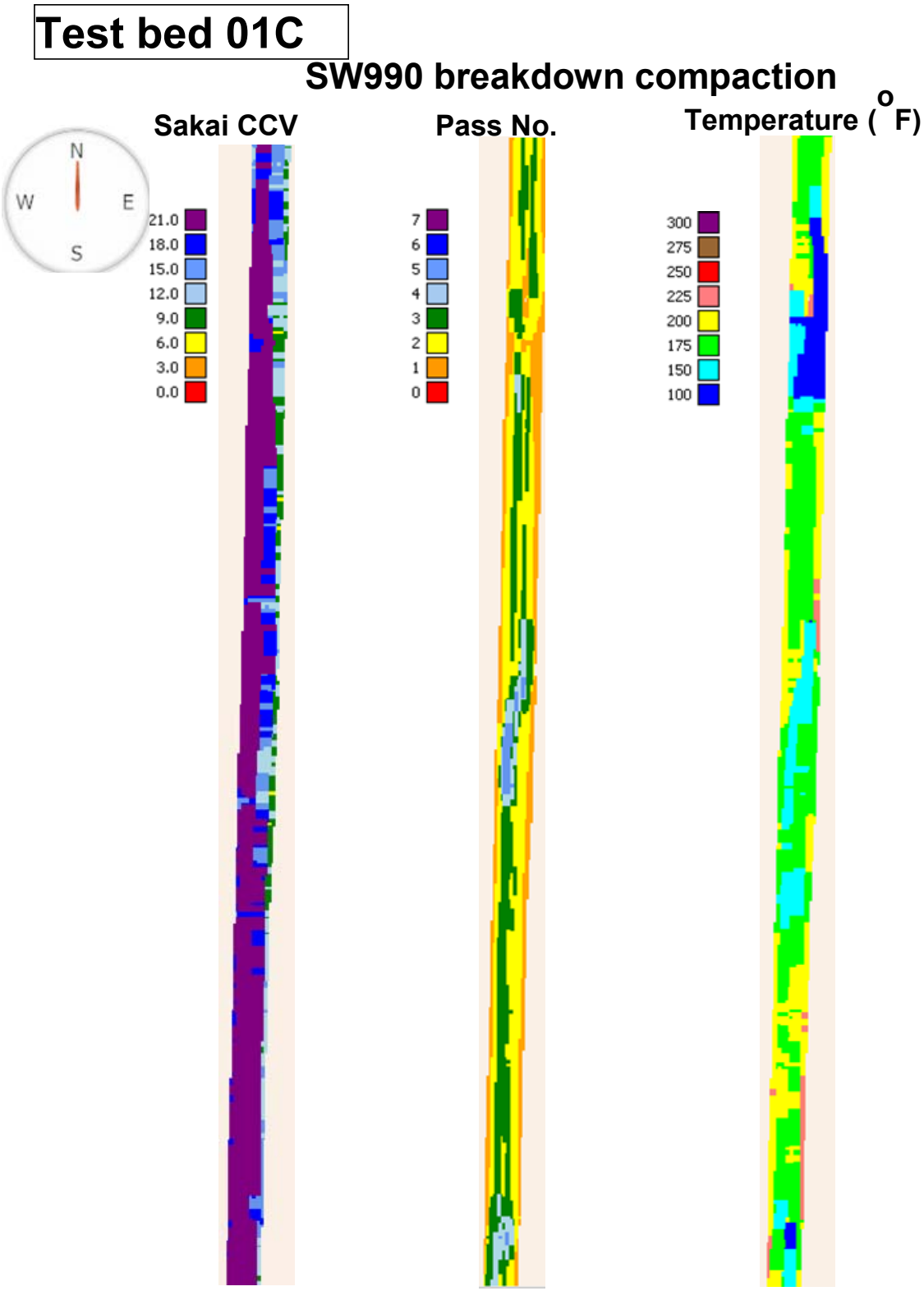

Figure 37. Sakai SW990 CCV, pass number, and surface temperatures for the breakdown compaction of the HMA intermediate course. (TB 01C)

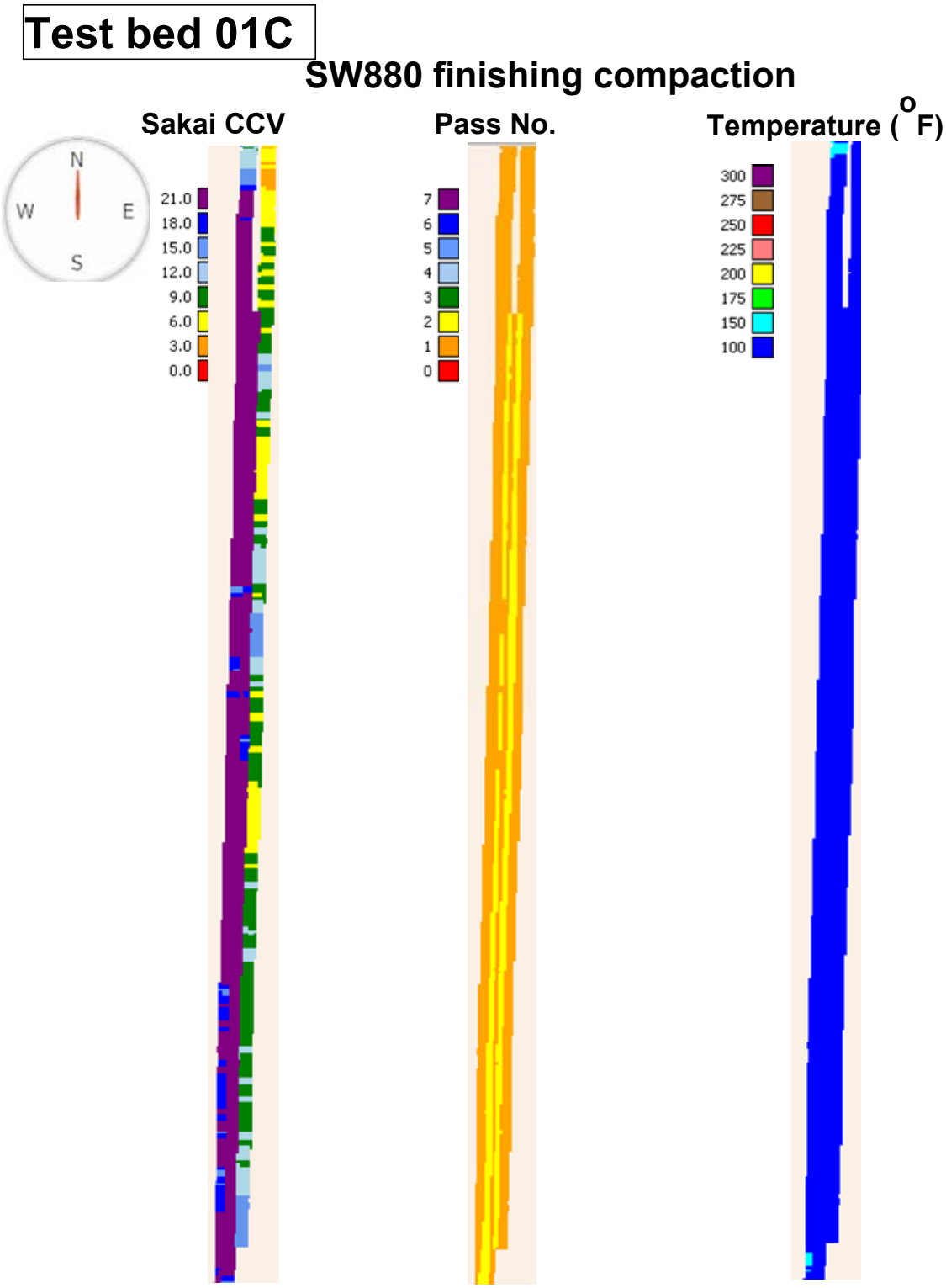

Figure 38. Sakai SW880 CCV, pass number, and surface temperatures for the finishing compaction of the HMA intermediate course. (TB 01C).

Test bed 01C_Section 1

SW990 breakdown compaction

Sakai CCV

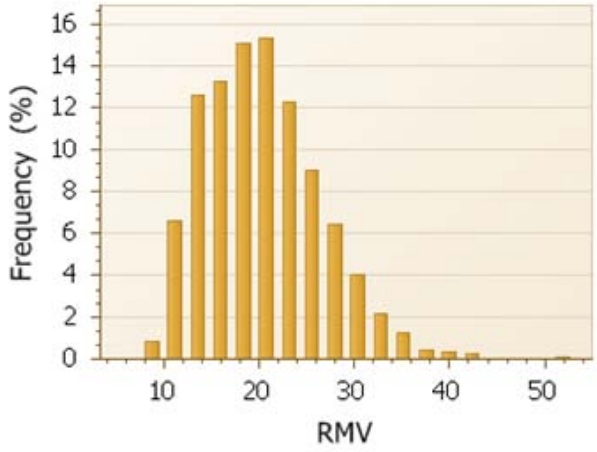

Mean: 19.15
STD: 6.10
COV: 0.32

Temperature

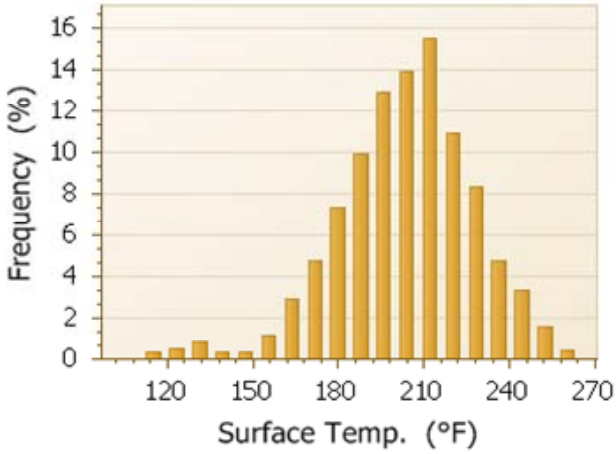

Mean: 199.4
STD: 23.59
COV: 0.12

Frequency

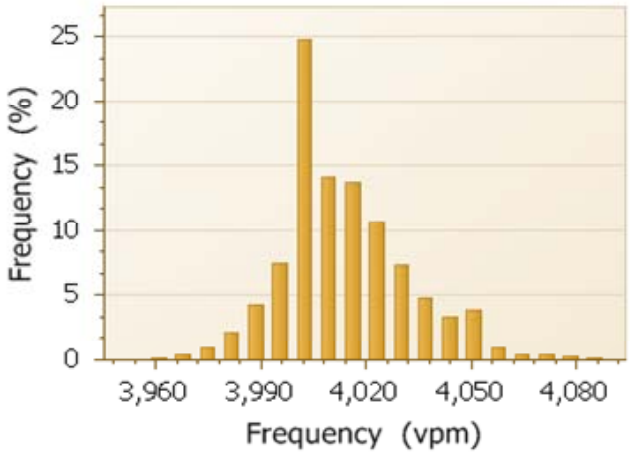

Mean: 4010
STD: 18
COV: 0.00

Figure 39. Sakai SW990 CCV, pass number, and surface temperatures for the breakdown compaction of the HMA intermediate course (TB01C - Section 1).

Test bed 01C_Section 2

SW990 breakdown compaction

Sakai CCV

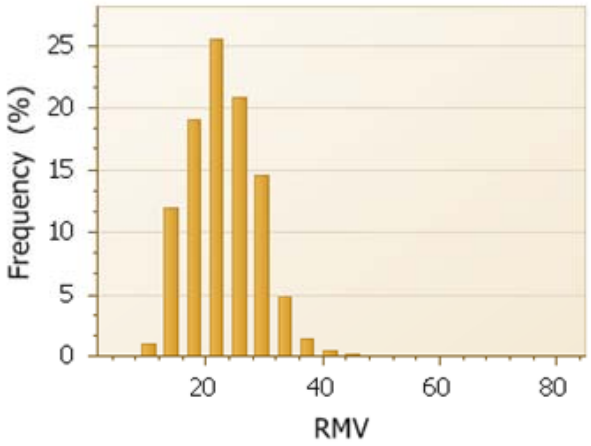

Mean: 21.07
STD: 6.04
COV: 0.29

Temperature

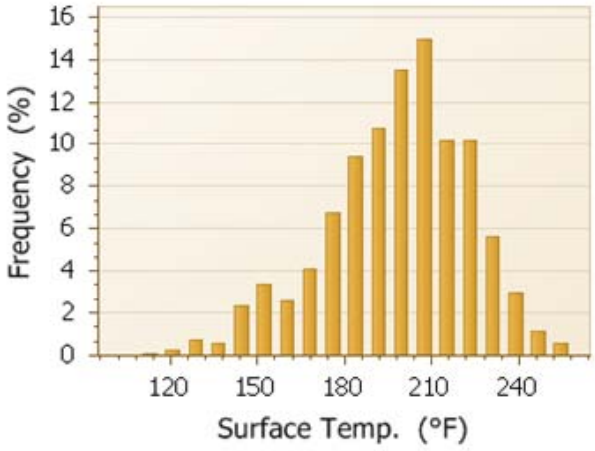

Mean: 194.4
STD: 24.50
COV: 0.13

Frequency

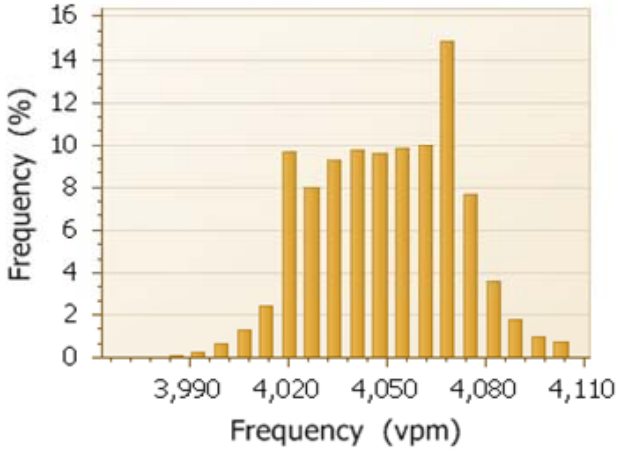

Mean: 4046
STD: 21
COV: 0.01

Figure 40. Sakai SW990 CCV, pass number, and surface temperatures for the breakdown compaction of the HMA intermediate course (TB01C - Section 2).

Test bed 01C_Section 1

Sakai CCV

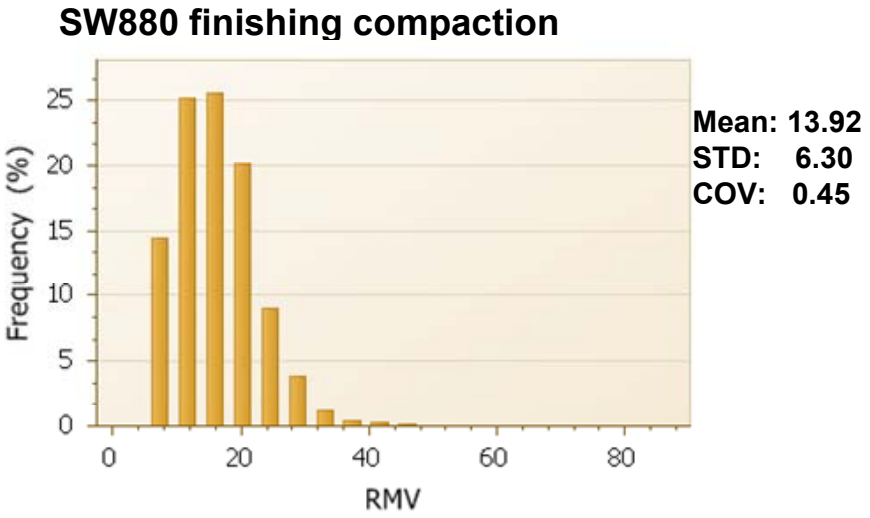

Temperature

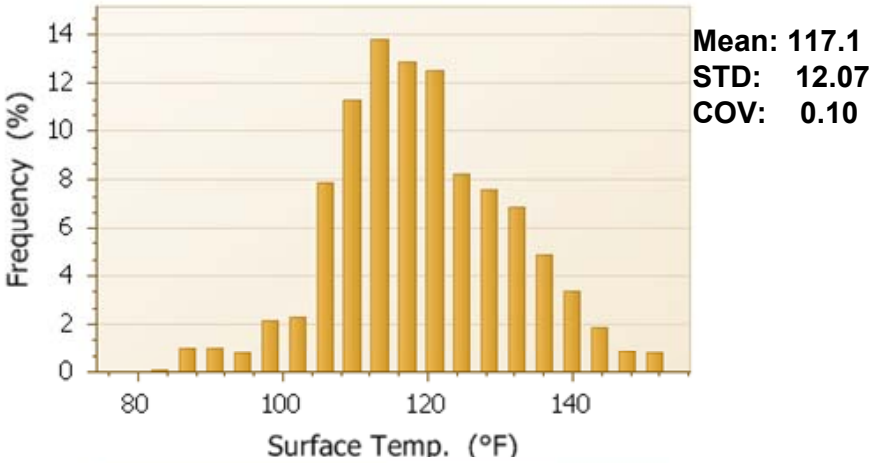

Frequency

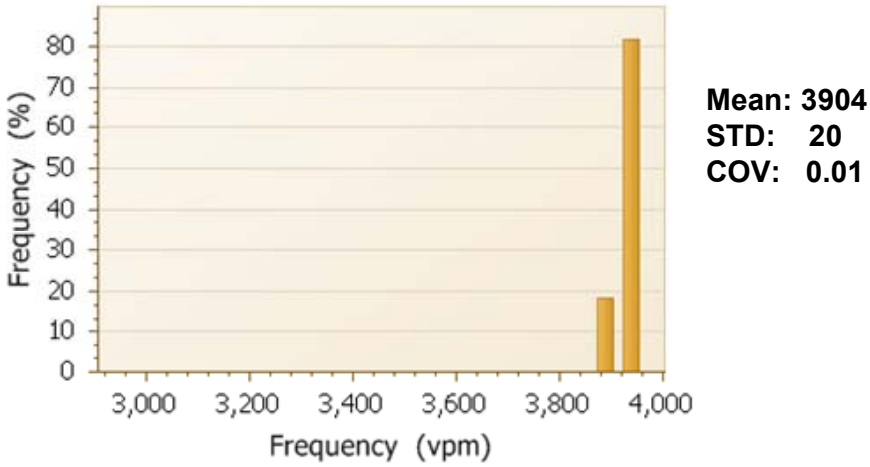

Figure 41. Sakai SW880 CCV, pass number, and surface temperatures for the finishing compaction of the HMA intermediate course (TB01C - Section 1).

Test bed 01C_Section 2

SW880 finishing compaction

Sakai CCV

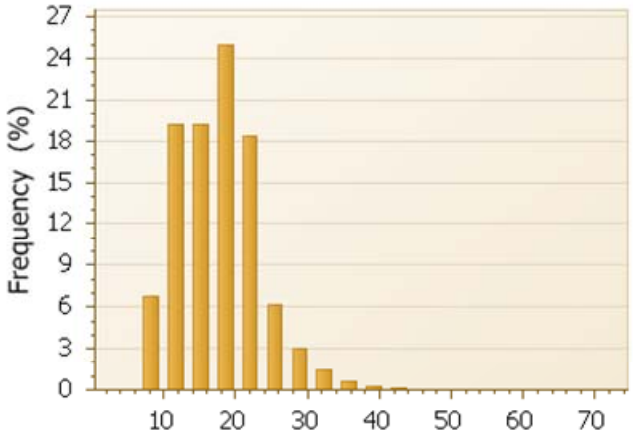

Mean: 15.96
STD: 5.85
COV: 0.37

Temperature

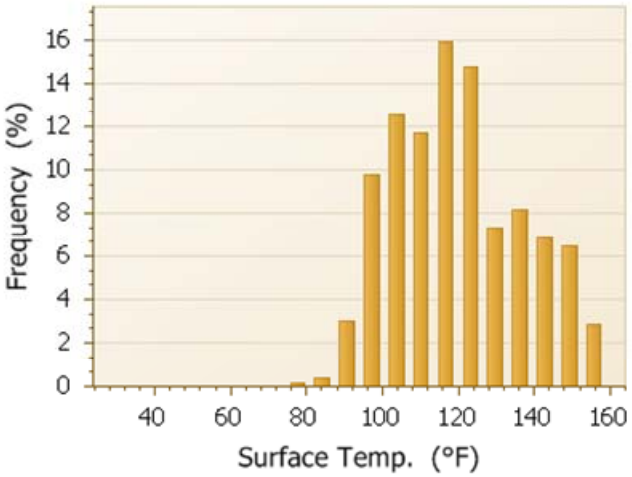

Mean: 116.8
STD: 17.09
COV: 0.15

Frequency

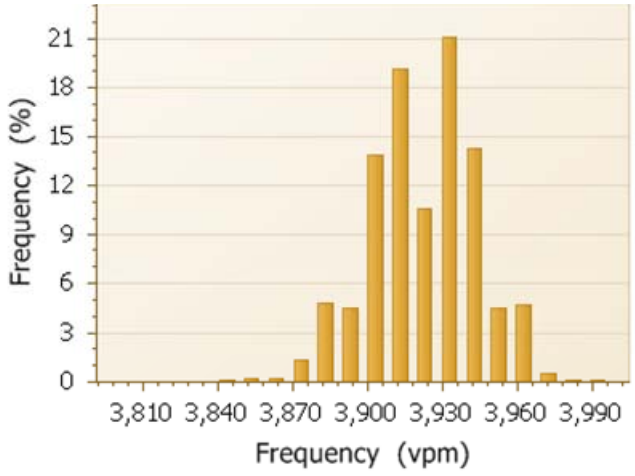

Mean: 3917
STD: 21
COV: 0.01

Figure 42. Sakai SW880 CCV, pass number, and surface temperatures for the finishing compaction of the HMA intermediate course (TB01C - Section 2).

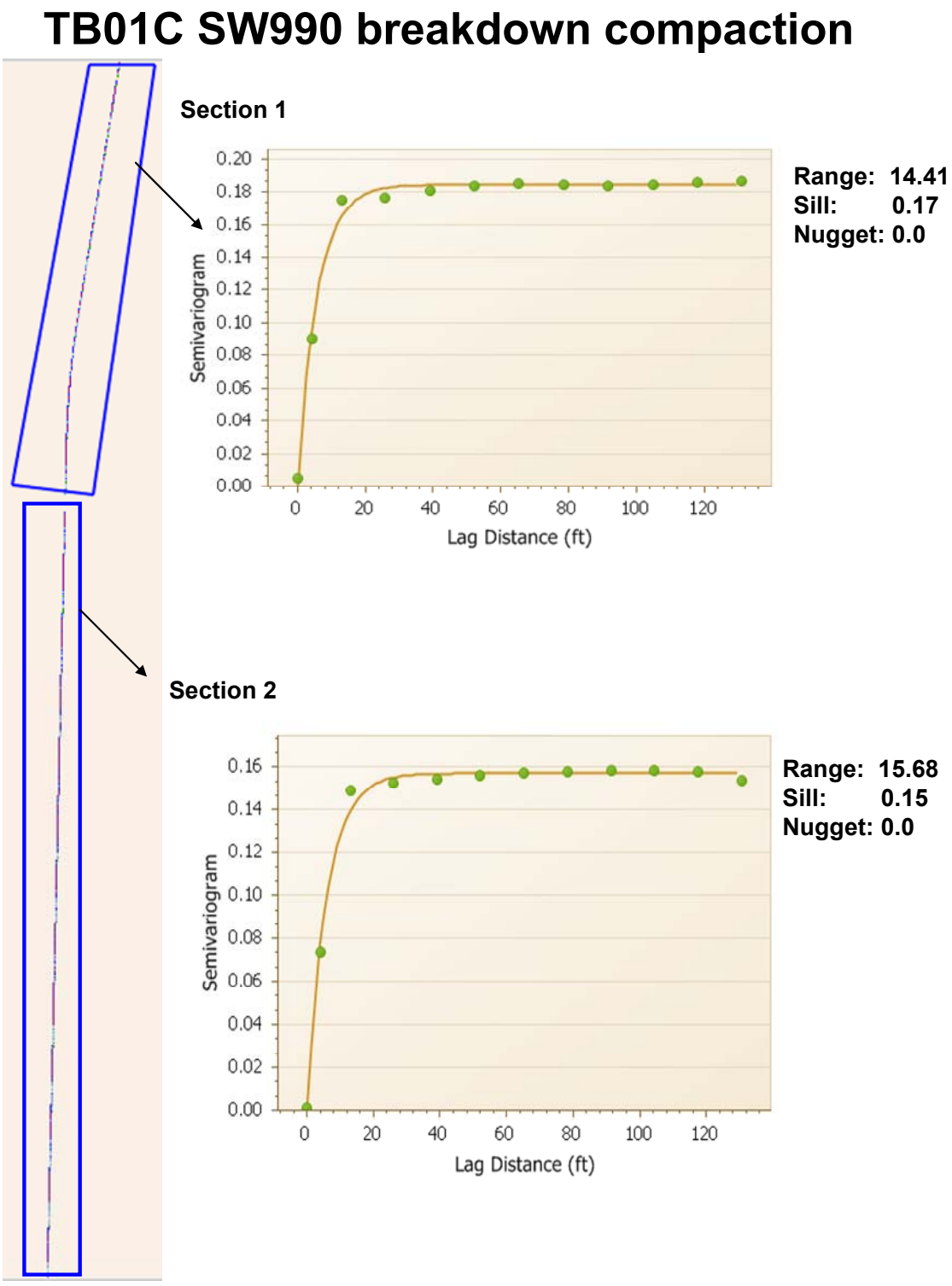

Figure 43. Semivariogram for the Sakai SW990 breakdown compaction of the HMA intermediate course. (TB 01C)

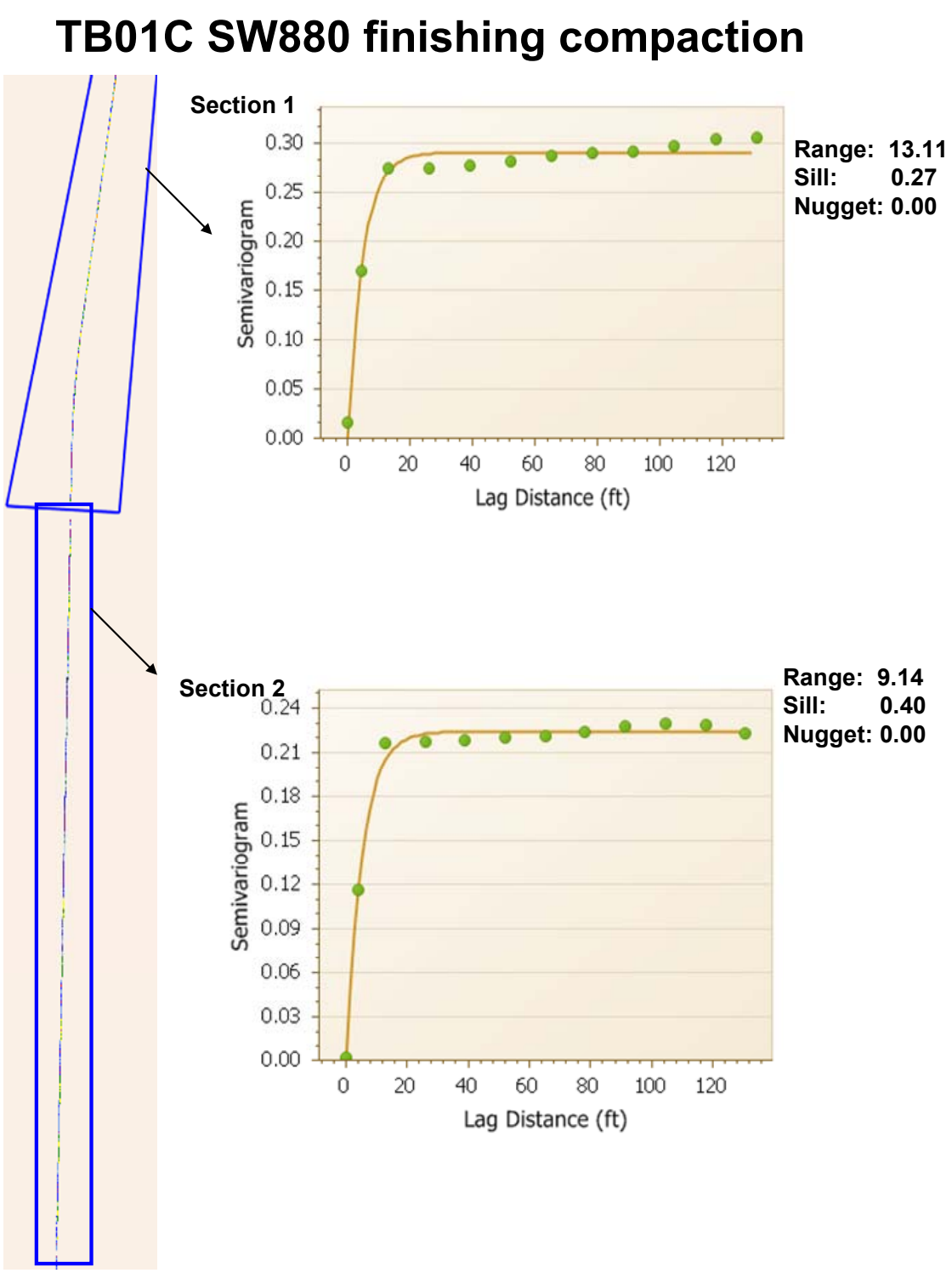

Figure 44. Semivariogram for the Sakai SW880 finishing compaction of the HMA intermediate course. (TB 01C)

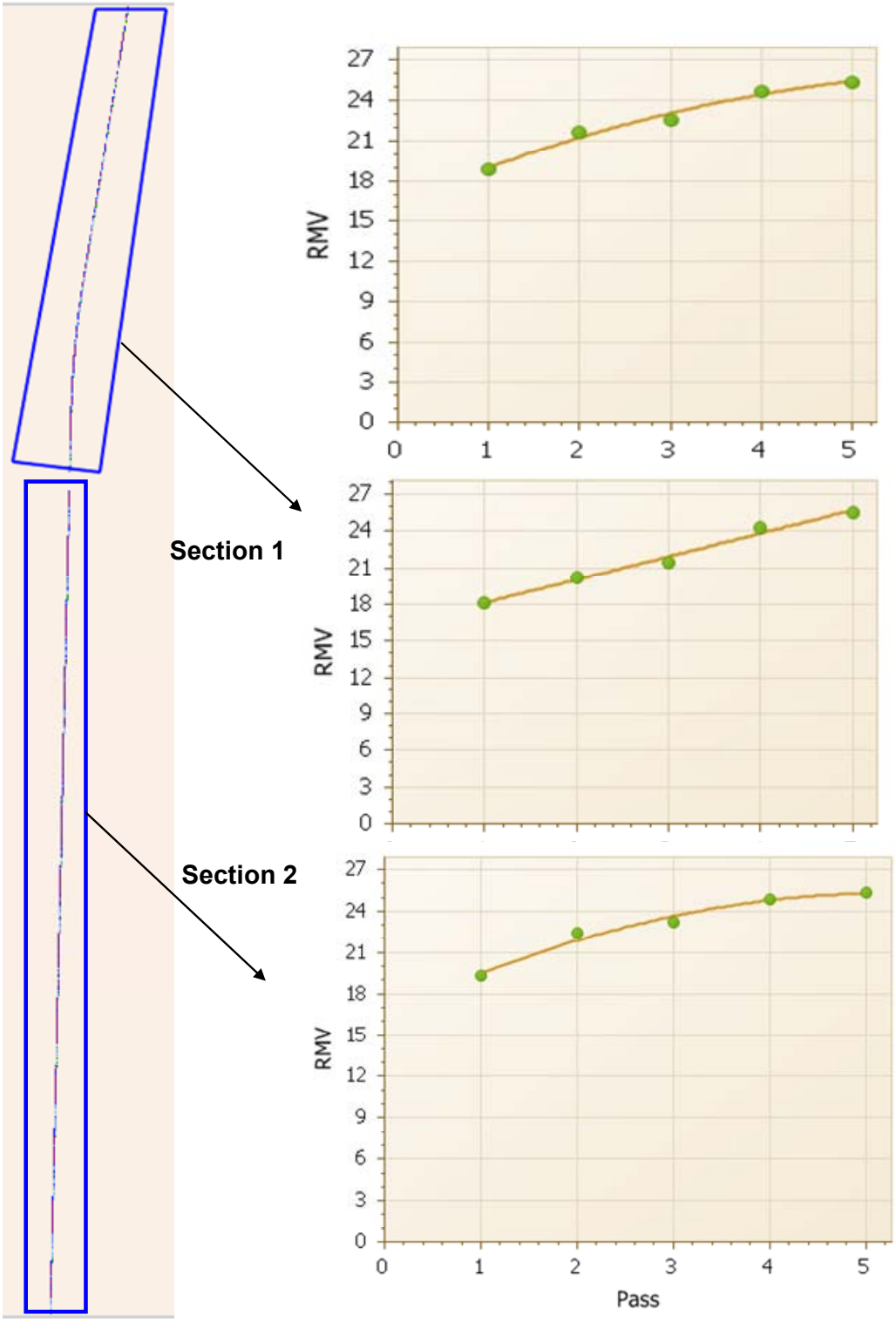

Figure 45. Compaction curves of the Sakai 990 compaction of the HMA intermediate layer(TB 01C).

TB 02M – Rubblized and crack-and-seat PCC Base on the Driving Lane

This test bed consists of mapping the rubblized and crack-and-seat PCC bases on the IH 39 SB driving lane. On May 12, the HMA surface layer was milled and removed, and then the PCC base was rubblized at the 1st section (before the bridge intersecting highway 153) and then cracked-and-seated at the 2nd section (after the bridge intersecting highway 153). The Sakai SW880 machine was used for mapping the PCC base with 1 roller pass. The Sakai machine settings were as follows: frequency of 3000 vpm; low amplitude; and speed of 3 mph; only the front drum was vibrated.

Figure 46 summarize the test location, roller machines and compaction parameters (frequency, amplitude, and speed), and the in-situ tests.

Figure 47 and Figure 48 present the maps of Sakai CCV, and roller pass number for the SW880 mapping on the rubblized and crack-and-seat PCC base, respectively.

Figure 49 and Figure 50 show the statistical histograms of the Sakai CCV and frequency for the SW880 mapping on the rubblized and crack-and-seat PCC base, respectively. The mean values of CCVs are 14.24 and 15.45 for the rubblized and crack-and-seat PCC base, respectively. The crack-and-seat PCC base has a little bit higher CCV than the rubblized PCC base, which could be due to its higher integrity of the PCC slab pieces.

Test bed 02M (5/12/2010)

Description
This test bed consists of mapping the rubblized and crack-and-seat PCC bases on the IH 39 SB driving lane. The surface HMA was milled and removed, then the PCC base was rubblized or cracked-and-seated. The Sakai SW880 double-drum IC roller was used to mapping the PCC base. The purpose is to evaluate the condition of the existing support prior to the asphalt construction.

Sakai SW880 Machine setting:

Vibration frequency was 3000 vpm; the low amplitude was used; the speed was set about 3 mph; only the front drum was vibrated.

Figure 46. Rubblization of the PCC base, Sakai IC mapping, and in-situ testing (TB 02M)

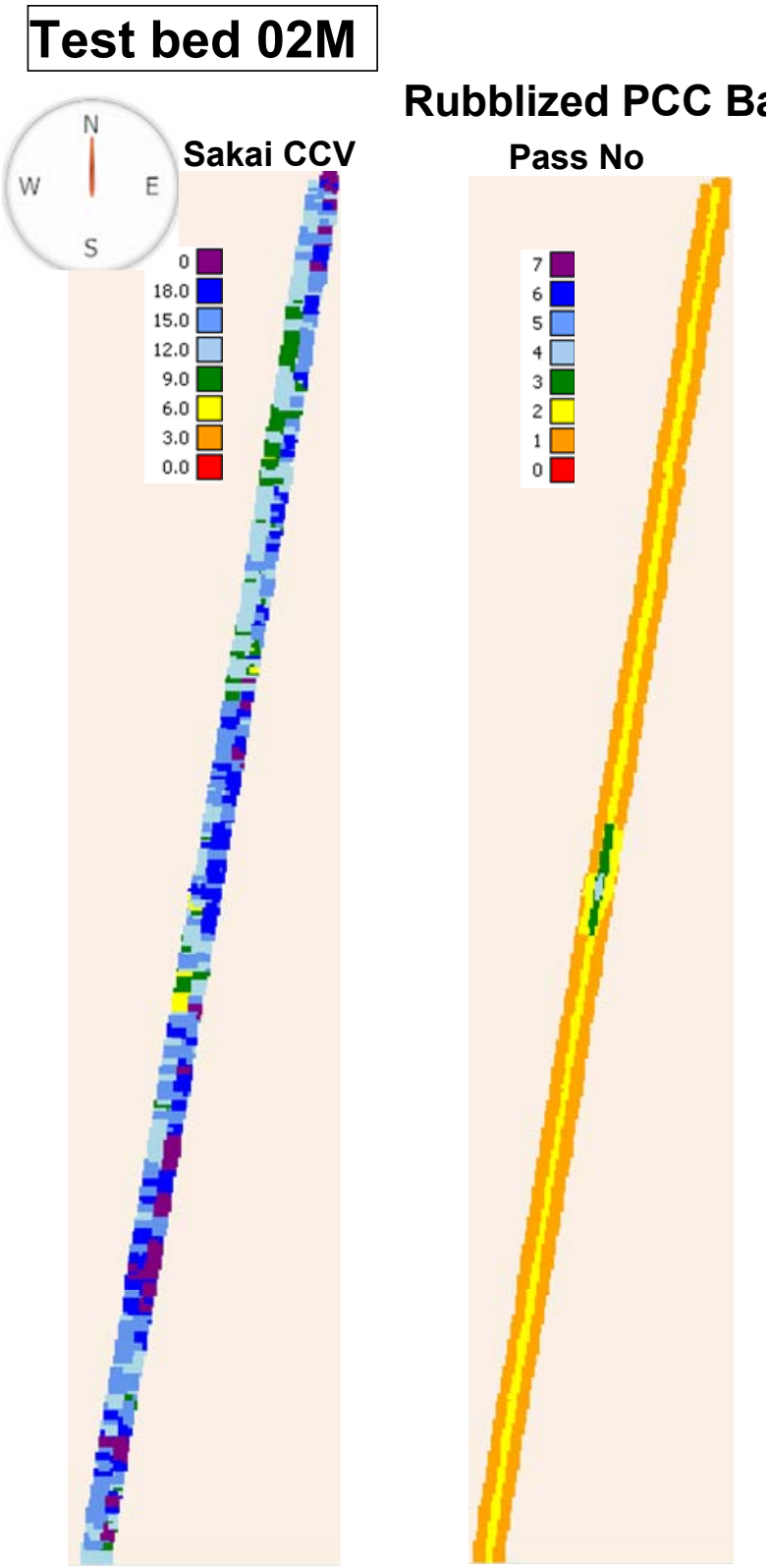

Figure 47. Sakai SW880 CCV and pass number for mapping TB01M rubblized PCC base.

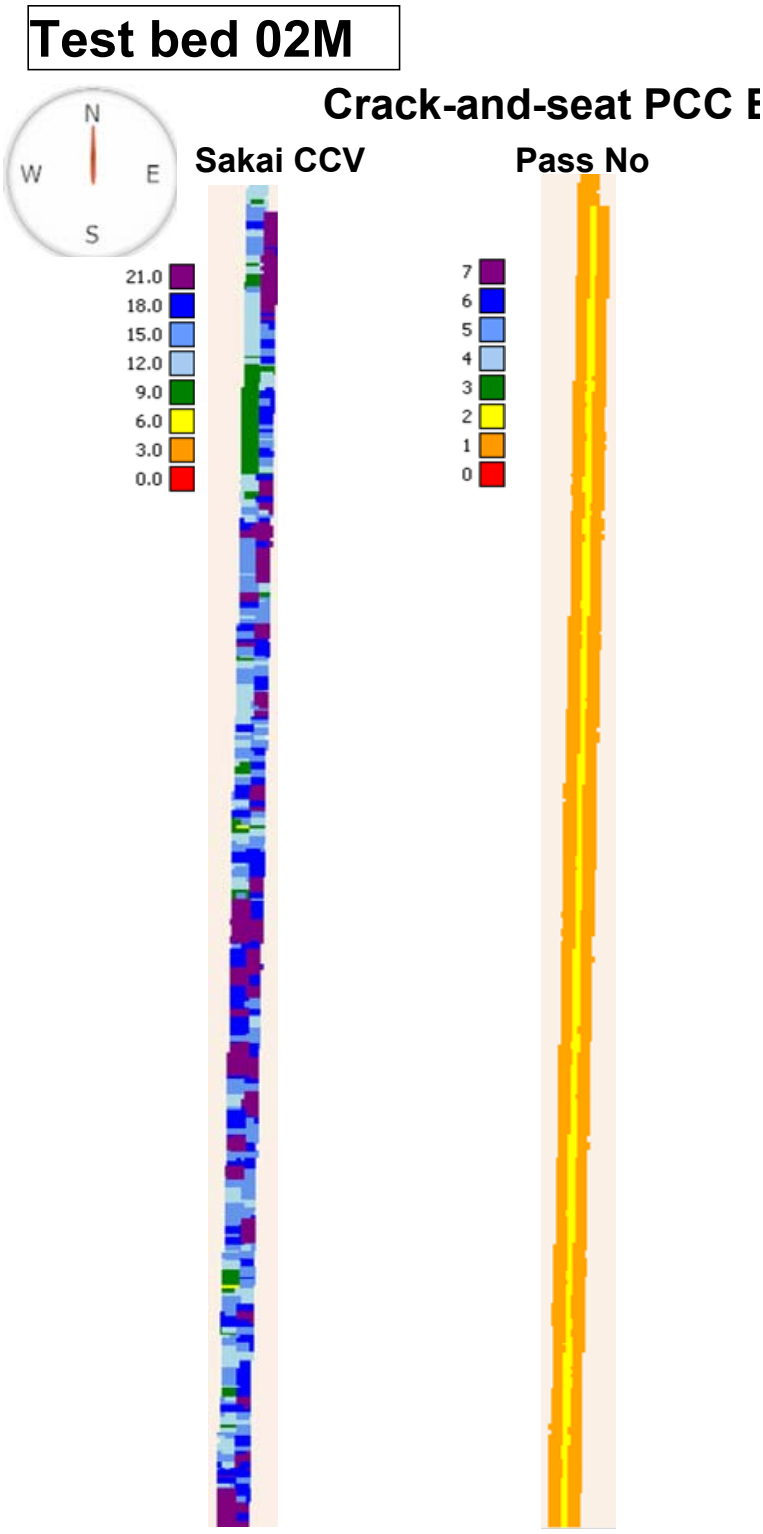

Figure 48. Sakai SW880 CCV and pass numbers of mapping the crack-and-seat PCC base. (TB 02M)

Test bed 02M

Rubblized PCC Base

Sakai CCV

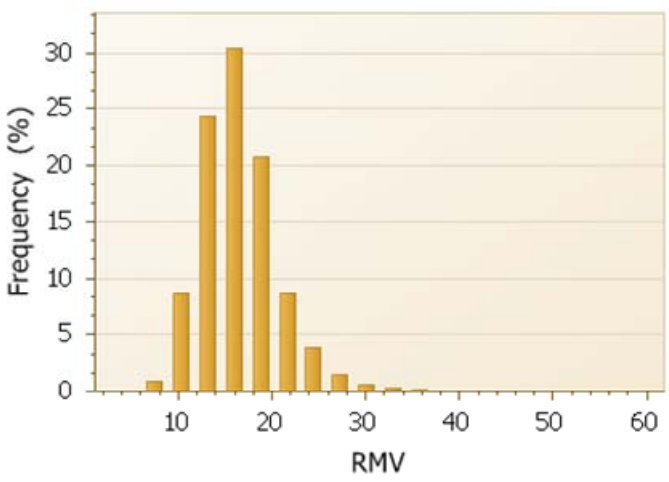

Frequency

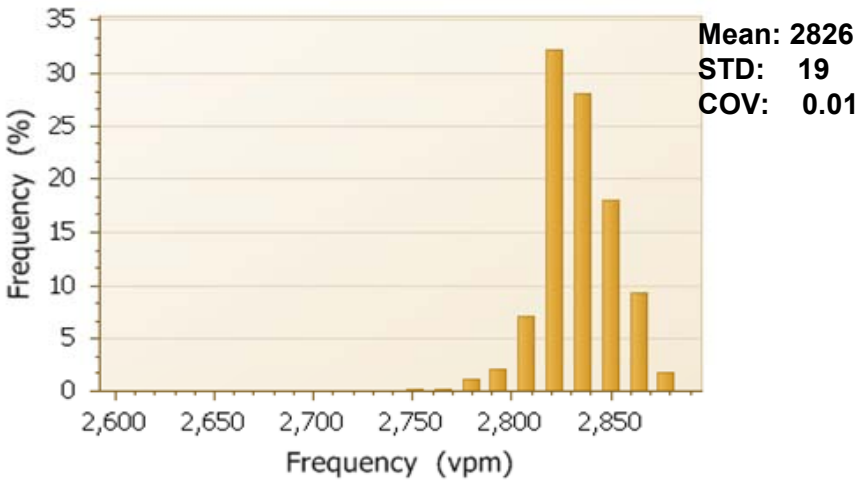

Figure 49. Sakai CCV and frequency histograms for mapping rubblized PCC base. (TB 02M – Section 1)

Test bed 02M

Crack-and-seat PCC Base

Sakai CCV

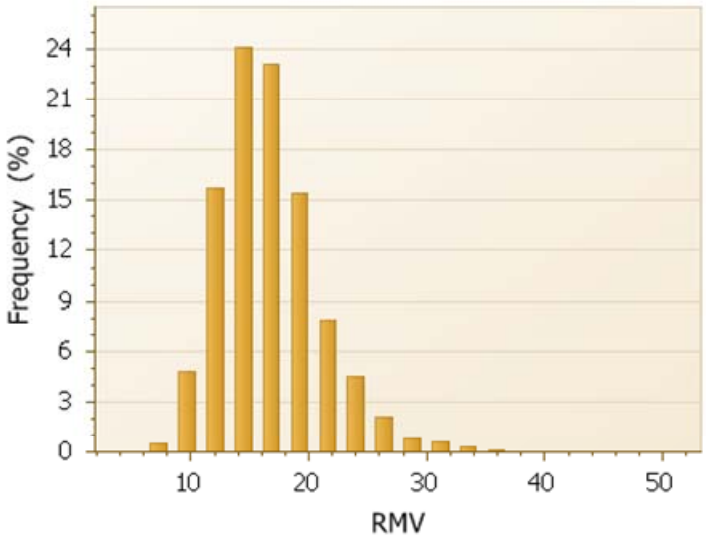

Mean: 15. 49
STD: 4.31
COV: 0.28

Frequency

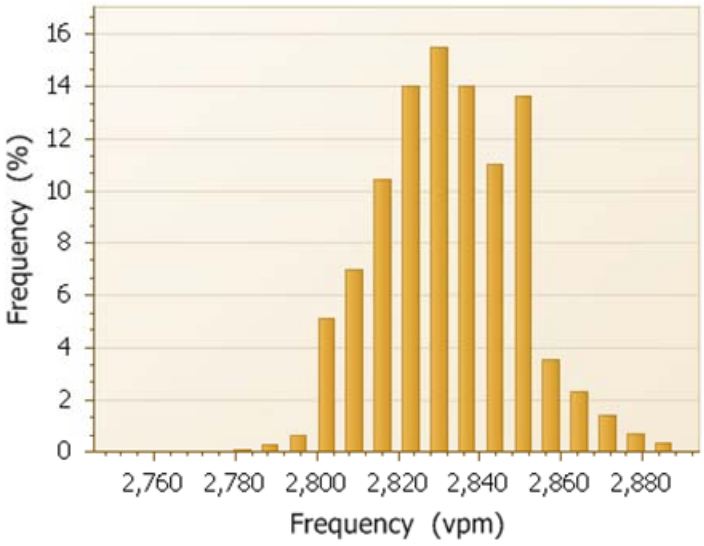

Mean: 2829
STD: 17
COV: 0.01

Figure 50. Sakai CCV and frequency histograms for mapping crack-and-seat PCC base. (TB02M – Section 2)

TB 02B – HMA Base Layer on the Driving Lane

This test bed consists of paving the HMA base on the rubblized and crack-and-seat PCC bases using the Sakai double-drum IC roller on May 12. The Sakai SW990 machine was used as the intermediate roller with 3 passes, and the Sakai SW880 was used as the finishing roller with 1-2 passes. The Sakai machine settings were as follows: frequency of 3000 vpm; low amplitude; and speed of 3 mph.

Figure 51 summarize the test location, roller machines and compaction parameters (frequency, amplitude, and speed), and the in-situ tests.

Figure 52 and Figure 53 present the maps of Sakai CCV, roller pass number, and HMA surface temperature of TB02B resulted from the SW990 intermediate and SW880 finishing compaction, respectively.

Figure 54 and Figure 55 show the statistical histograms of the Sakai CCV, HMA surface temperature, and frequency for the 1st and 2nd sections HMA base under the SW990 intermediate compaction, respectively. The mean CCVs of the 1st and 2nd section of HMA base under the SW990 intermediate compaction are 13.58 and 15.28, respectively.

Figure 56 and Figure 57 show the statistical histograms of the Sakai CCV, HMA surface temperature, and frequency for the 1st and 2nd section of HMA base under the SW880 finishing compaction, respectively. The mean CCVs of the 1st and 2nd section of HMA base under the SW880 finishing compaction are 14.28 and 12.11, respectively. The CCVs of the 2nd section paved on the crack-and-seat base is lower than that of the 2nd section paved on the rubblized PCC base, which could be due to the improved integrity and interlock of slab pieces after repeated compaction on the rubblized PCC base. It is noted that obviously HMA temperatures under SW990 intermediate compaction is higher than that under the SW880 finishing compaction.

Figure 58 and Figure 59 display the semi-variograms of the HMA base under the Sakai SW990 intermediate and SW880 finishing compaction, respectively. Results show that for the SW990 breakdown compaction section 2 has a larger range yet lower sill value than section 1, indicating its better uniformity.

Figure 60 presents the compaction curves of the HMA base layer under the SW990 breakdown compaction. It shows that the roller pass number doesn't have significant impact on the CCV, but it seems that the optimum CCV is achieved under the roller pass of 4.

Test bed 02B (5/12/2010)

Description

This test bed consists of compacting the HMA base layer on the rubblized and crack-and-seat PCC bases on the IH 39 SB driving lane. The Sakai SW990 double-drum IC roller was used as the intermediate roller and the SW880 machine was used as finishing roller. The in-situ FWD and LWDmeasurements were performed.

Sakai Machine Settings:

Vibration frequency was 3000 vpm; the low amplitude was used; the speed was set about 3 mph.

Figure 51. Paving/Compaction and in-situ tests of the HMA base Course (TB 02B).

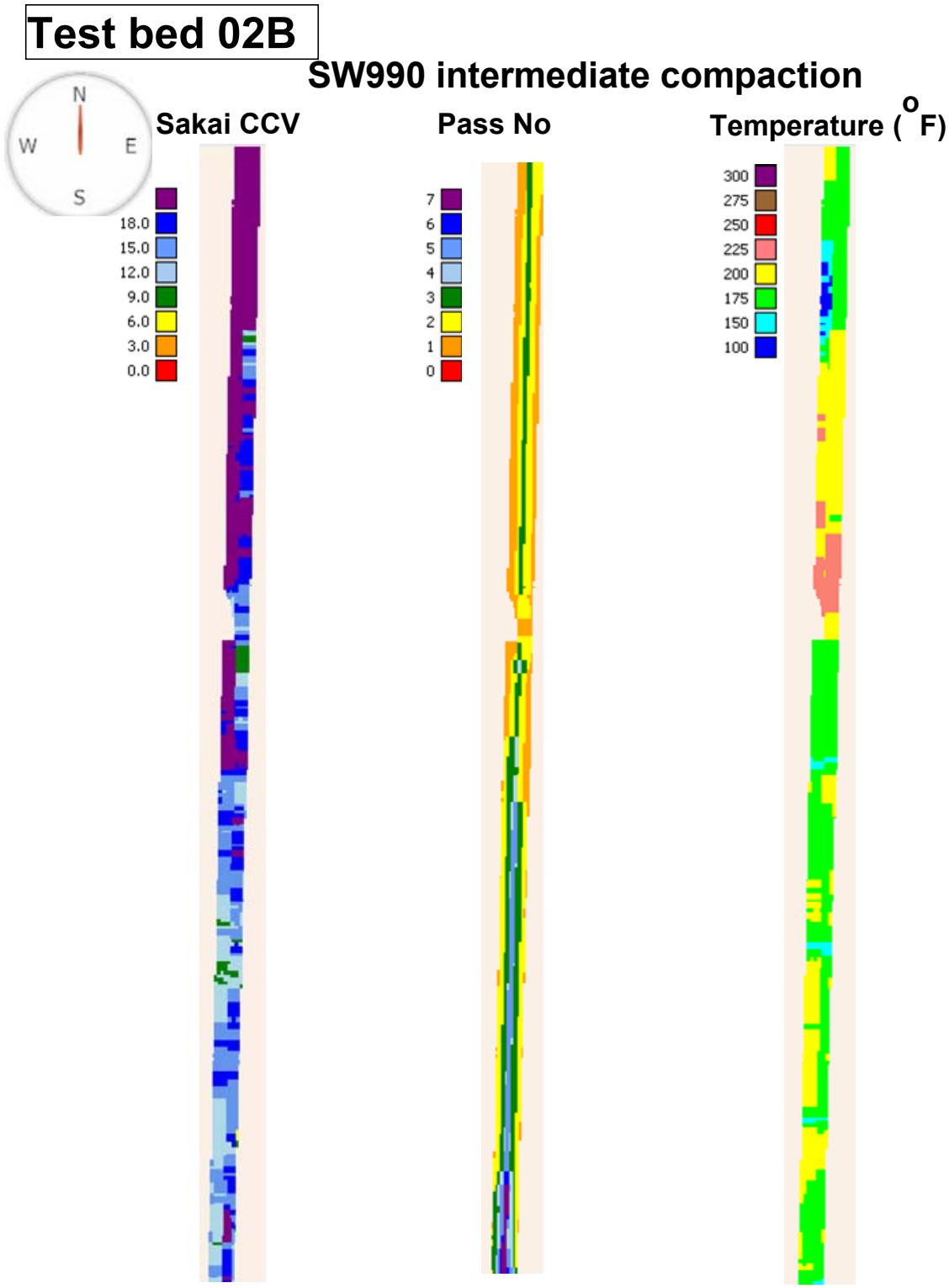

Figure 52. Sakai CCV, pass number, and surface temperatures for the Sakai SW990 intermediate compaction of the HMA base course. (TB 02B)

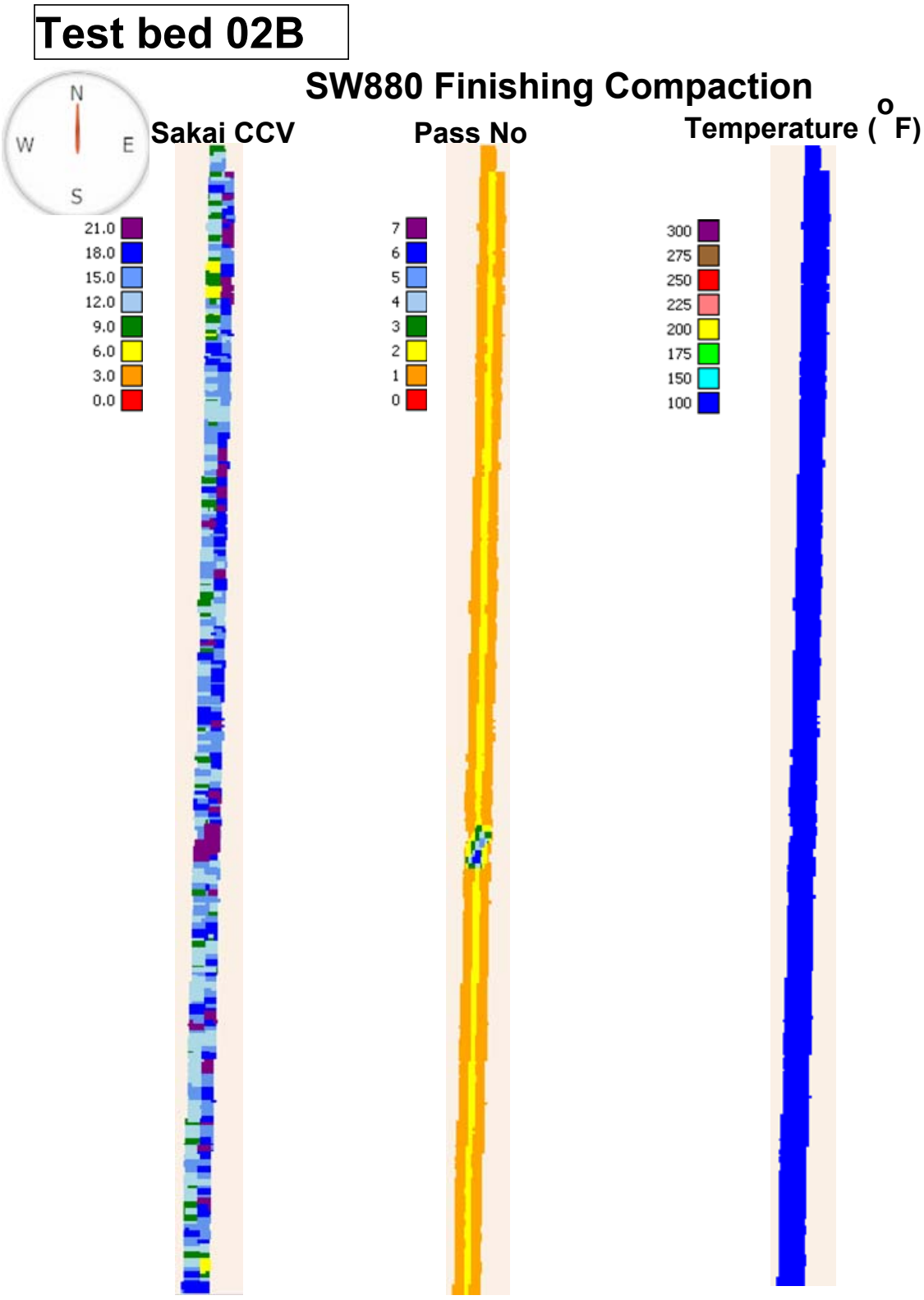

Figure 53. Sakai CCV, pass number, and surface temperatures for the Sakai SW880 finishing compaction of the HMA base course. (TB 02B)

Test bed 02B_section 1

SW990 intermediate compaction

Sakai CCV

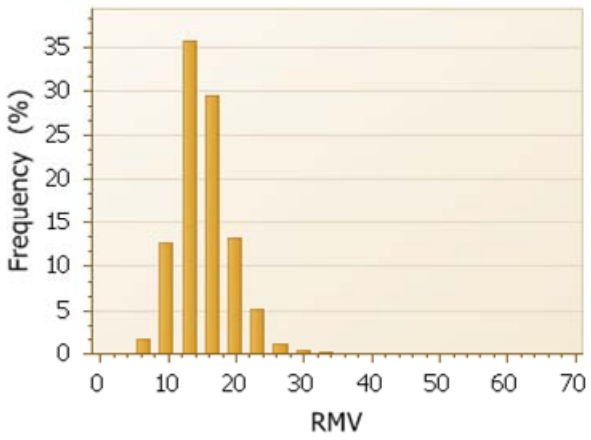

Mean: 13. 58
STD: 4.21
COV: 0.31

Temperature

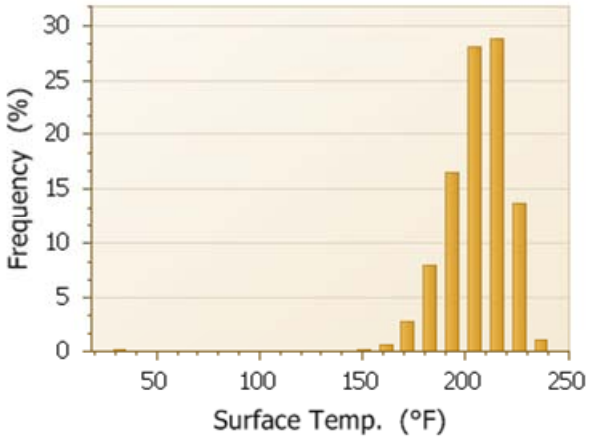

Mean:200.3
STD: 15.81
COV: 0.08

Frequency

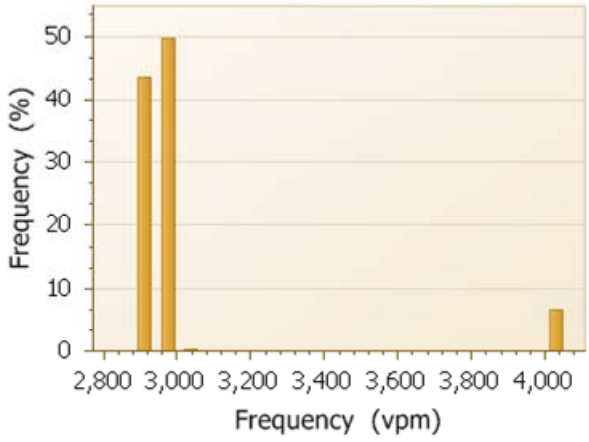

Mean: 2990
STD: 277
COV: 0.09

Figure 54. Sakai CCV, surface temperatures, and frequency histograms for the Sakai SW990 intermediate compaction of the HMA base course (TB 02B – Section 1).

Test bed 02B_section 2

SW990 intermediate compaction

Sakai CCV

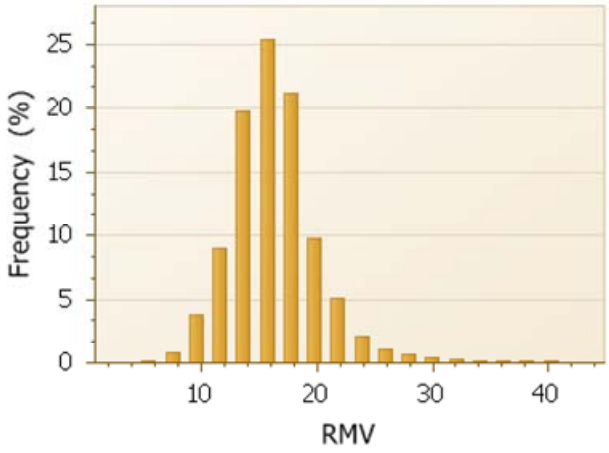

Mean: 15. 28
STD: 3.92
COV: 0.26

Temperature

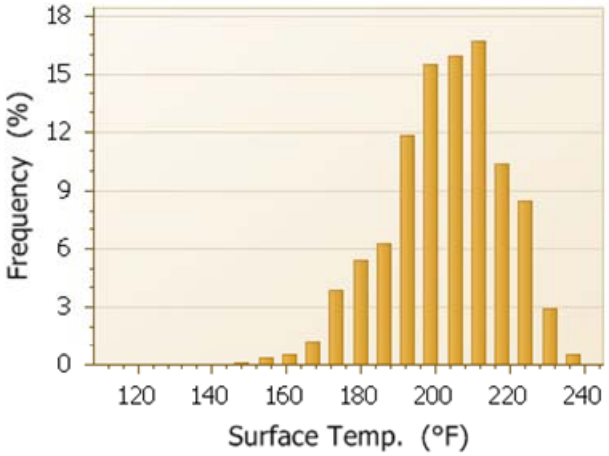

Mean:199.7
STD: 15.33
COV: 0.08

Frequency

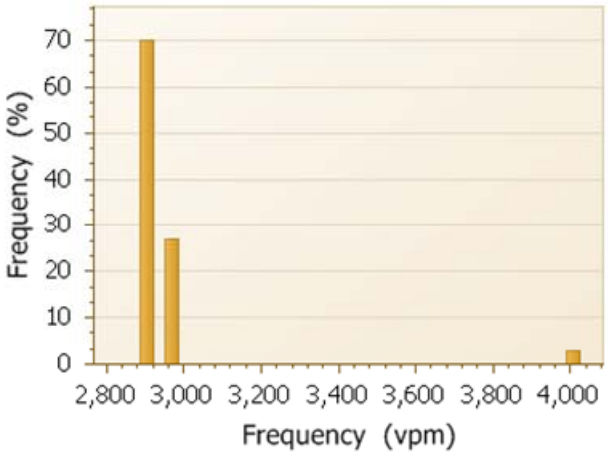

Mean: 2930
STD: 288
COV: 0.06

Figure 55. Sakai CCV, surface temperatures, and frequency histograms for the Sakai SW990 intermediate compaction of the HMA base course (TB 02B – Section 2).

Test bed 02B_section 1

SW880 finishing compaction

Sakai CCV

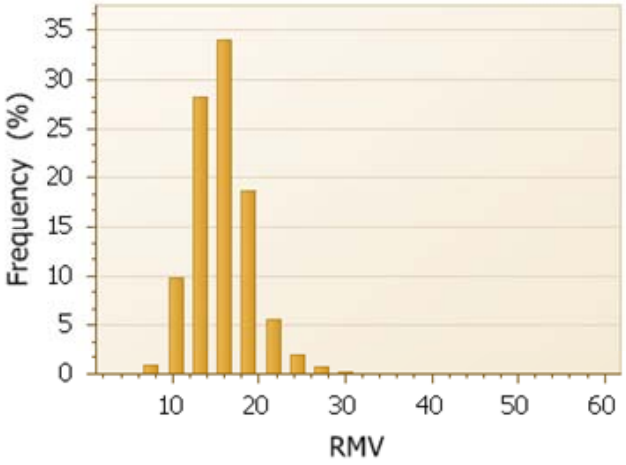

Mean: 14.28
STD: 3.58
COV: 0.25

Frequency

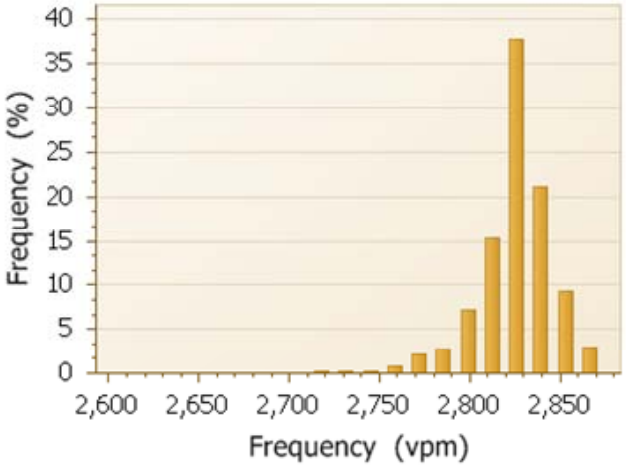

Mean: 2819
STD: 22
COV: 0.01

Figure 56. Sakai CCV, surface temperatures, and frequency histograms for the Sakai SW880 finishing compaction of the HMA base course (TB 02B – Section 1).

Test bed 02B_section 2

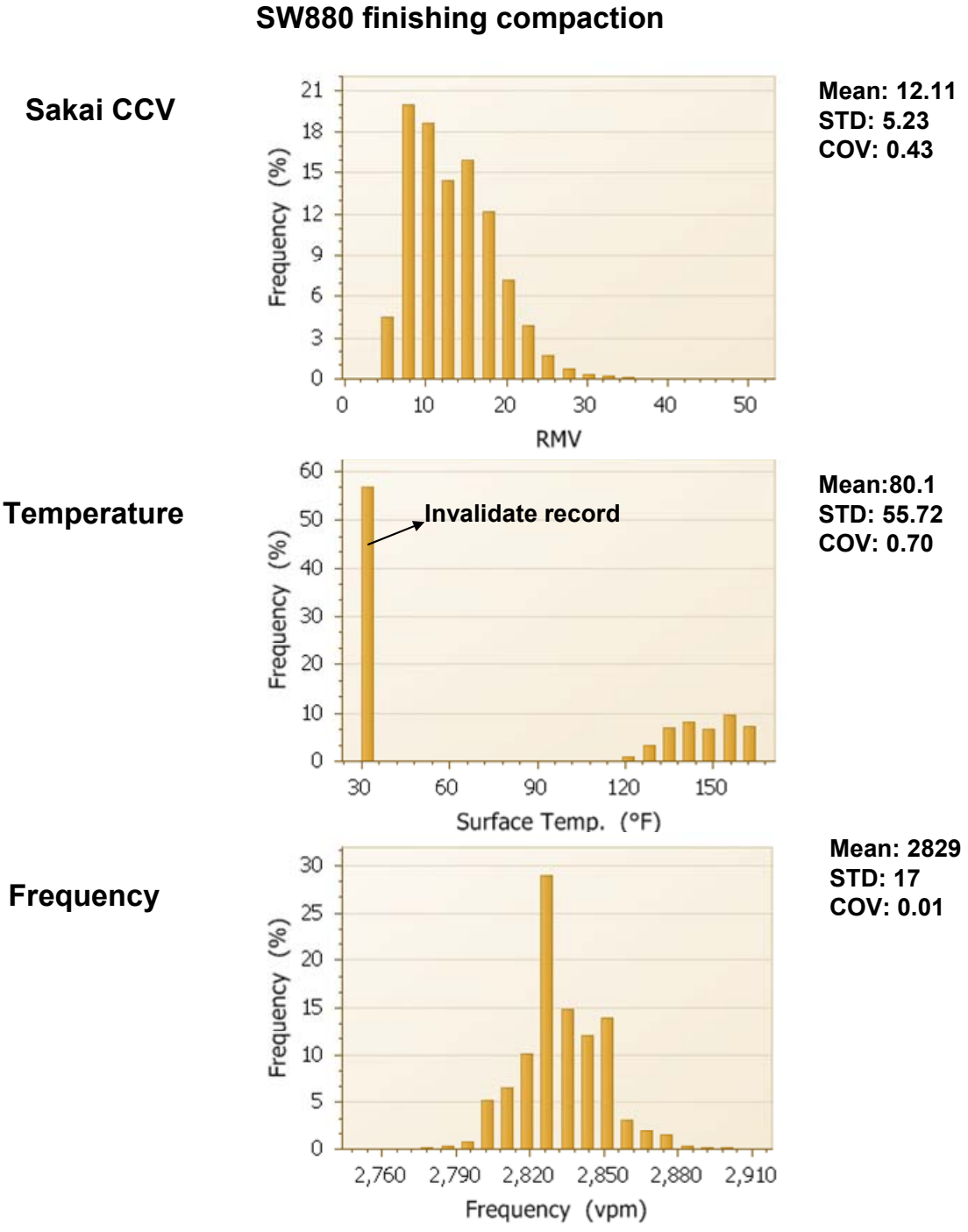

Figure 57. Sakai CCV, surface temperatures, and frequency histograms for the Sakai SW880 finishing compaction of the HMA base course (TB 02B – Section 2).

TB01B SW990 intermediate compaction

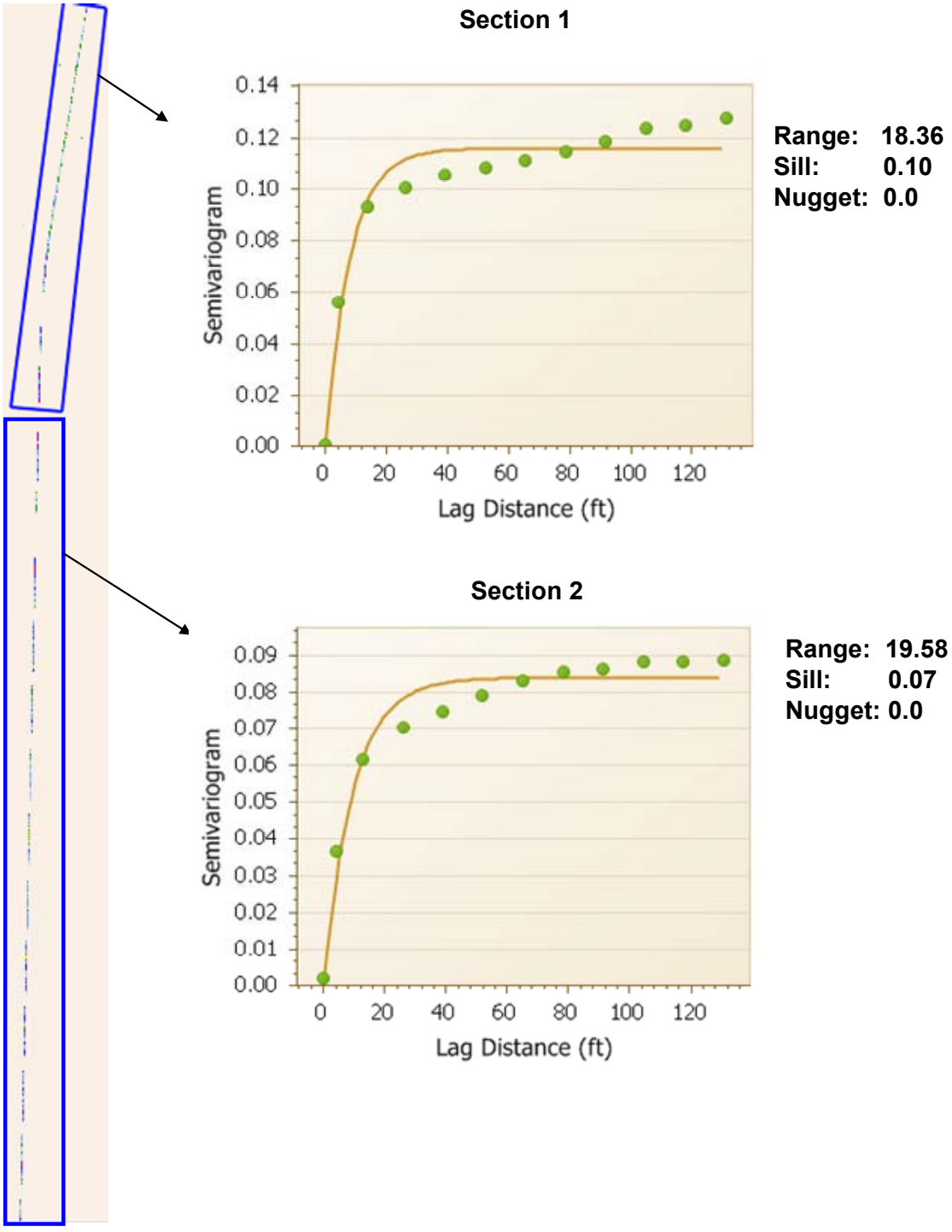

Figure 58. Semivariogram for the Sakai SW990 intermediate compaction of the HMA base course (TB 02B).

TB02B SW880 finishing compaction

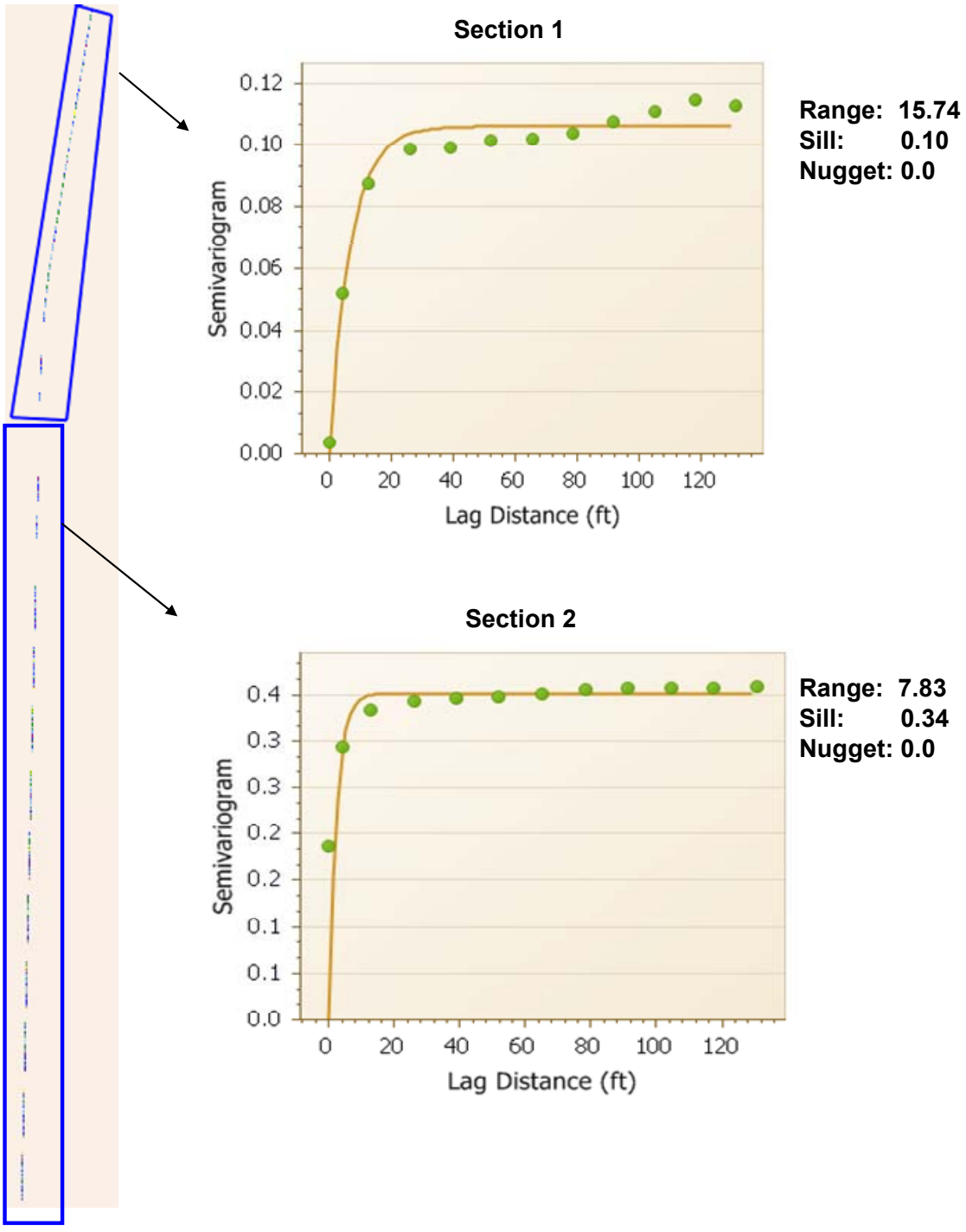

Figure 59. Semivariogram for the Sakai SW880 finishing compaction of the HMA base course (TB 02B).

TB01B SW990 intermediate compaction

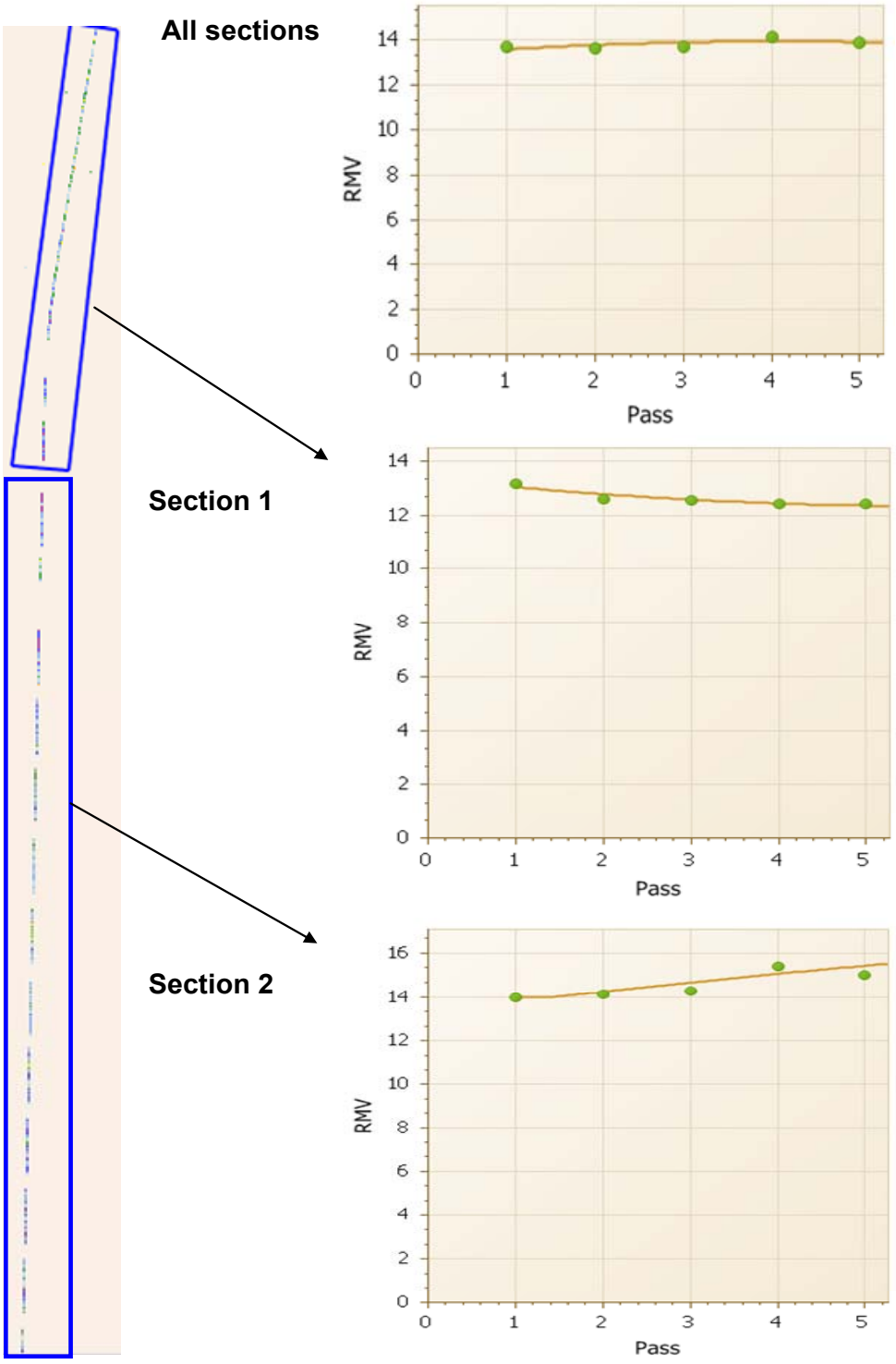

Figure 60. Compaction curves for the Sakai SW990 intermediate compaction of the HMA base course (TB 02B).

TB 02C – HMA 2nd Lift Intermediate Layer on the Driving Lane

This test bed consists of paving the 2nd lift HMA intermediate layer on the HMA bases using the Sakai double-drum IC rollers on May 12 to 13, and night paving was successfully implemented. The Sakai SW990 machine was used as the breakdown roller with 3 passes, and the Sakai SW880 was used as the finishing roller with 1-2 passes. The Sakai machine settings were as follows: frequency of 4000 vpm for SW990 breakdown compaction, 3000 and 4000 vpm for SW880 finishing compaction; low amplitude; and speed of 3 mph.

Figure 61 summarize the test location, roller machines and compaction parameters (frequency, amplitude, and speed), and the in-situ tests.

Figure 62 and Figure 63 present the maps of Sakai CCV, roller pass number, and HMA surface temperature of TB02C resulted from the SW990 breakdown and SW880 finishing compaction, respectively.

Figure 64 and Figure 65 show the statistical histograms of the Sakai CCV, HMA surface temperature, and frequency for the 1st and 2nd sections under the SW990 breakdown compaction, respectively. The mean CCVs of the 1st and 2nd section are 23.13 and 24.35, respectively.

Figure 66 and Figure 67 show the statistical histograms of the Sakai CCV, HMA surface temperature, and frequency for the 1st and 2nd sections under the SW880 intermediate compaction, respectively. The mean CCVs of the 1st and 2nd section are 12.55 and 16.84, respectively. The CCVs of the 2nd section is higher than that of the 1st section, one of the important reasons would be due to its higher vibration frequency (4000 vpm compared to 3000 vpm used in the 1st section). The same as discussed before, HMA temperatures under SW990 breakdown compaction is significantly higher than that under the SW880 finishing compaction.

Figure 68 and Figure 69 display the semi-variograms of the HMA base under the Sakai SW990 breakdown and SW880 finishing compaction, respectively. Results show that for section 1 the uniformity of the 2nd lift HMA has improved in comparison with that of the HMA base, with a longer range while lower sill value.

Figure 70 presents the compaction curves of the HMA 2nd lift intermediate layer under the SW990 breakdown compaction. It shows that CCV increases first and then decreases with increasing roller pass number, and an optimum CCV is achieved at the roller pass of 4.

Test bed 02C (5/12/2010)

Description

This test bed consists of compacting the 2nd lift HMA intermediate layer on the HMA base on the IH 39 SB driving lane. Sakai SW990 was used as the breakdown roller and SW880 was used as the finishing roller. The in-situ FWD, LWD, and NG density measurements were performed.

Sakai Machine Setting:

Vibration frequency was 4000 vpm for SW990, 3000 and 4000 vpm for SW880; the low amplitude was used; the speed was set about 3 mph.

Figure 61. Paving/Compaction and in-situ tests of the HMA intermediate layer (TB 02C)

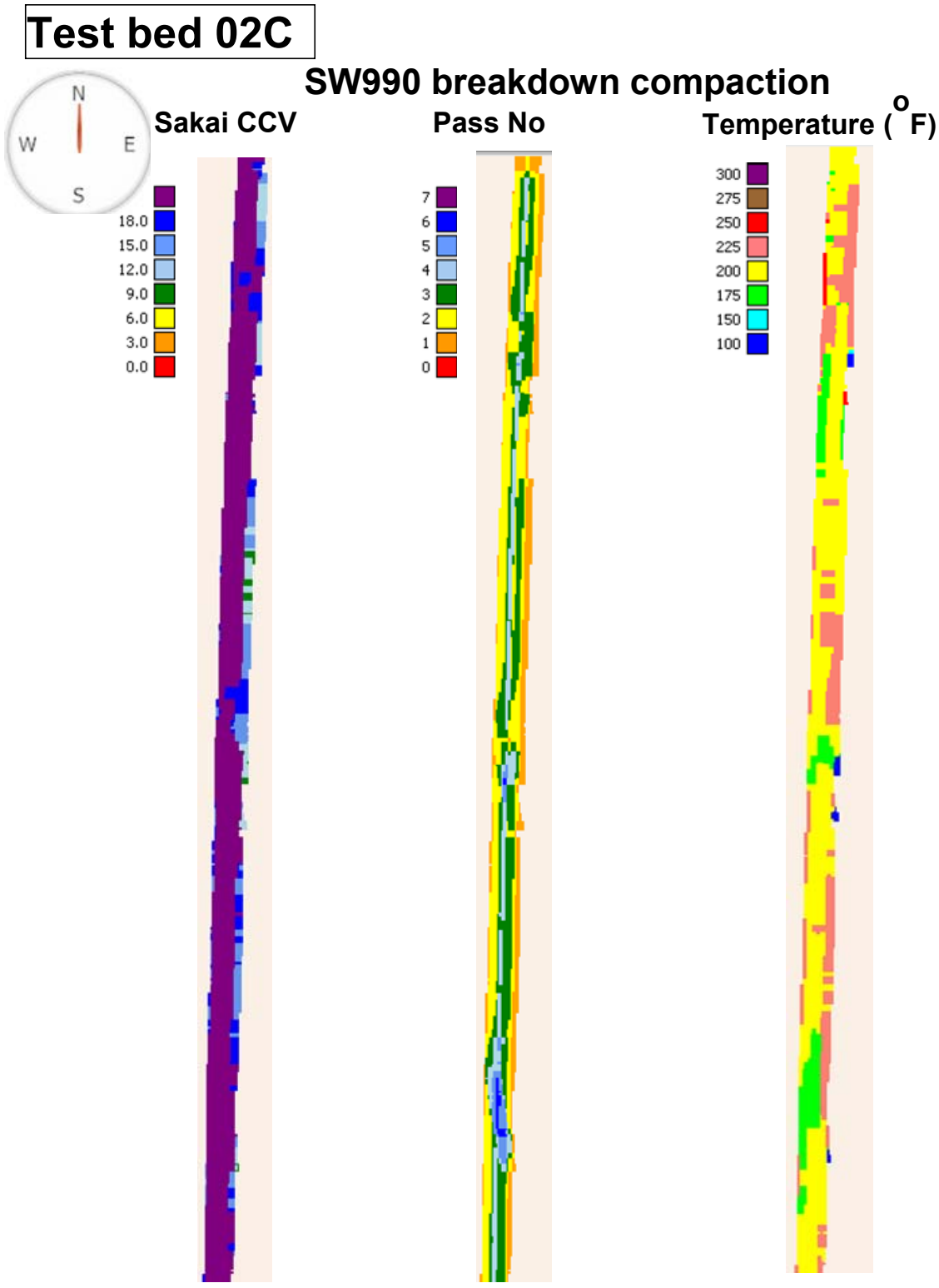

Figure 62. Sakai CCV, pass number, and surface temperatures for the Sakai SW990 breakdown compaction of the HMA intermediate course (TB 02C).

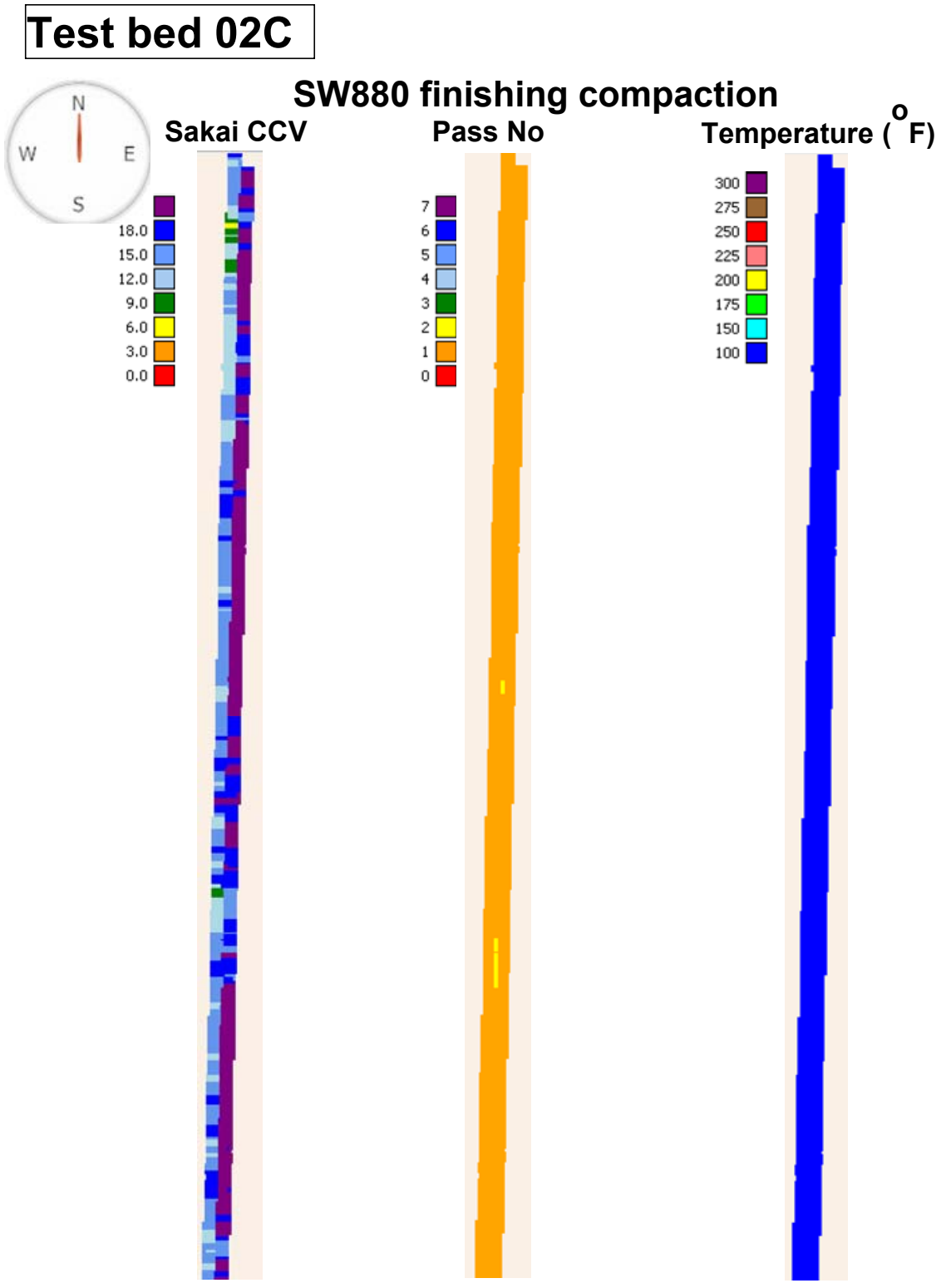

Figure 63. Sakai CCV, pass number, and surface temperatures for the Sakai SW880 finishing compaction of the HMA intermediate course (TB 02C).

Test bed 02C_Section 1

SW990 breakdown compaction

Sakai CCV

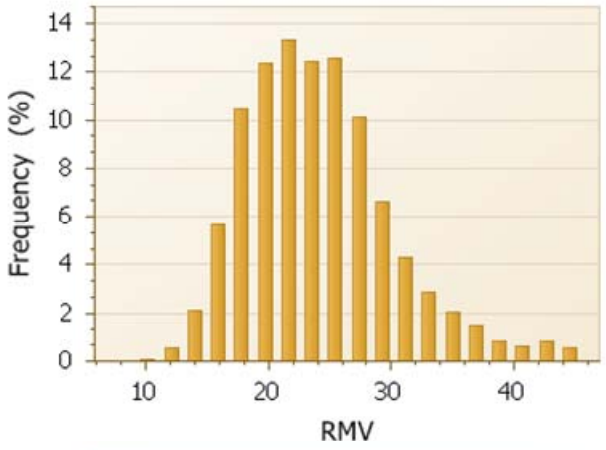

Mean: 23.13
STD: 5.91
COV: 0.26

Temperature

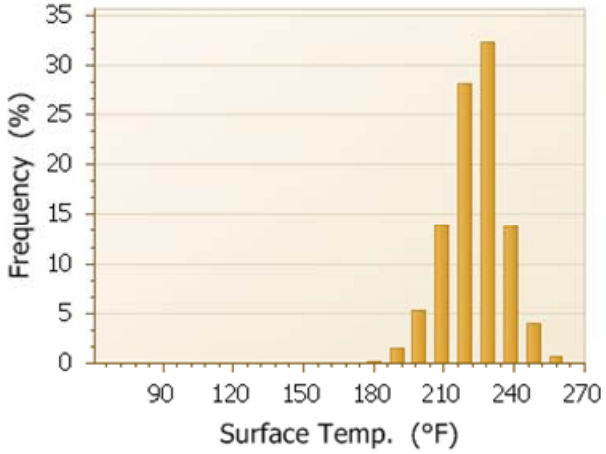

Mean: 218.2
STD: 13.27
COV: 0.06

Frequency

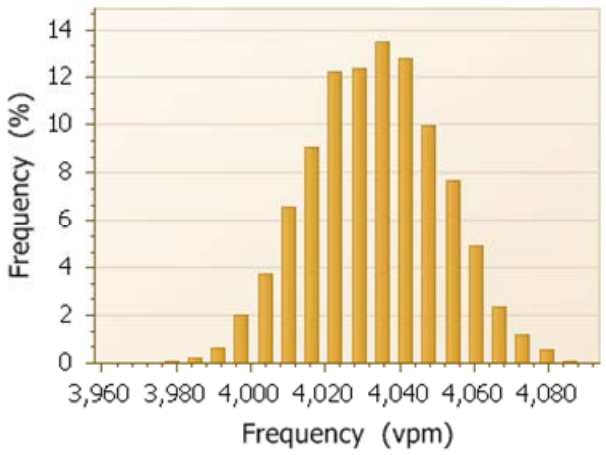

Mean: 4030
STD: 17
COV: 0.00

Figure 64. Sakai CCV, surface temperatures, and frequency histograms for the Sakai SW990 breakdown compaction of the HMA intermediate course (TB 02C – Section 1).

Test bed 02C_Section 2

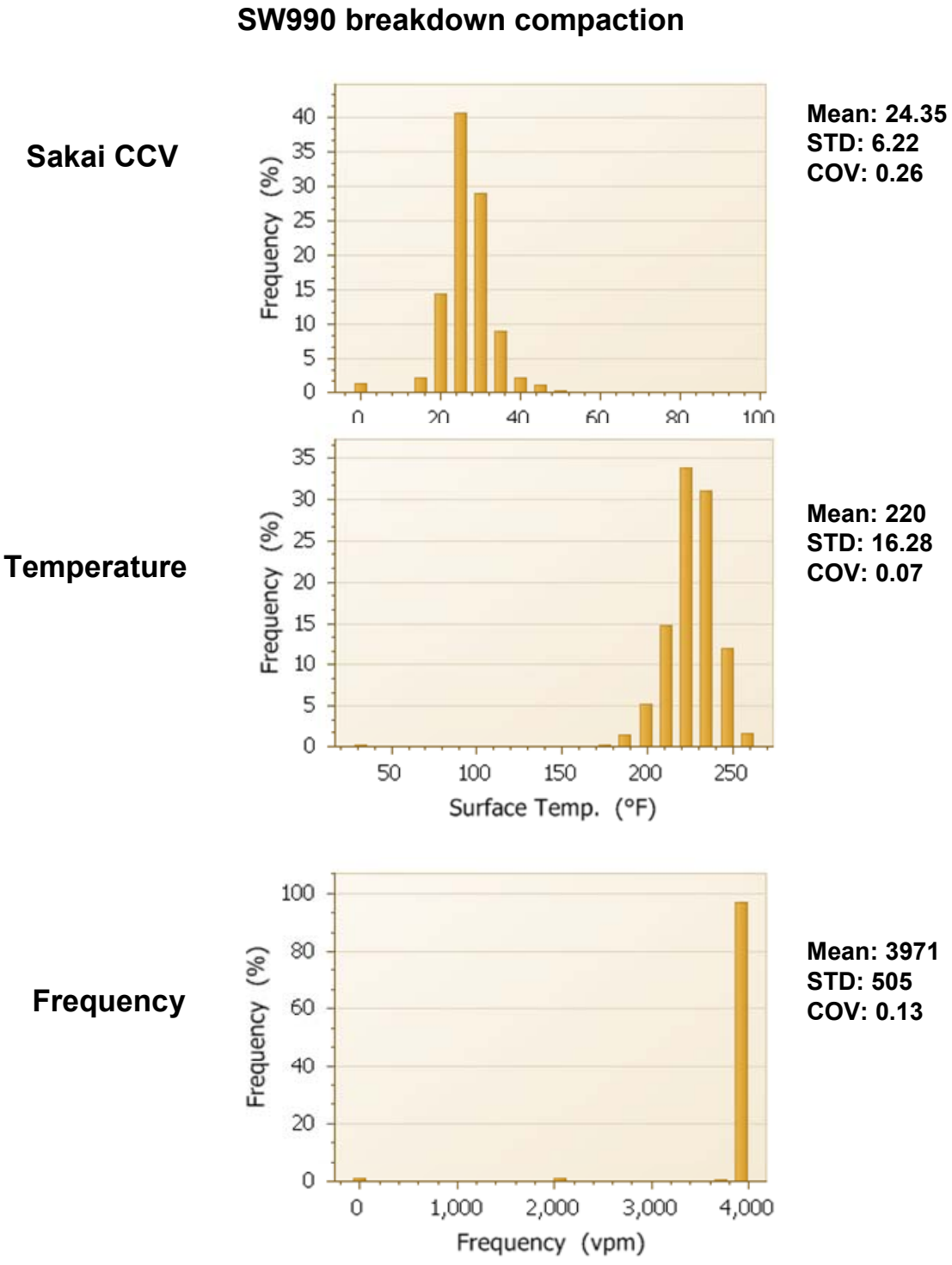

Figure 65. Sakai CCV, surface temperatures, and frequency histograms for the Sakai SW990 breakdown compaction of the HMA intermediate course (TB 02C – Section 2).

Test bed 02C_section 1

SW880 finishing compaction

Sakai CCV

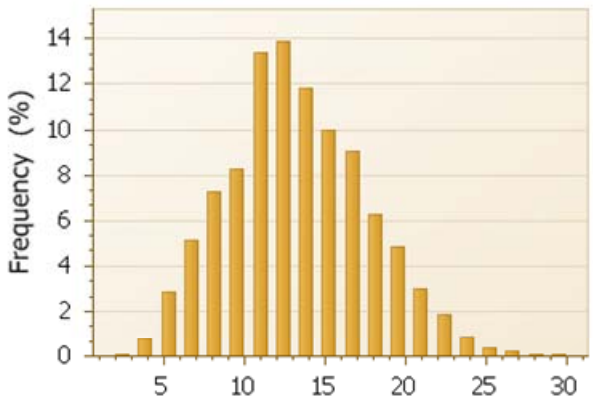

Mean: 12.55
STD: 4.34
COV: 0.35

Temperature

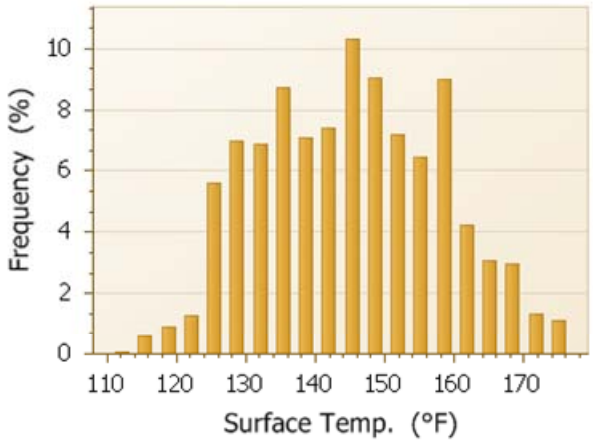

Mean:143.4
STD: 13.03
COV: 0.09

Frequency

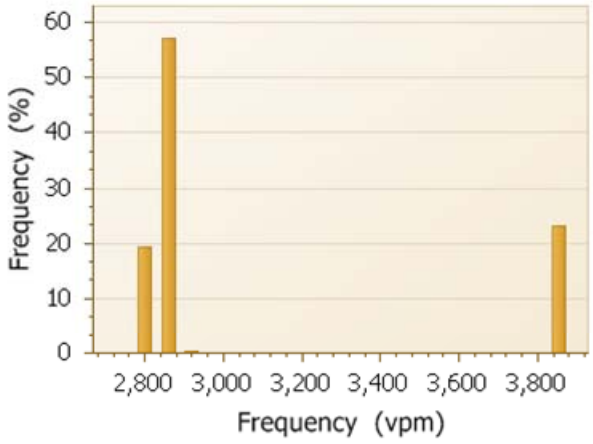

Mean: 3056
STD: 442
COV: 0.14

Figure 66. Sakai CCV, surface temperatures, and frequency histograms for the Sakai SW880 finishing compaction of the HMA intermediate course (TB 02C – Section 1).

Test bed 02C_section 2

SW880 finishing compaction

Sakai CCV

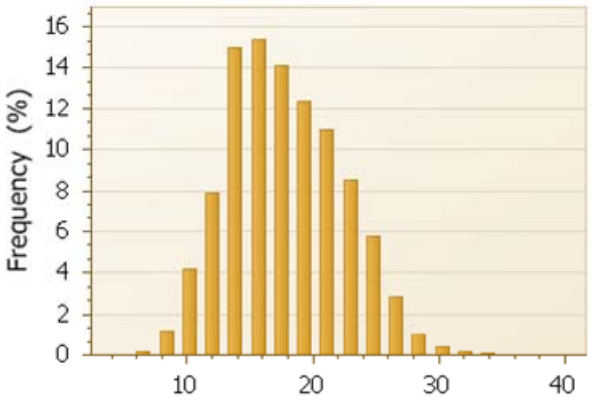

Mean: 16.84
STD: 4.51
COV: 0.27

Temperature

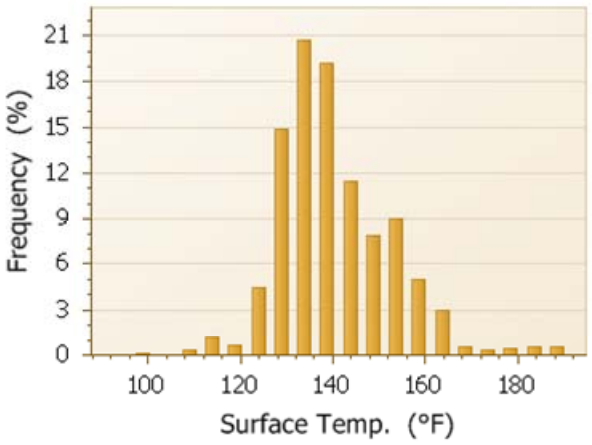

Mean:137.9
STD: 12.22
COV: 0.09

Frequency

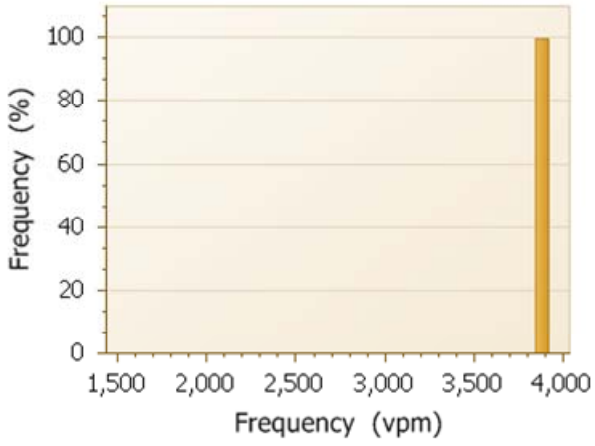

Mean: 3890
STD: 79
COV: 0.02

Figure 67. Sakai CCV, surface temperatures, and frequency histograms for the Sakai SW880 finishing compaction of the HMA intermediate course (TB 02C – Section 2).

TB02C SW990 breakdown compaction

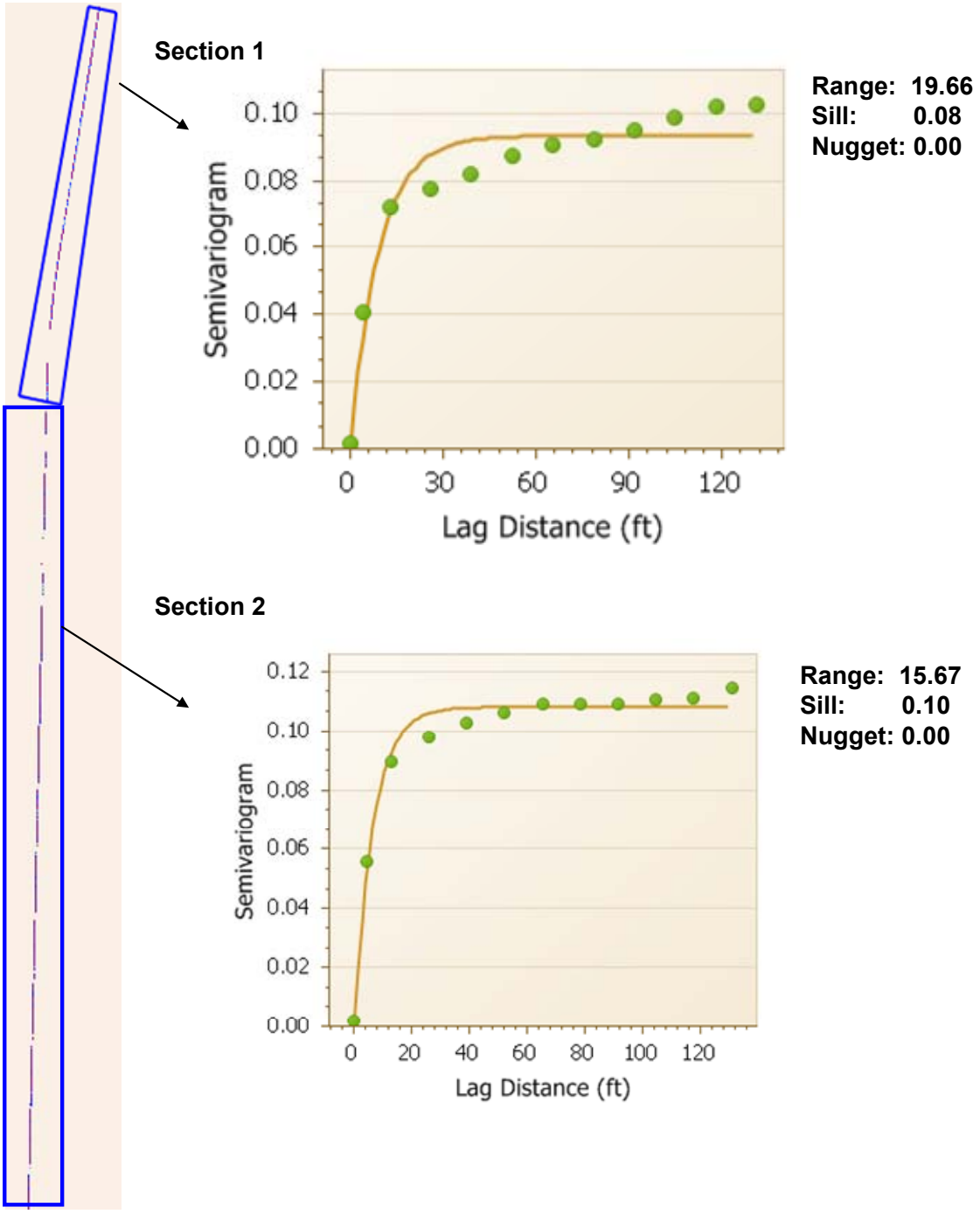

Figure 68. Semivariogram for the Sakai SW990 breakdown compaction of the HMA intermediate course (TB 02C).

TB02C SW880 finishing compaction

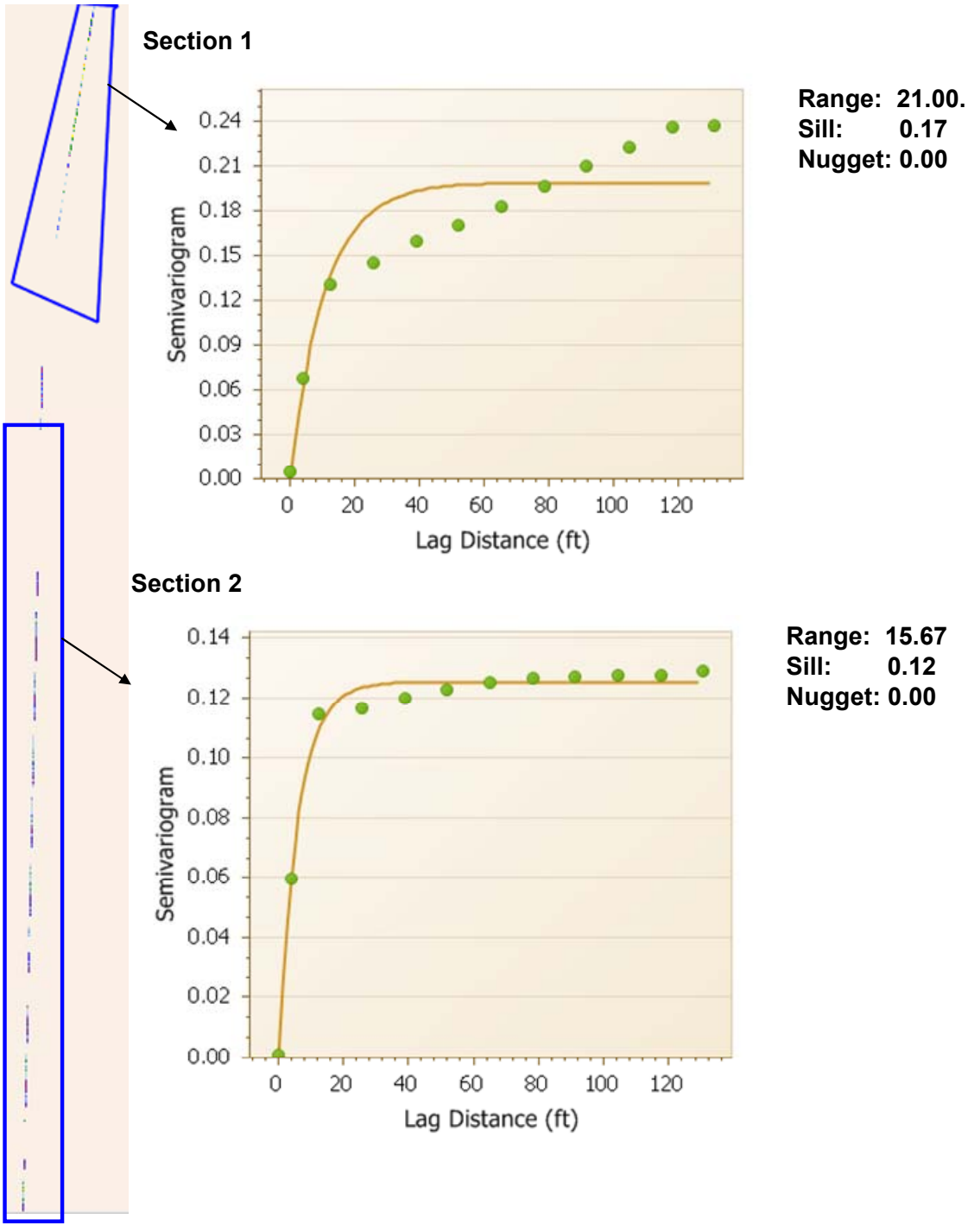

Figure 69. Semivariogram for the Sakai SW880 breakdown compaction of the HMA finishing course (TB 02C).

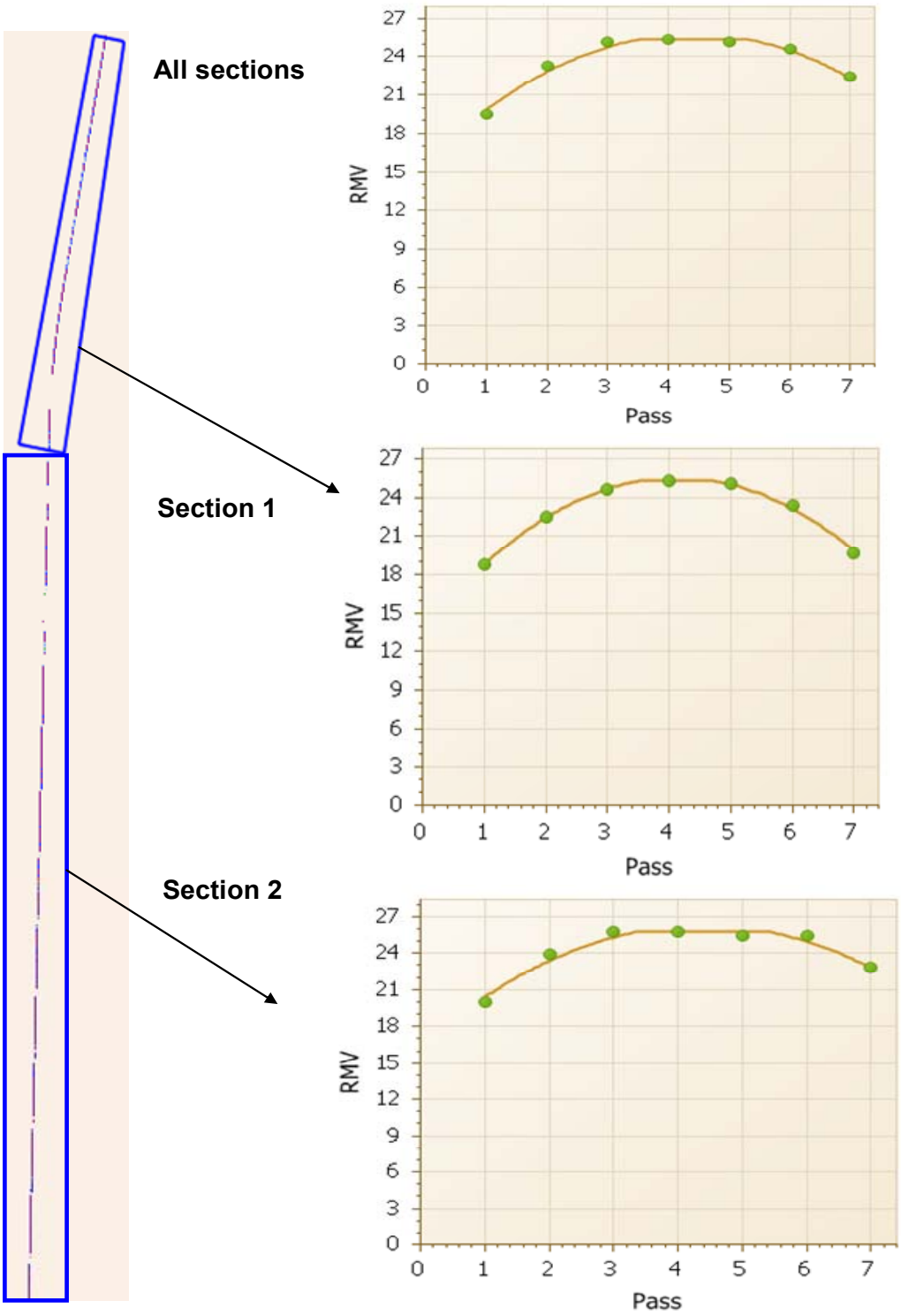

Figure 70. Compaction curves for the Sakai SW990 breakdown compaction of the HMA intermediate course (TB 02C).

In-Situ Test Results

NG of HMA

Figure 71 presents all the measured NG densities following the Sakai SW990 breakdown and/or SW880 finishing compactions. No obvious trend of density variation with roller pass could be found due to limited measurements. However, results show that the NG density after finishing roller is higher than that following breakdown roller, indicating the contribution of finishing compaction to improving density. It is also noted that the 2nd lift HMA intermediate layer has a higher NG density than the HMA base, which would be primarily due to the material components and mix design (e.g. the smaller max normal aggregate size of 19mm of 2nd lift HMA compared to 25mm of HMA base).

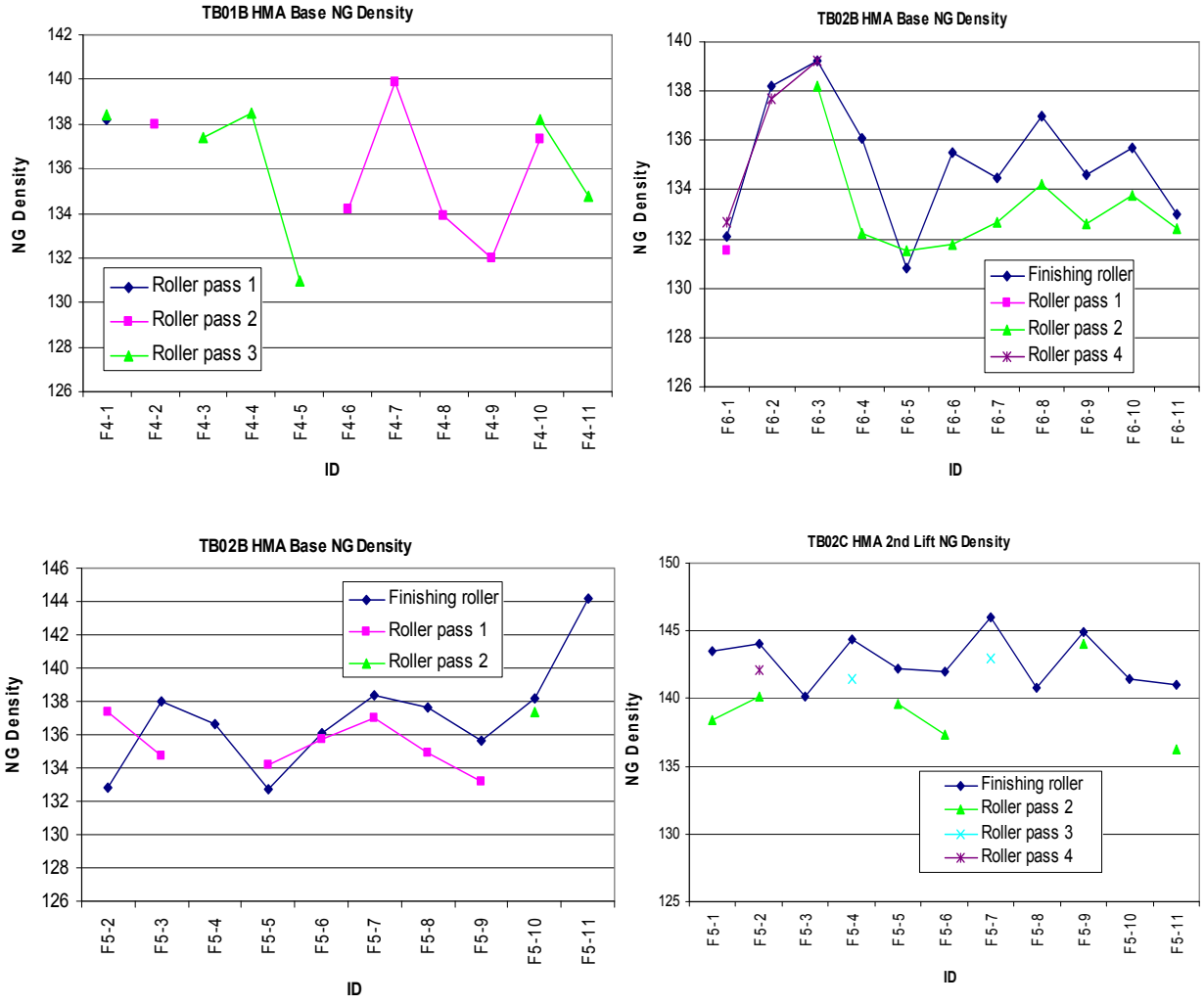

Figure 71. NNG density of HMA course after Saki compaction.

FWD Tests

Figure 72 presents the FWD deflections at plate center. Results show that deflections reduce from the underlying layer of PCC base to the upper layer of HMA base and then the 2nd lift HMA due to the improved integral strength with paving more HMA layers on the top. It is also noted that the pavement deflections and the deflection differences between adjacent pavement layers for the 2nd section is lower than that for the 1st section. This result may be explained by the better integral strength of the crack-and-seat PCC base of the 2nd section than that of the rubblized PCC base of the 1st section. However, this finding does not guarantee that the HMA pavement of the 2nd section on the crack-and-seat will result in better long-term performance. In comparison, the rubblized PCC base of the 1st section has better interlock effect with smaller PCC block sizes and stronger interaction between PCC blocks and asphalt mixtures.

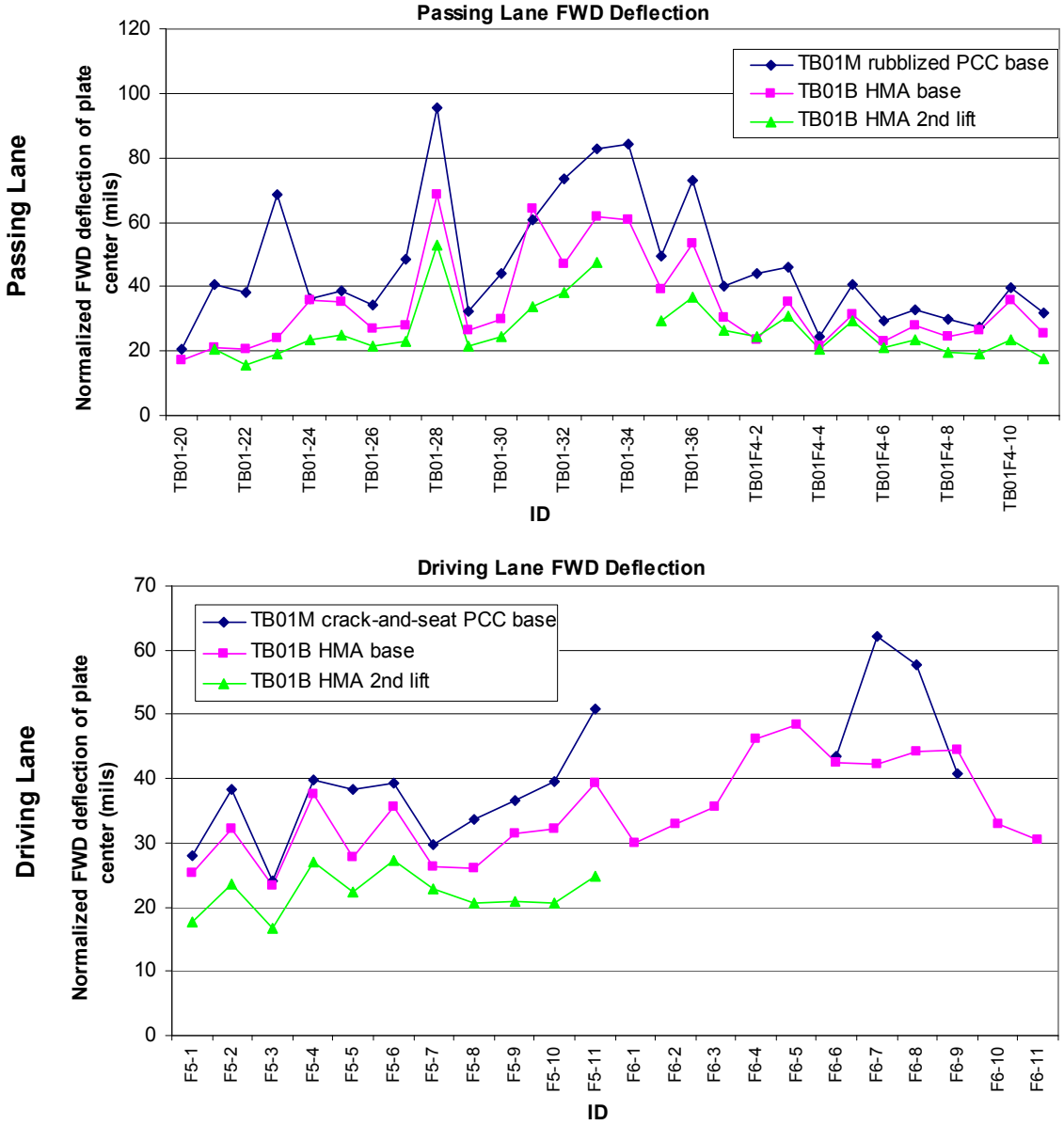

Figure 72. FWD deflections at the plate center.

LWD Tests

Figure 73 shows the measured LWD deflections on the rubblized/crack-and-seat PCC base, HMA base and 2nd lift HMA for both the passing lane and driving lane. Apparently, the 2nd lift HMA has a significantly lower deflection while higher moduli than PCC base and HMA base.

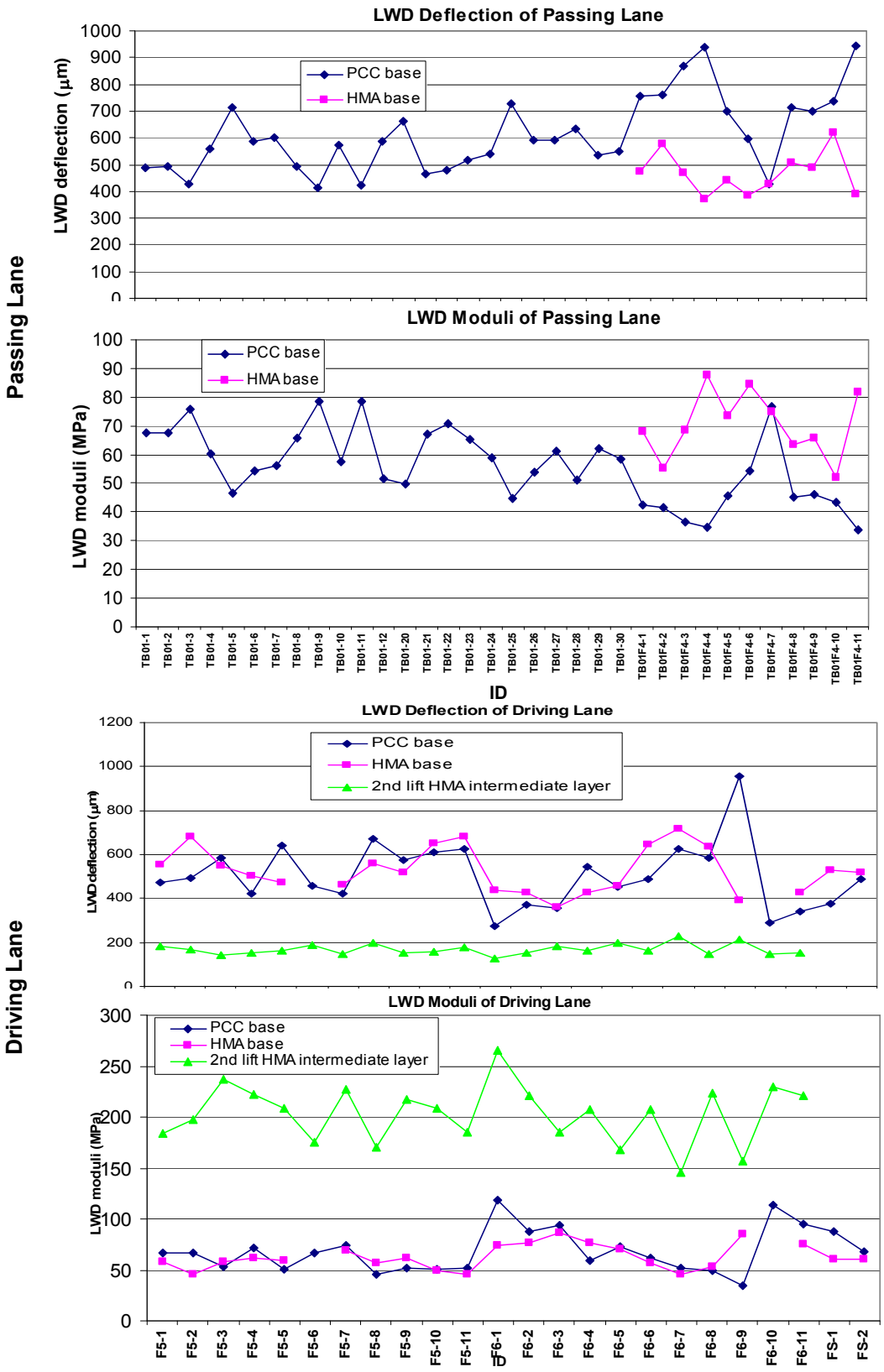

Figure 73. LWD Measurements.

Correlation of IC Data and In-Situ Test Data

When correlating results from various different tests, it is important to recognize that the differences in nature of these test devices and test methods. As seen in Figure 74, the "influence depths" of various devices are quite different. The test results are also affected by the in-situ conditions: such as moistures to soil/aggregate tests and temperatures to asphalt tests.

Furthermore, the roller measurement values (RMV) at various stages (subbase paving, base course paving, and HMA wearing course paving) cover the influence depths incrementally as pavement layers being laid on (see Figure 75). Also, the RMVs represent the measurements at "points" in time and in space when roller drums contact the underlying of pavement structure: i.e., the "states" of the pavement (e.g. HMA layer temperatures and compacted levels) are unique at these locations.

As stated by Scherocman (2007) to comment on the RMV vs. asphalt densities, "the RMV represent a relative value that computed from the acceleration signal (i.e., roller-pavement interaction) but this value does not give the absolute percent compaction, stiffness, or density measured (i.e. the level and state of compaction of the HMA bound layer)". Therefore, cautions should be taken when interpretation of any correlations of RMVs with any other measurements in the following sections.

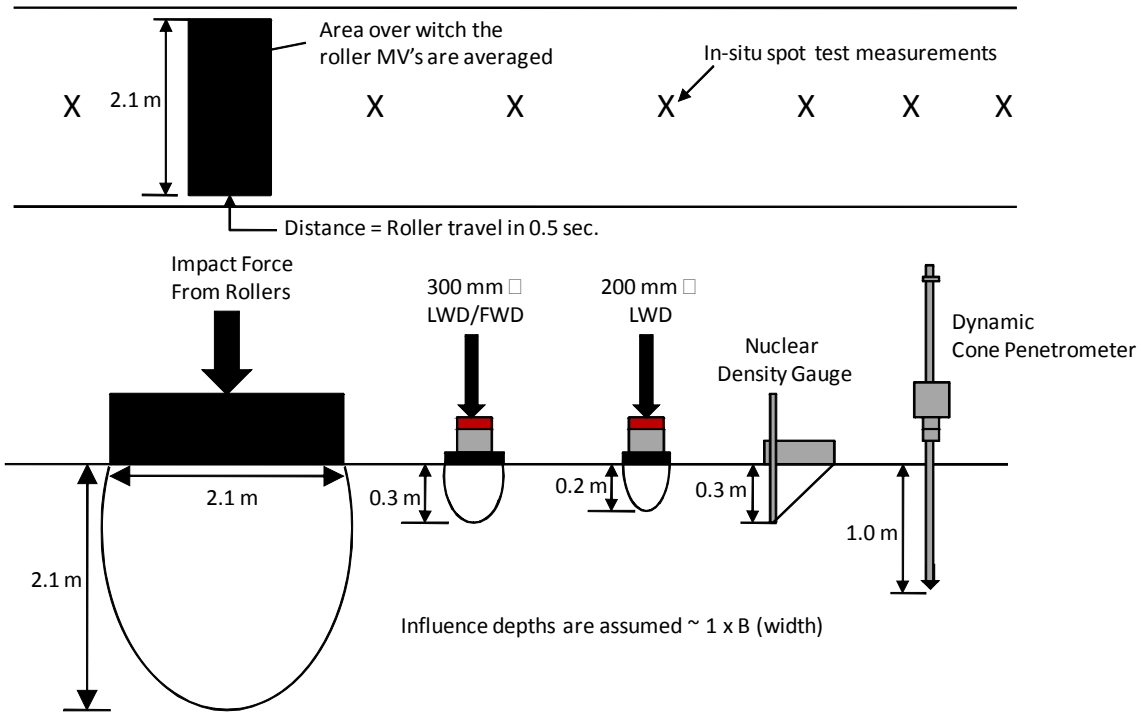

(Courtesy of Dr. David White)

Figure 74. Influence depths of various test methods.

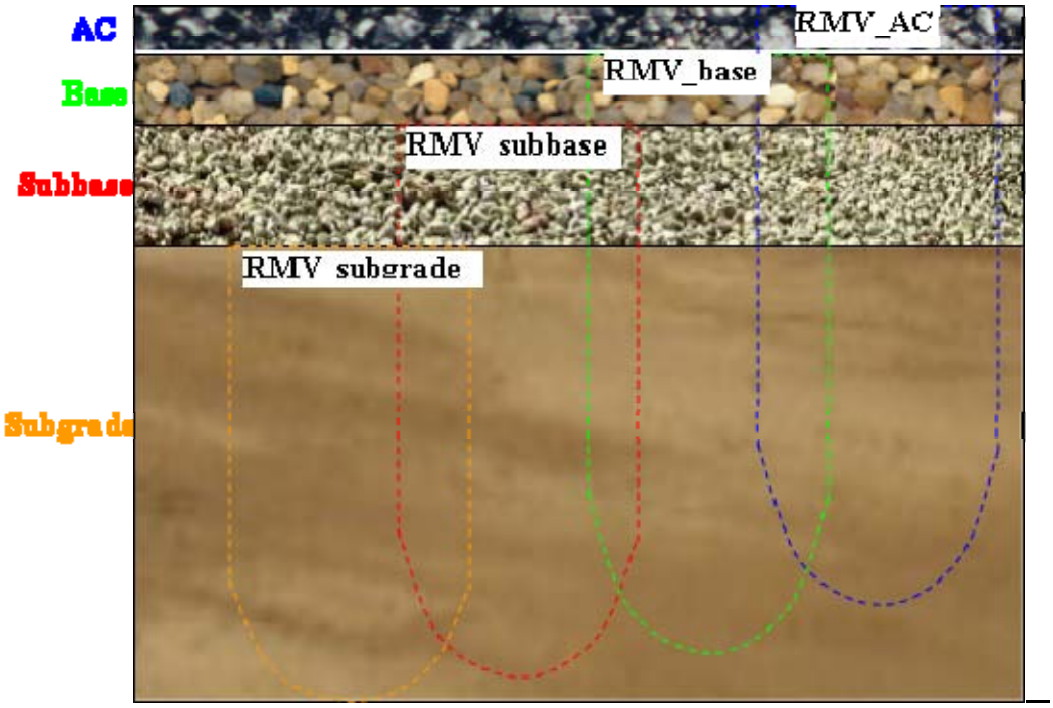

Figure 75. Influence depths of RMVs at various paving stages.

Sakai IC Measurements vs. FWD Deflections

Figure 76 to Figure 79 present the correlation results between the Sakai measurements of CCV, frequency, and surface temperature and the measured FWD deflection under the loading plate. Results show that Sakai CCV decreases with increasing FWD deflection, indicating that a lower stiffness of material corresponds to a larger deflection as expected. However, the linear correlation is relatively low as indicated by the relatively small R^2 value. One of the most important reasons could be due to the discontinuous environmental or roller conditions on those test spots, such as the very scattered distributions of HMA temperature (see Figure 79) and/or vibration frequency (see Figure 77). Since the CCV as a stiffness index is dependent on the HMA temperature and roller vibration frequency, a more accurate correlation would be achieved given a more uniform HMA temperature and vibration frequency distribution on those test spots. Another possible factor is the loose contact between the FWD loading plate and the rubbilized PCC base that may result in unreliable deflections.

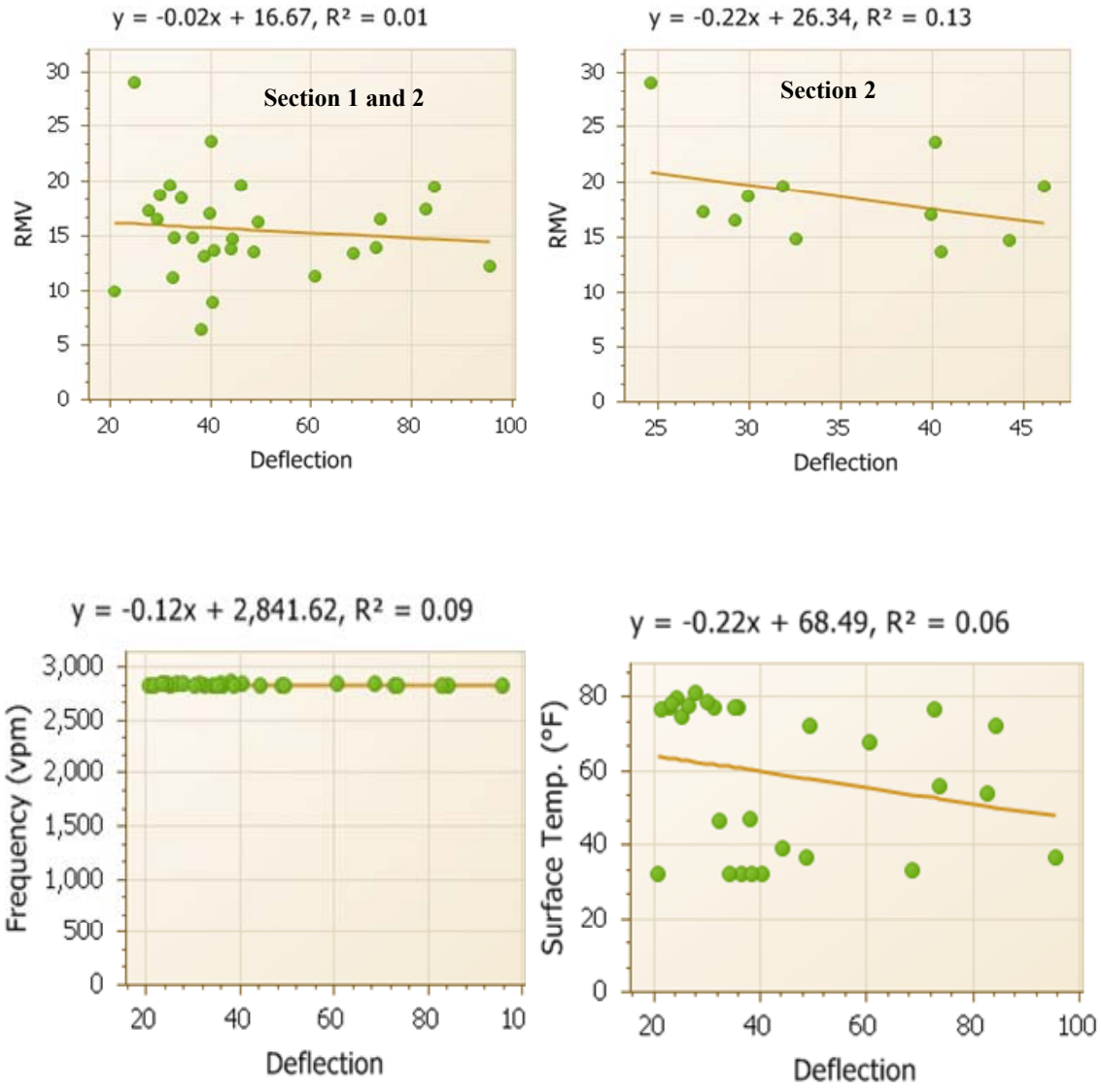

Figure 76. TB01M PCC base, Sakai IC measurements vs. FWD deflection of plate center.

TB01B SW990 breakdown, FWD all sections

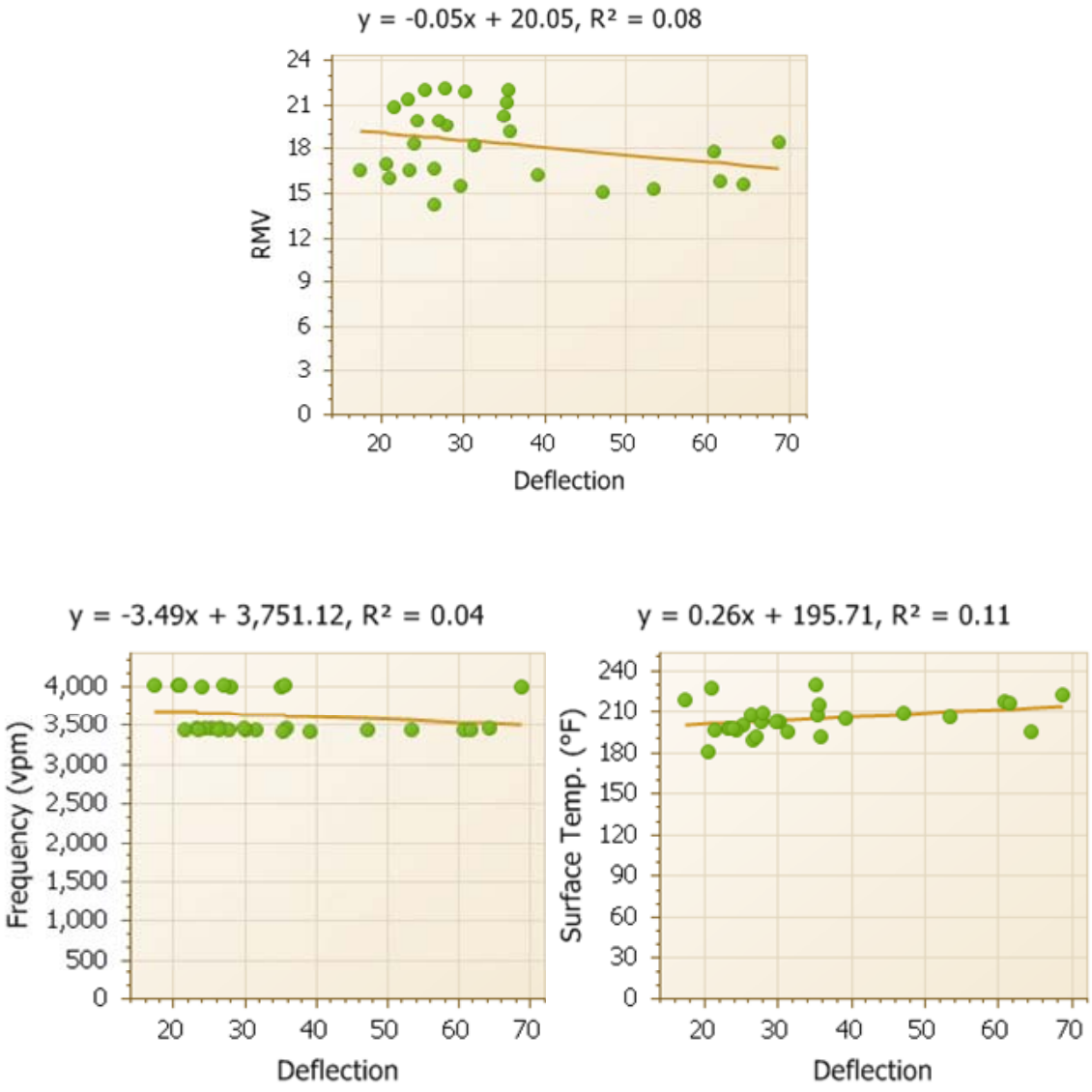

Figure 77. TB01B HMA base, Sakai IC measurements vs. FWD deflection of plate center.

TB01C SW990 breakdown FWD All data

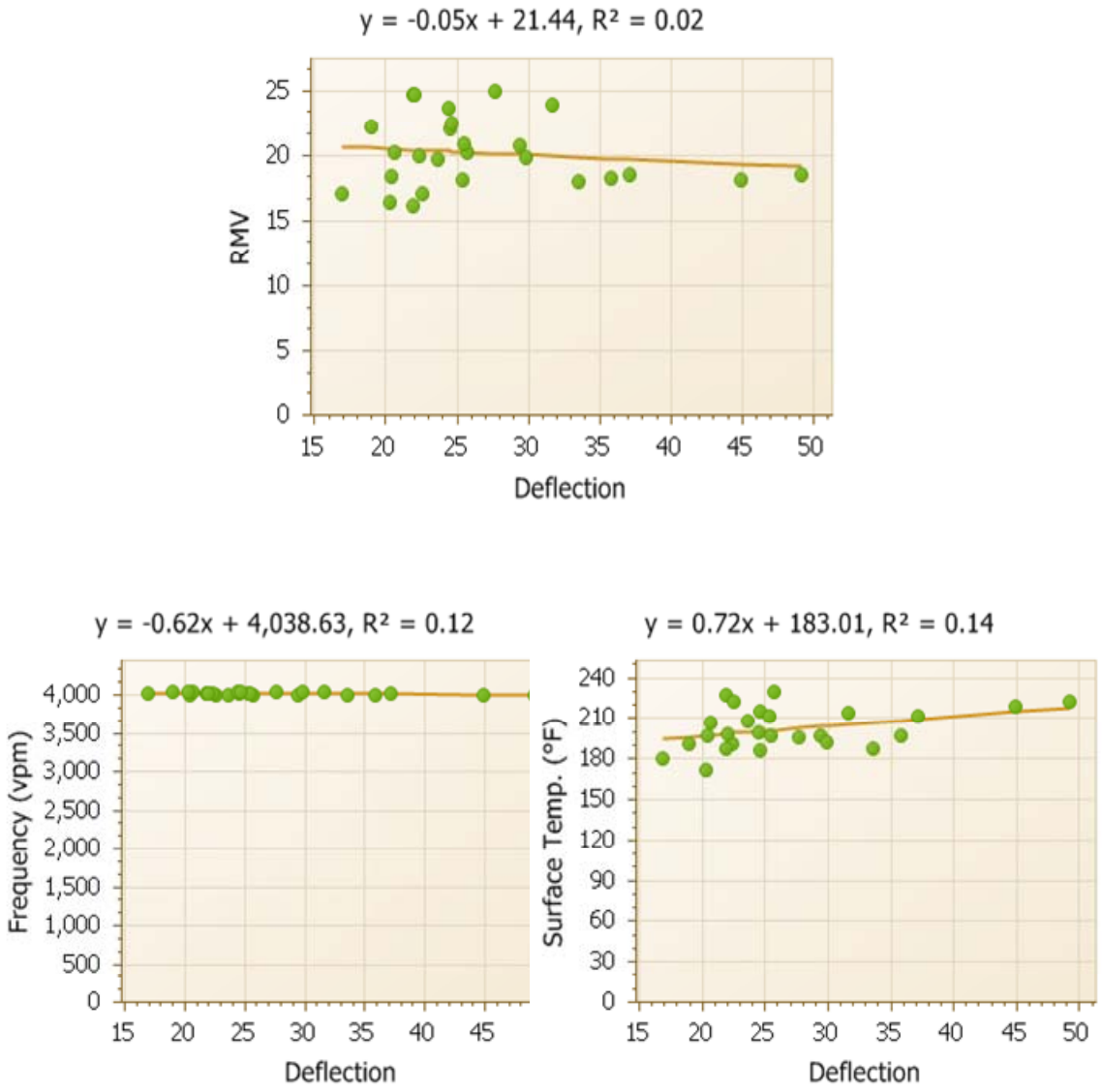

Figure 78. TB01C HMA 2nd lift, Sakai IC measurements vs. FWD deflection of plate center.

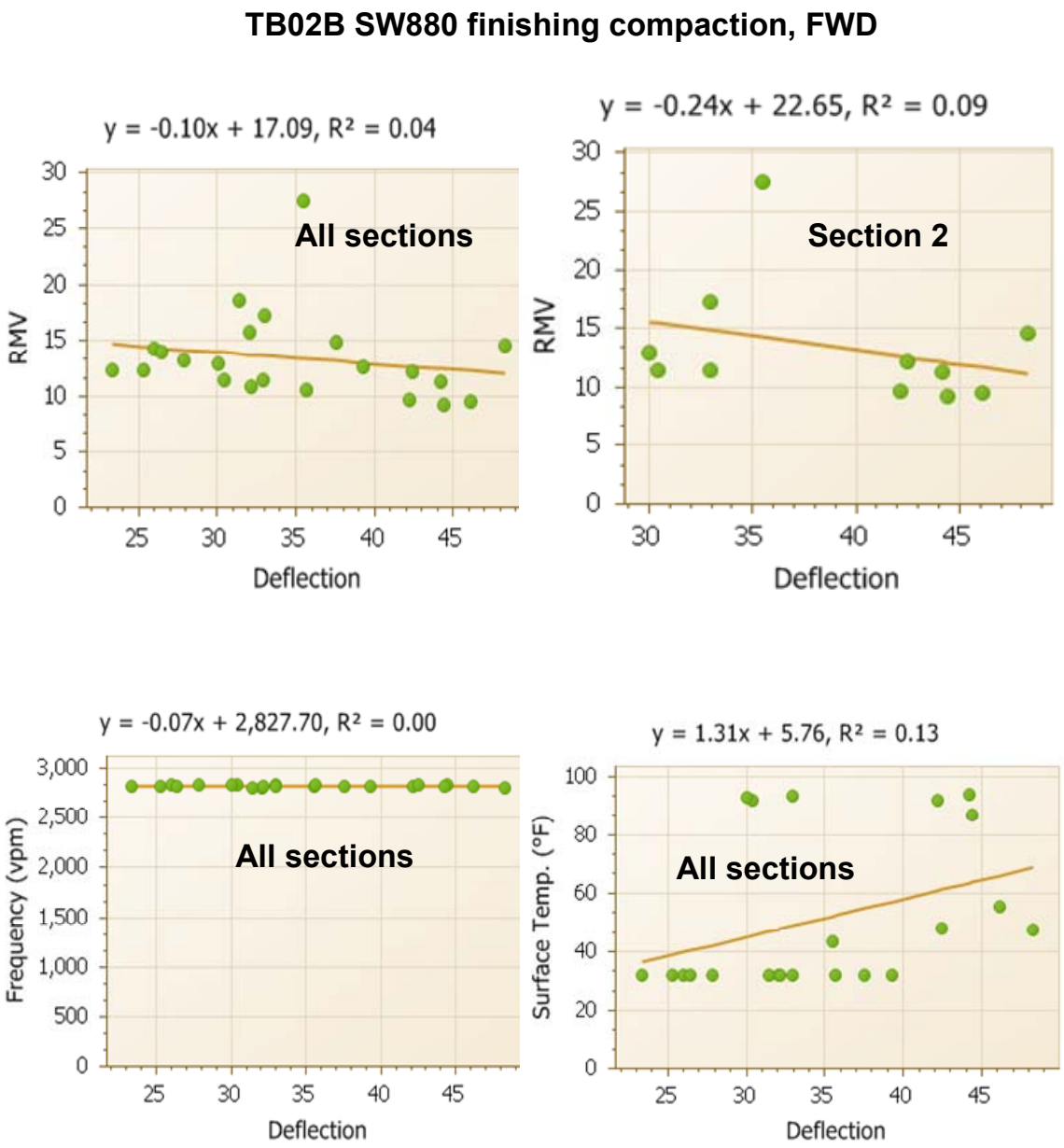

Figure 79. TB02B HMA base, Sakai IC measurements vs. FWD deflection of plate center.

Sakai IC Measurements vs. LWD Deflections and Moduli

Figure 80 to Figure 84 show the correlations between the Sakai measurements of CCV, frequency, and surface temperature and the measured LWD deflections and moduli. Results show that Sakai CCV decreases with increasing deflection while increases with increasing moduli, indicating that a lower stiffness of material corresponds to a larger deflection or a higher modulus as expected. The linear correlation is relatively good for some test beds, e.g. it has a R^2 value of 0.34 for the TB01B HMA base (see Figure 81).

For some test beds, the liner correlation is relatively poor such as that for the TB02B HMA base (see Figure 83). One of the most important reasons affecting the correlation could be due to the uniformity of the environmental or roller conditions of test spots, as discussed above for the FWD test correlation. E.g., TB02 HMA base has a scattered HMA temperature distribution for the test spots (see Figure 83 and Figure 84), resulting in a lower linear correlation between Sakai CCV and in-situ tests.

However, TB01B HMA base has a uniform HMA temperature distribution for the test spots (see Figure 81), resulting in a higher linear correlation. This result further confirms the significant effect of HMA temperature as discussed in previous IC demonstration reports. Therefore, it becomes urgent to make temperature correction in order to achieve a more accurate correlation. However, the challenges would be to develop a reliable IC model to accurately adjust for the temperature effect.

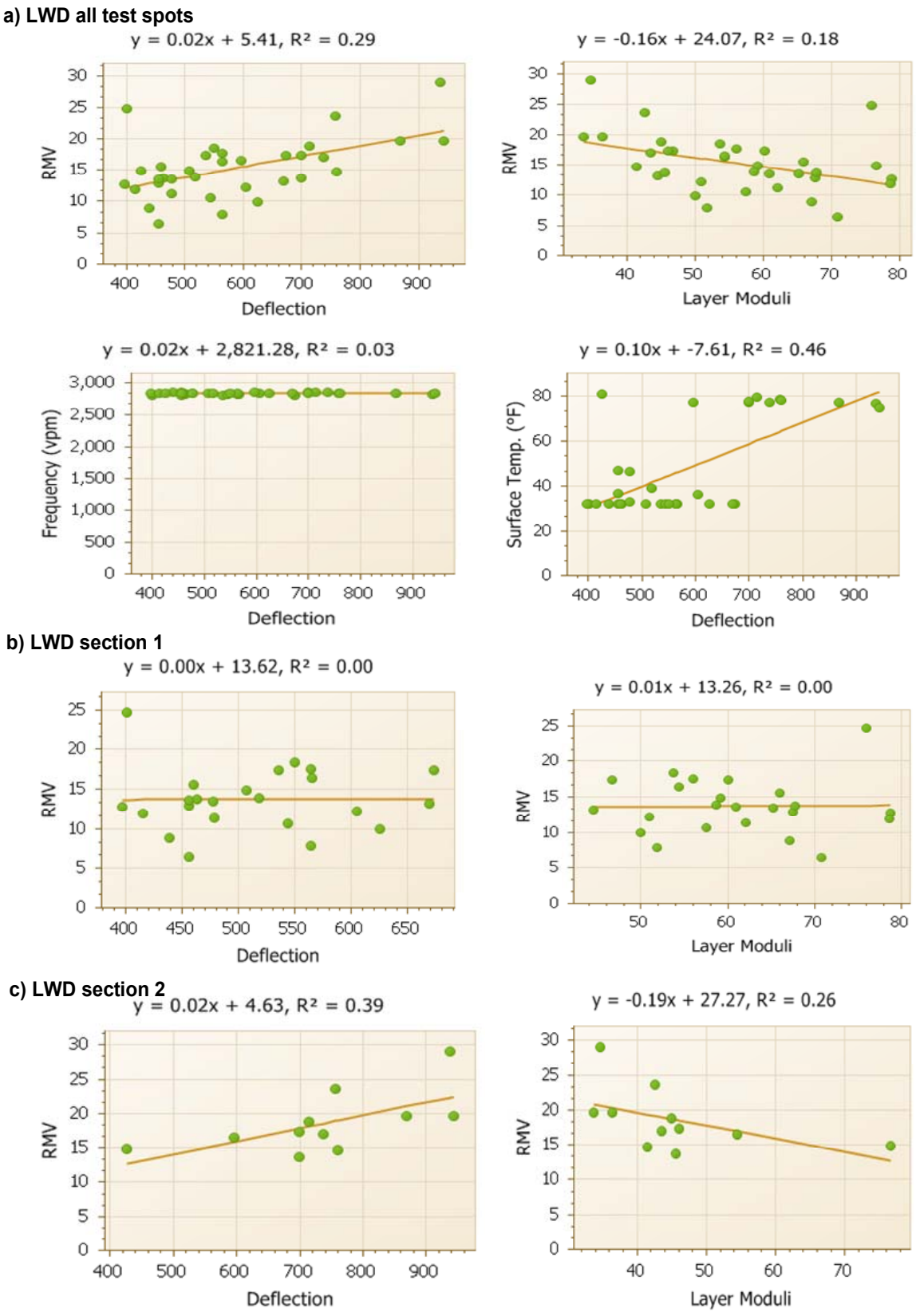

Figure 80. TB01M PCC base, Sakai IC measurements vs. LWD deflection and moduli.

TB01B SW990 breakdown LWD

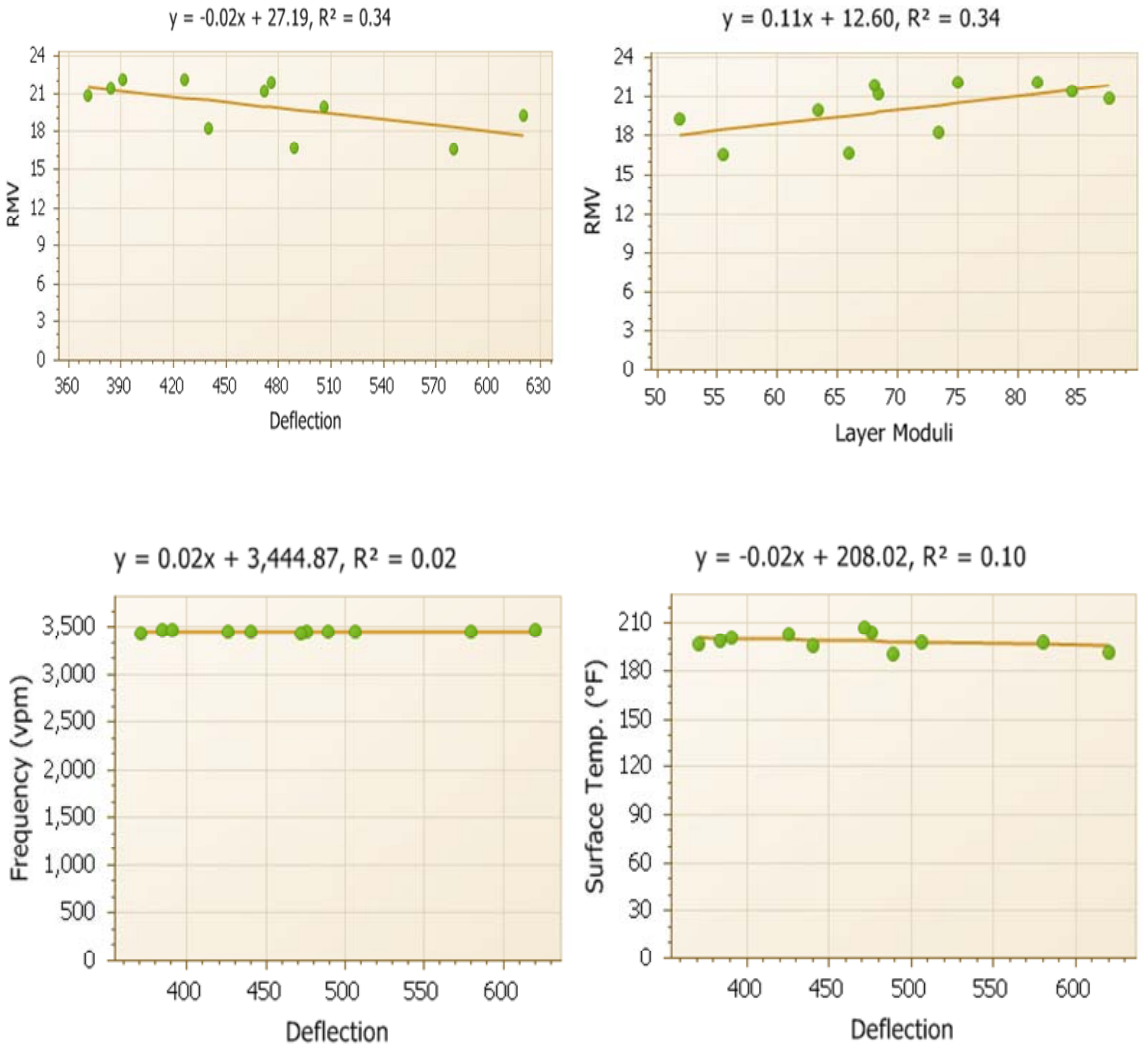

Figure 81. TB01B HMA base, Sakai IC measurements vs. LWD deflection and moduli.

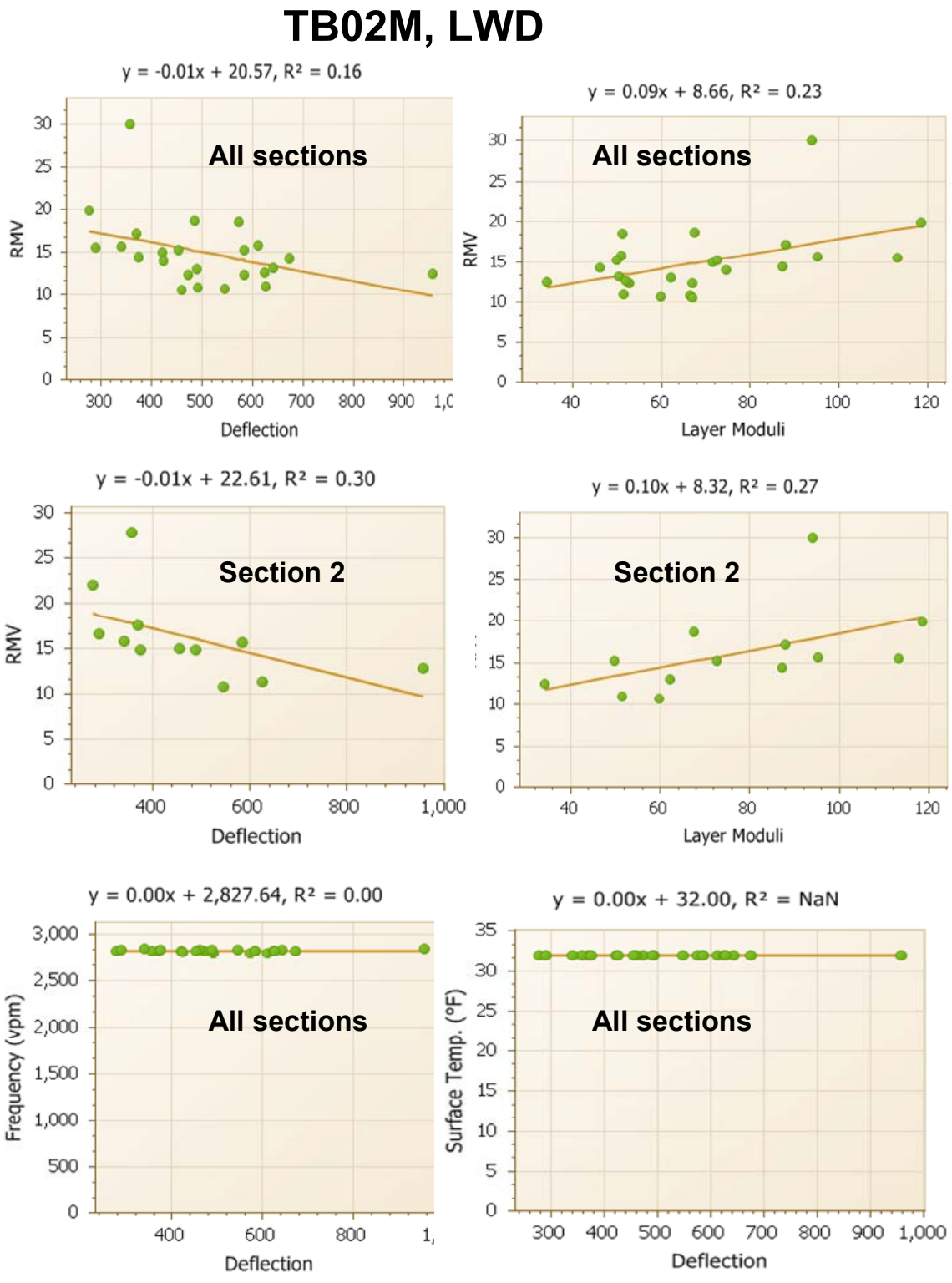

Figure 82. TB02M PCC base, Sakai IC measurements vs. LWD deflection and moduli.

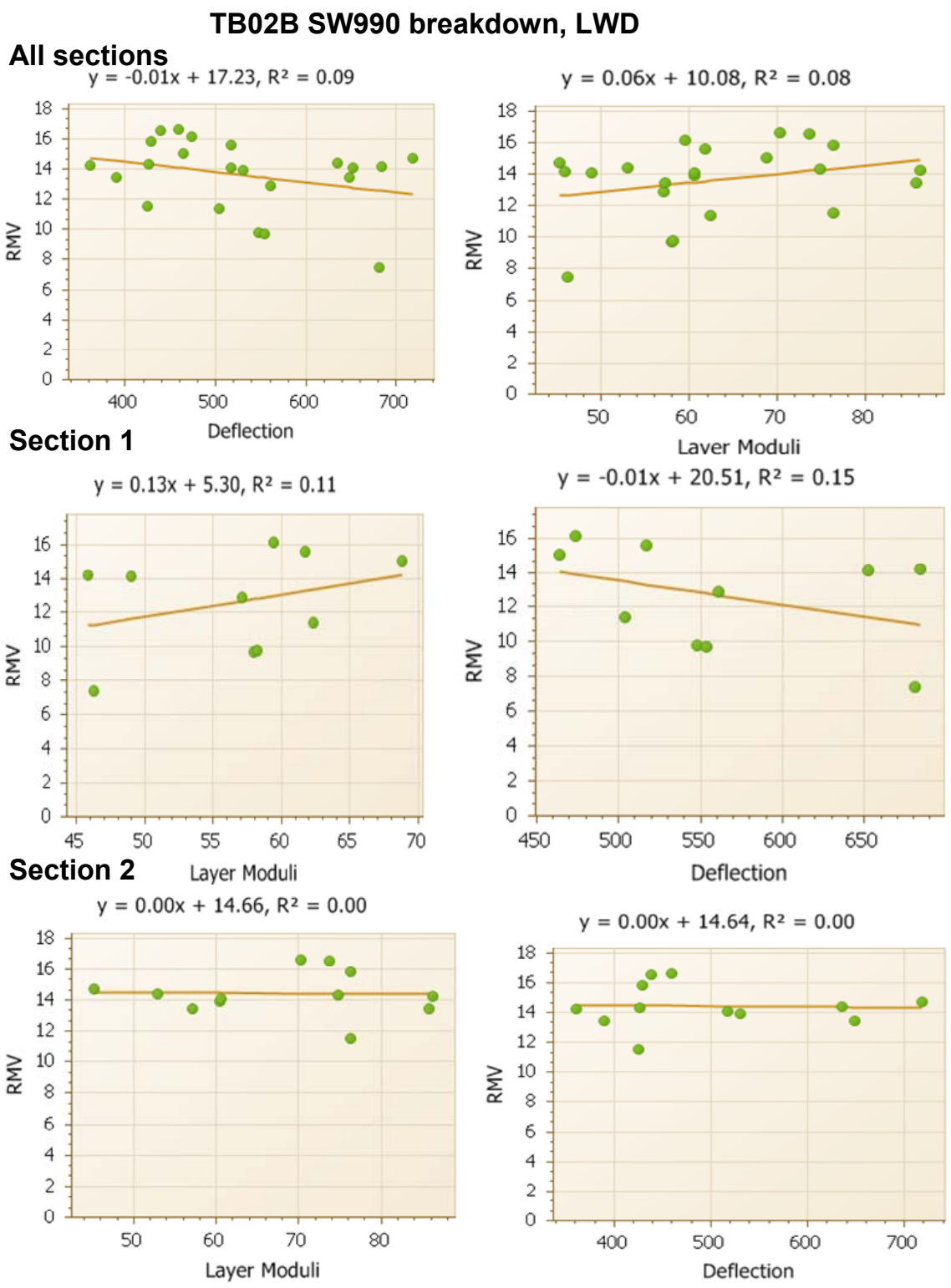

Figure 83. TB02B HMA base, Sakai SW990 IC measurements vs. LWD deflection and moduli.

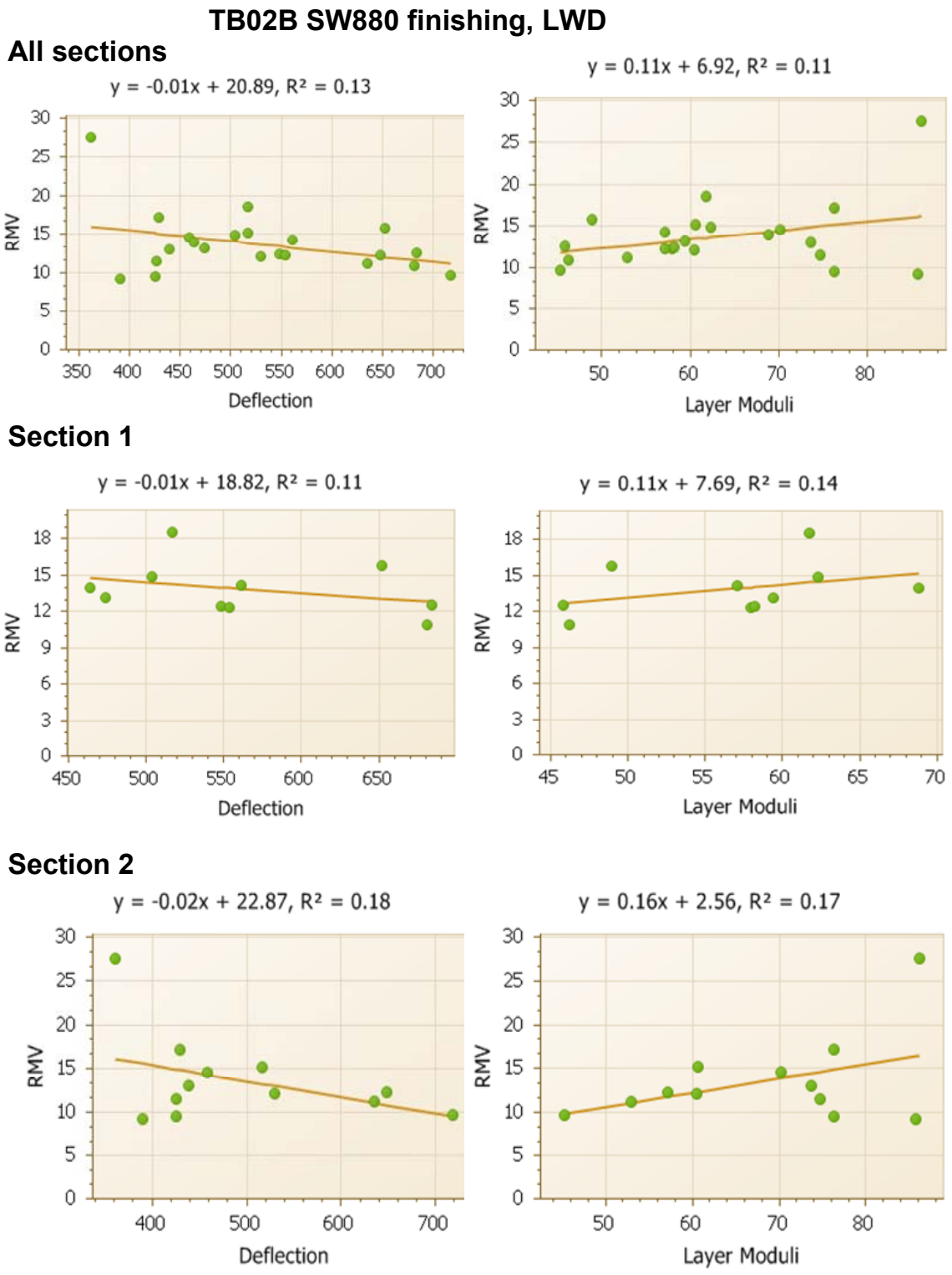

Figure 84. TB02B HMA base, Sakai SW880 IC measurements vs. LWD deflection and moduli.

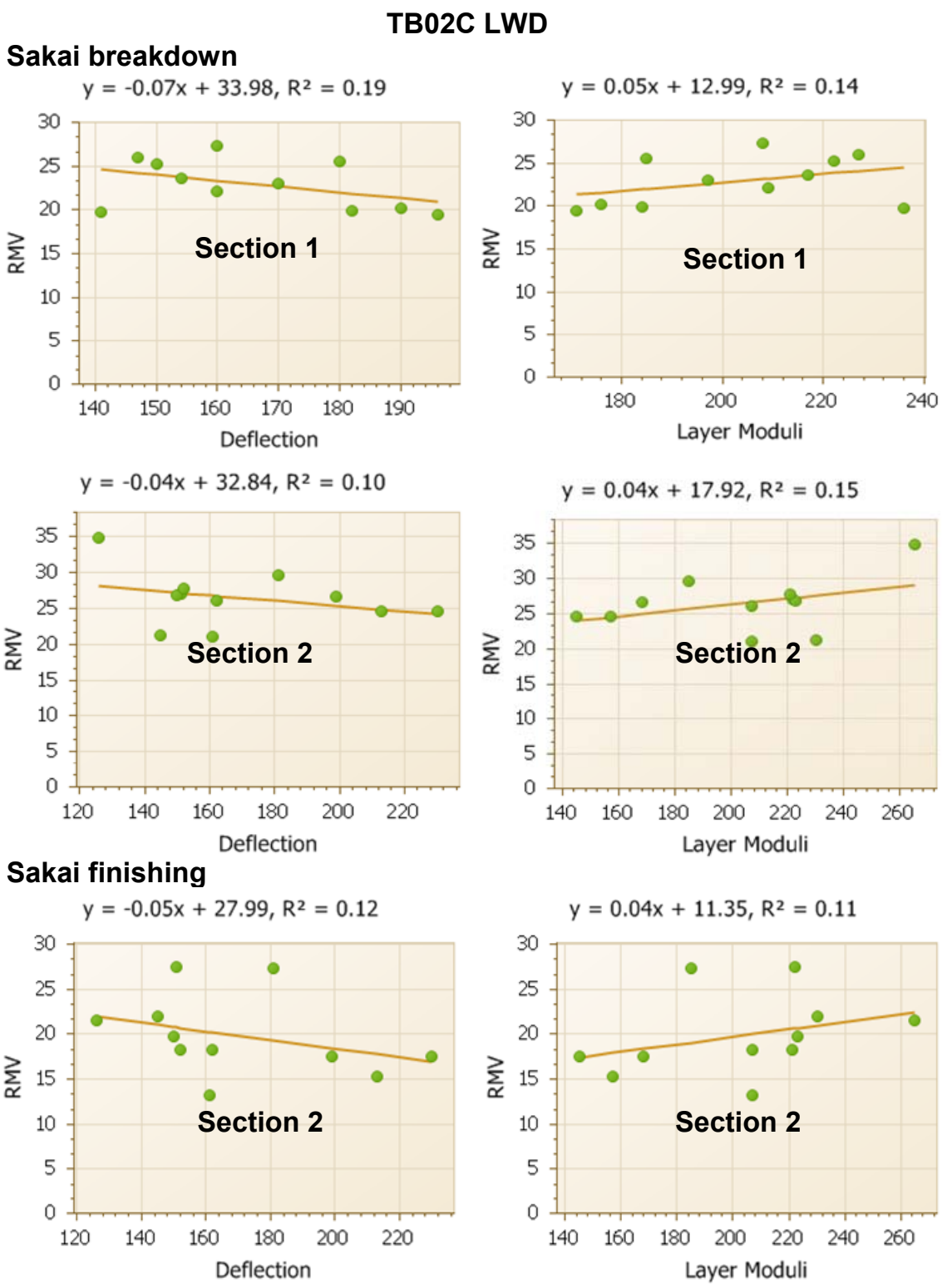

Figure 85. TB02C HMA 2nd lift, Sakai IC measurements vs. LWD deflection and moduli.

Sakai IC Measurements vs. HMA NG Densities

Figure 86 to Figure 89 show the correlations between the Sakai measurements of CCV, frequency, and surface temperature and the NG density. Results show that Sakai CCV increases with increasing NG density, and usually a higher density corresponds to a higher stiffness of material.

For some test beds the linear correlation is relatively good. E.g. a R^2 value of 0.85 (Figure 89) and 0.36 (see Figure 87) are achieved for the proof data of the TB02C 2nd lift HMA course and the TB01C 2nd lift HMA course, respectively.

However, for some other test beds the liner correlation is relatively poor such as that for the TB02B HMA base (see Figure 88). One of the most important reasons affecting the correlation could be due to the uniformity of the HMA temperature distribution on test spots as discussed for the FWD and LWD test correlations. E.g., TB02 HMA base has a very scattered HMA temperature distribution on test spots (see Figure 88), resulting in a relatively poor correlation since the used Sakai CCV is not adjusted for temperature effect.

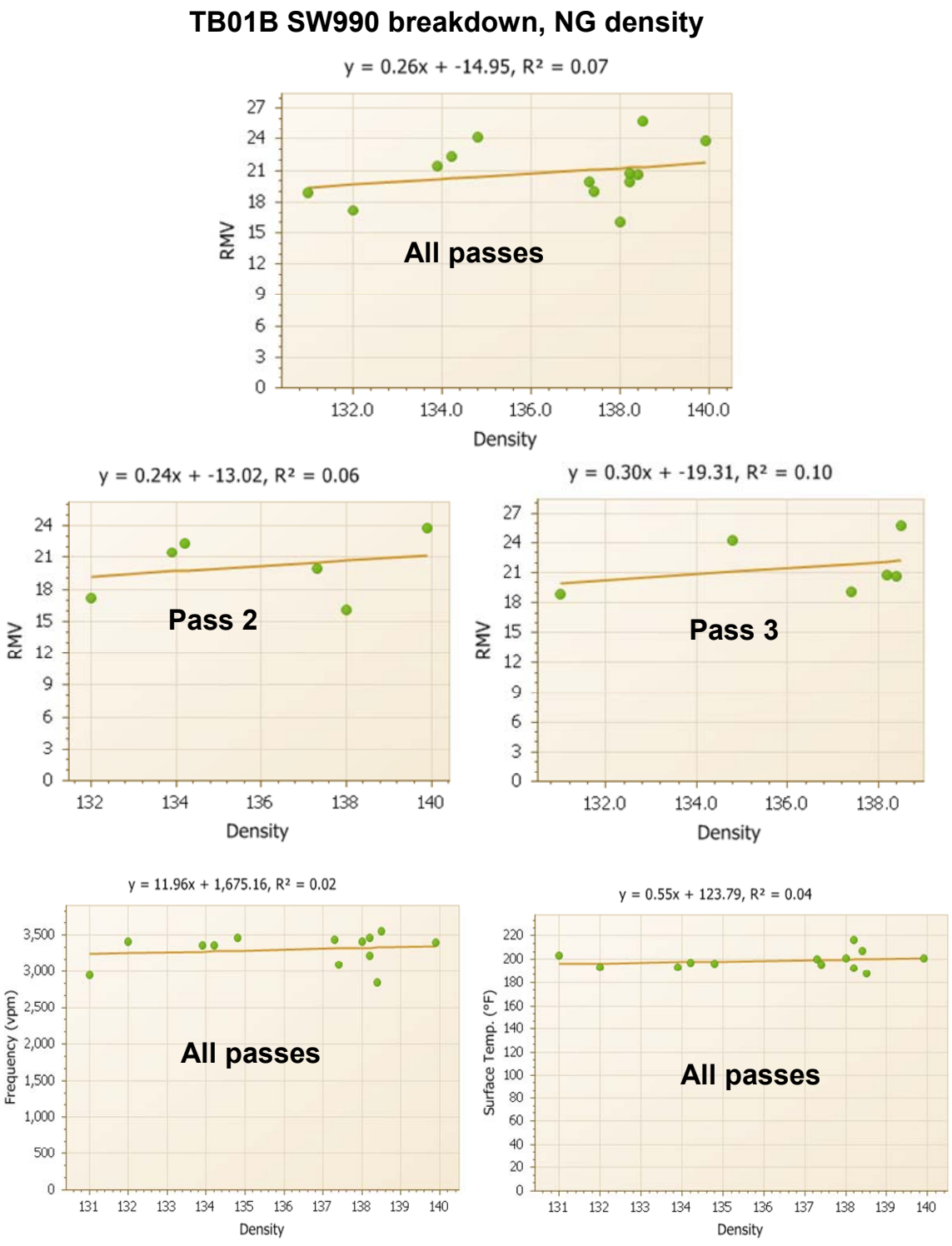

Figure 86. TB01B HMA base Sakai CCV, frequency, surface temperatures vs. NG density.

TB01C SW990 breakdown NG All Sections

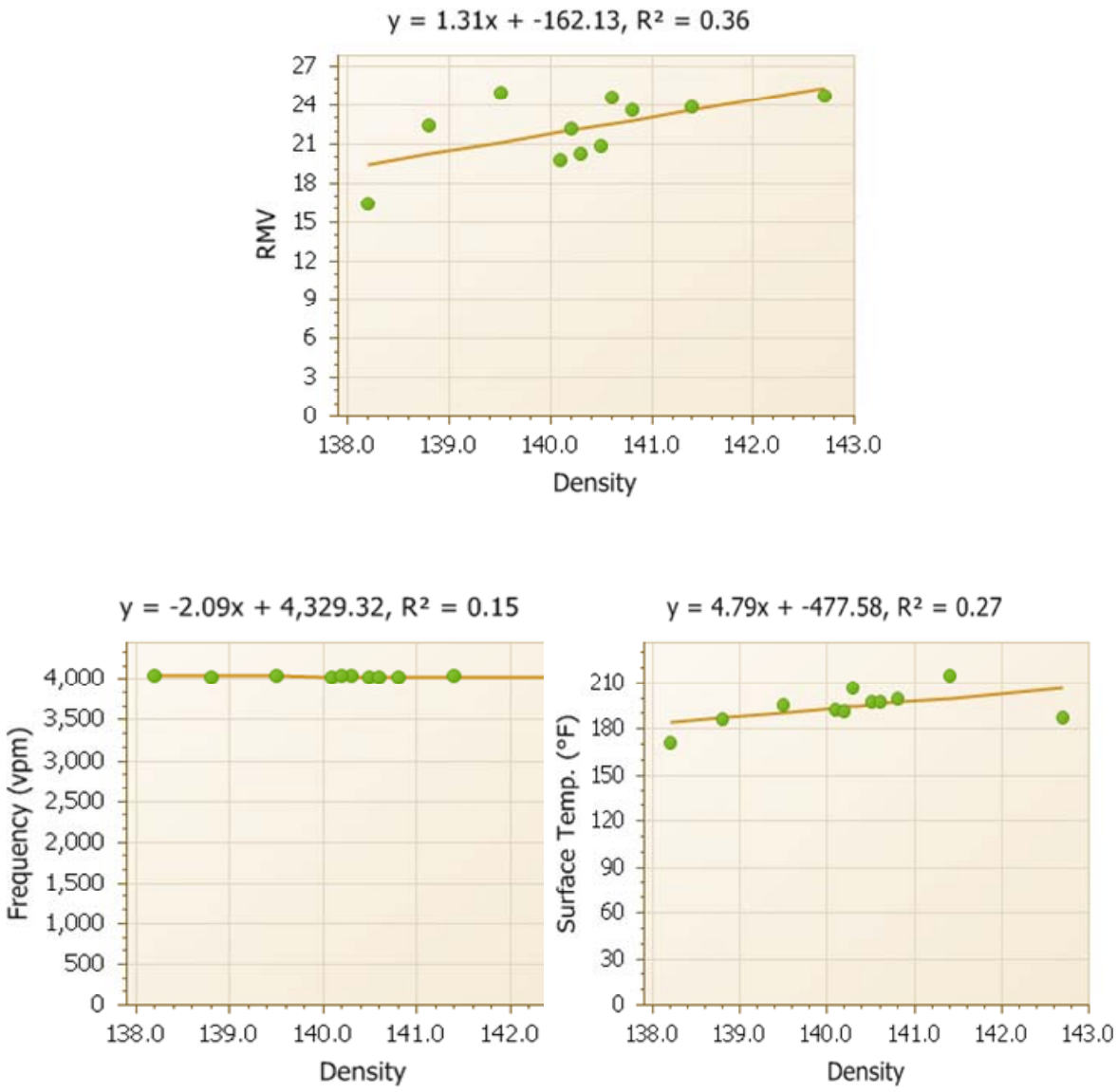

Figure 87. TB01C HMA 2nd lift Sakai CCV, frequency, surface temperatures vs. NG density.

TB02B, NG

Sakai SW990

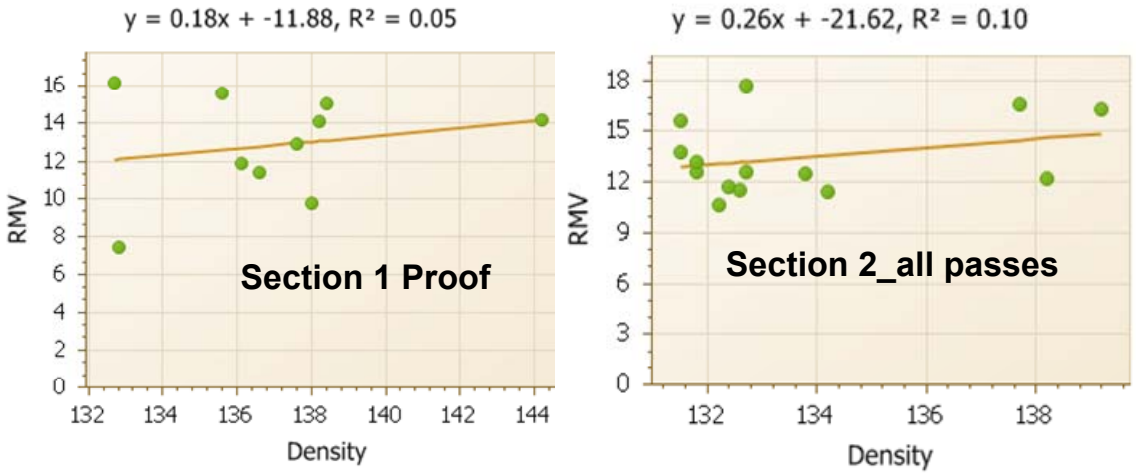

Sakai SW880

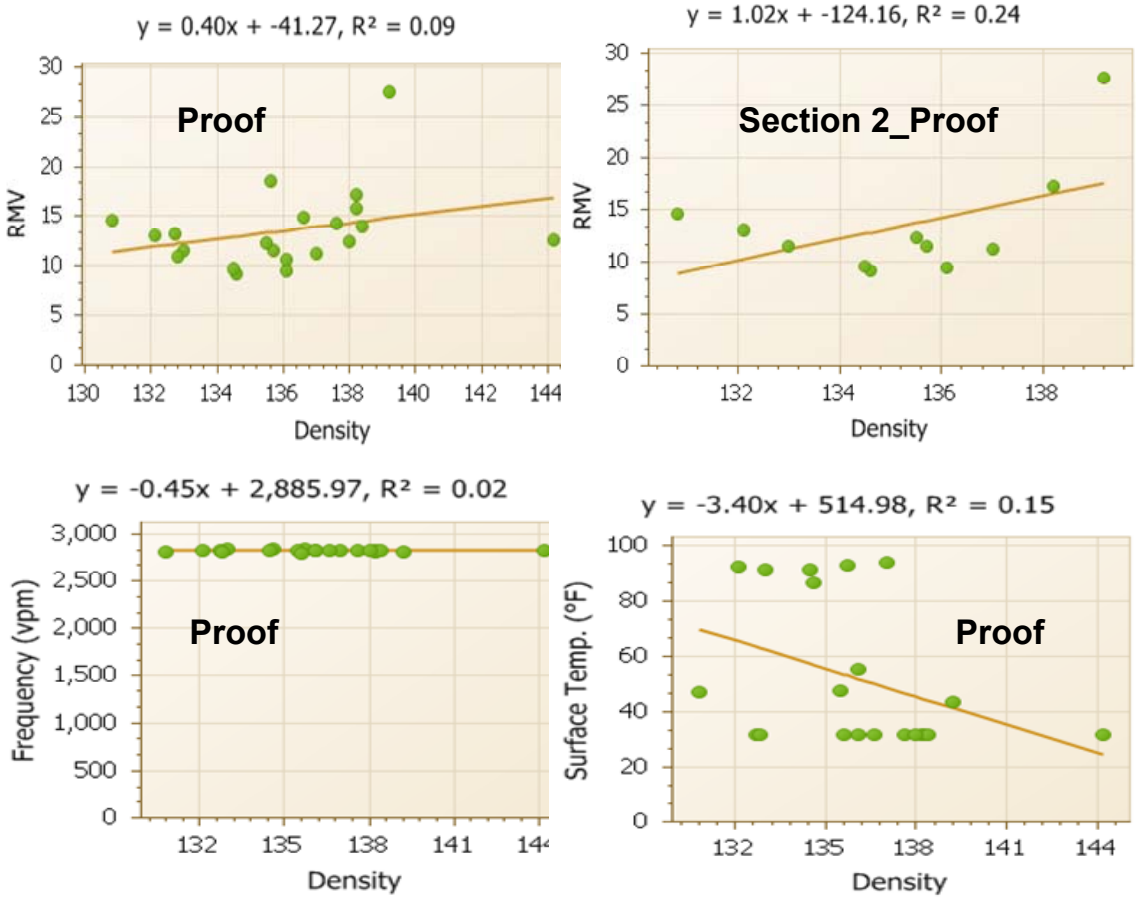

Figure 88. TB02B HMA base Sakai CCV, frequency, surface temperatures vs. NG density.

TB02C , NG

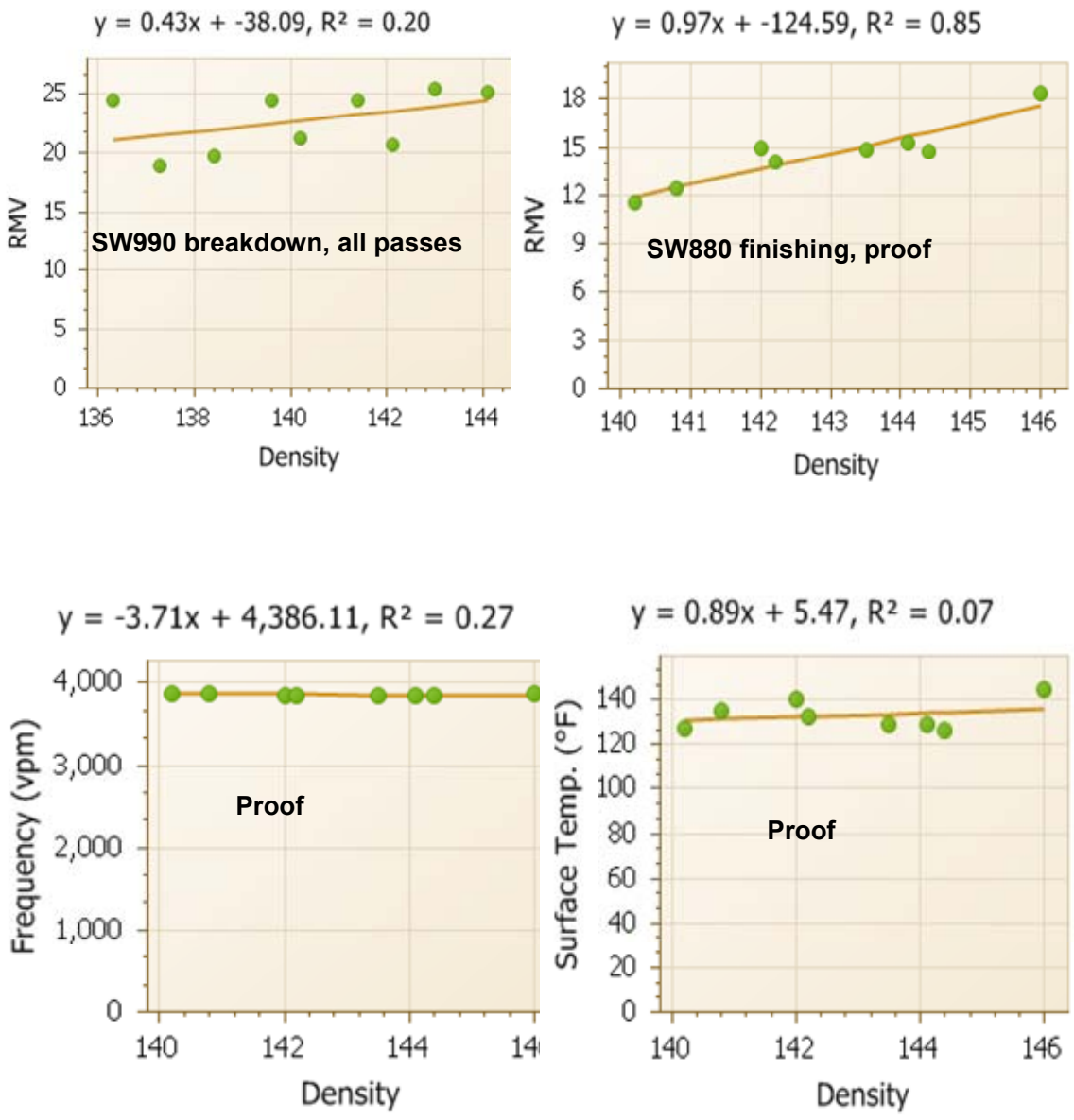

Figure 89. TB02C HMA 2nd lift Sakai CCV, frequency, surface temperatures vs. NG density.

Summary Tables

Roller Measurement Value

Table 4 summarizes the RMV (Sakai CCV) for each test bed. Results show that overall the Sakai CCV increases from the rubblized/crack-and-seat PCC base, to the HMA base, and then the 2nd lift HMA intermediate layer, indicating that the integral strength of pavement system increases with paving more HMA layer on the top. However, it would be noted that for the TB02 (driving lane) Section 1 under the Sakai SW880 finishing compaction, Sakai CCV of the 2nd lift HMA is lower than that of the HMA base. This could be due to the limited available IC data for the TB02C Section 1 2nd lift HMA course (see Figure 69) when the Sakai SW880 roller was not working stably at that time and some IC data was not collected.

Table 4: Roller measurement value, Sakai CCV

	Sakai SW990 breakdown		Sakai SW880 finishing	
Sections	Section 1	Section 2	Section 1	Section 2
TB01M PCC Base	N/A	N/A	10.49	12.06
TB01B HMA Base	17.49	18.03	13.88	12.63
TB01C 2nd HMA lift	19.15	21.07	13.92	15.96
TB02M PCC Base	N/A	N/A	15.1	15.49
TB02B HMA Base	13.58	15.28	14.28	12.11
TB02C 2nd HMA lift	23.13	24.35	12.55	16.84

Optimum Roller Passes from Compaction Curves

Table 5 summarizes the optimum roller passes for each test bed determined by the compaction curves. Results show that mostly 4 or 5 roller pass has resulted in the maximum Sakai CCV for this project. Therefore, this finding is specifically important for avoid under/over-compaction by using the IC technology.

Table 5: Optimum roller passes

	All sections	Section 1	Section 2
TB01B HMA Base	4	4	4
TB01C 2nd HMA lift	5	5	5
TB02B HMA Base	4	1	4
TB02C 2nd HMA lift	4	4	4

Compaction Uniformity

Table 6 summarizes the semi-variogram parameters for each test bed. Results show that generally increased uniformity (i.e. a longer range with a lower sill value) is achieved from the "ground up": i.e., from rubblized/crack-and-seat PCC base to the HMA base , and then the 2nd lift HMA intermediate layer. However, it should be noted for the section 2 under the SW990 breakdown compaction, this trend is not evident.

Table 6: Summary of Semi-variogram parameters for Sakai CCV

a) SW990 breakdown compaction

	Section 1			Section 2		
	Range	Sill	Nugget	Range	Sill	Nugget
TB01B HMA Base	11.78	0.29	0.00	13.06	0.28	0.00
TB01C 2nd HMA lift	14.41	0.17	0.00	15.68	0.15	0.00
TB02B HMA Base	18.36	0.10	0.00	19.58	0.07	0.00
TB02C 2nd HMA lift	19.66	0.08	0.00	15.67	0.10	0.00

b) SW880 finishing compaction

	Section 1			Section 2		
	Range	Sill	Nugget	Range	Sill	Nugget
TB01B HMA Base	13.10	0.27	0.00	9.14	0.40	0.00
TB01C 2nd HMA lift	13.11	0.27	0.00	9.14	0.40	0.00
TB02B HMA Base	15.74	0.10	0.00	7.83	0.34	0.00
TB02C 2nd HMA lift	21.00	0.17	0.00	15.67	0.12	0.00

Conclusions and Recommendation

Conclusions and Findings

This HMA IC demonstration project has successfully demonstrated the ability of the IC roller to map the rubblized and crack-and-seat PCC bases, and tracking the compaction levels for the HMA courses. Major findings of this project included:

- Double-drum IC rollers can be used to map the rubblized and crack-and-seat PCC bases prior to the paving of HMA layer;
- IC mapping of the rubblized and crack-and-seat PCC bases and soil shoulder was shown to be crucial in identifying the pavement conditions prior to the paving of the HMA base;
- Night paving has been successfully implemented with the assistance of IC technology;
- LWD measured deflection and moduli, and NG density have relatively good linear correlation with the roller measurement values for some test beds, and HMA temperature has significant effect on the correlation result;
- Mostly compaction uniformity increases from the rubblized/crack-and-seat PCC base to the HMA base and then the 2nd lift HMA course as indicated by the semi-variogram parameters;
- Mostly at the roller pass of 4 or 5 the optimum roller measurement value is achieved, which offers very important information to help achieve the best compaction quality, while avoid over compaction or under compaction with IC technology;
- The IC rollers can track well the roller pass numbers, roller speeds, HMA surface temperatures, and the RMVs, which provides important metrics for the compaction quality;
- With the real-time information of IC roller passes, HMA surface temperatures and RMVs displayed on the screen, the roller operator can adjust rolling patterns to improve the compaction quality.

Recommendations

- Validation of the IC Global Positioning System (GPS) setup prior to the compaction operation using a survey grade GPS hand-held unit is crucial to providing precise and correct measurements. The process should require IC rollers moving forward and backward to validation locations.
- To correlate in-situ tests with IC data properly, in-situ test locations must be established using a hand-held GPS “rover” unit that is tied into the project base station and offers survey grade accuracy.
- It is highly recommended to perform IC measurements (mapping) of the underlying layers prior to the paving of upper layers in order to identify possible weak spots and facilitate the interpretation of the measurements on the asphalt surface layers.
- Long term pavement performance monitoring is recommended in order to identify performance trends that may relate to RMV values.
- Temperature correction for the RMV of HMA material is recommended with developing models.

- Indicators of undesirable IC measurement conditions (such as bouncing, sudden start/stop, etc.) are strongly recommended to be stored in order to filter out invalid IC data.
- Standardization is strongly recommended to accelerate the implementation IC for State agencies. The recommended items include: a standard IC data storage format, an independent viewing/analysis software tool, and detailed data collection plan (include any in-situ/lab test results). The research team is currently developing guidelines for IC data collection, storage requirements, data processing, and a prototype of an independent software tool.
- Further investigation on a global scale (e.g., segment-by-segment analysis of entire paved sections) is recommended to provide guidance of usage of IC mapping data on existing pavement layer with subsequent IC measurements during HMA paving. This would include: setting a target RMV value from test trip data based on the onsite support condition and asphalt job mix formula.

Open House

An Open House was conducted on May 13, 2010 as part of this field investigation. There were about 60 people attended the Open House including WisDOT engineers/technicians, academics, paving contractors, roller manufacturers/dealer personnel, GPS manufacturers/technical supports, etc. The Open House included a two-hour indoor presentation and question-&-answer session, and followed by a one-hour equipment demonstration.

The in-door presentation included:

- FHWA/TPF Intelligent Compaction Project - by Dr. George Chang (Transtec Group)
- Asphalt Intelligent Compaction - by Bob Horan (Asphalt Institute)
- Sakai Intelligent Compaction System - by Todd Mansell (Sakai America)
- WisDOT HMA IC Demo and Prelim Results - by Dr. George Chang (Transtec Group)
- Trimble GPS System - by Adam Patrow (Fabco/Trimble)
- TopCon GPS System - by Brian Lingobardo (TopCon) and Tom Walrath (Position Solutions)

Issues discussed during the question-&-answer (Q&A) session included:

Q: What fundamental properties of the pavement materials that the IC rollers measure? A: Both CCV and Evib generally related to the levels of compaction – though based on slightly different technologies - and both can be related to other conventional in-situ measurements.

Q: Can RMV tell how deep the weak spots are? A: No. A coring or trench digging will be needed to verify these weak spots.

Q: How can we as an agency to implement IC in our specifications? A: You may simply perform correlation tests using the conventional test devices specified in your specifications and establish a target RMV for acceptance.

Q: What factors affect RMVs? A: There are many factors including machine sizes, operational amplitudes, material stiffness, etc.

The equipment demonstration included a Sakai IC onboard display unit, Sakai double-drum IC rollers, TopCon and Trimble rovers.

Figure 90. Open House –introduction by WisDOT.

Figure 91. Open House – participants.

Figure 92. Open House – participants (II).

Figure 93. Open House –Research team's presentation (Bob Horan).

Figure 94. Open House –TopCon's presentation.

Figure 95. Open House – Trimble's presentation.

Figure 96. Open House – Sakai equipement demonstration.

Figure 97. Open House – TopCon equipment demonstration.

Figure 98. Open House – Trimble equipment demonstration.

References

Aouad, M. F., Stokoe II, K. H., and Briggs, R.C (1993). Stiffness of Asphalt Concrete Surface Layers from Stress Wave Measurements. Transportation Research Record 1384, Washington, DC, pp. 29-35.

Li, Y., and Nazarian, S. (1994), "Evaluation of Aging of Hot-Mix Asphalt Using Wave Propagation Techniques," Engineering Properties of Asphalt Mixtures And the Relationship to Their Performance, ASTM STP 1265, Philadelphia, Pa., pp.166-179.

Nazarian, S., and Desai, M., (1993). "Automated Surface Wave Testing: Field Testing," Journal of Geotechnical Engineering (American Society of Civil Engineers, New York) 119, no. GT7:1094-112.

Nazarian, S., Yuan, D., Tandon, V., and Arellano, M., (2004) "Quality Management of Flexible Pavement Layers with Seismic Methods," Research Report 1735-3, Center for Transportation Infrastructure Systems, UTEP, El Paso, TX, 120 p.

Nohse, Y., and Kitano, M. (2002). "Development of a new type of single drum vibratory roller," Proc. 14th Intl. Conf. of the Intl. Soc. For Terrain-Vehicle Systems, Vicksburg, MS, October 20-24.

Powell, W.D., Potter, J.F., Mayhew, H.C., and Nunn, M.E., (1984) "The Structural Design of Bituminous Roads," TRRL Report LR 1132, 62 pp.

Sakai Heavy Industries, Ltd. Vibrating Roller Type Soil Compaction Quality Controller RMV (Compaction Control Value), Operating & Maintenance Instructions.

Scherocman, J., Rakowski, S., and Uchiyama, K. (2007). “Intelligent compaction, does it exist?” 2007 Canadian Technical Asphalt Association (CTAA) Conference, Victoria, BC, July.

Tandon, V., Nazarian, S., and Bai, X., (2009), "Assessment of Relationship between Seismic and Dynamic Modulus of Hot Mix Asphalt Concrete," International Journal of Road Materials and Pavement Design (accepted for publication).

Von Quintus, H.L.; Rao, C.; Minchin, R.E.; Nazarian, S.; Maser, K.R; Prowell, B.D. (2009), “NDT Technology for Quality Assurance of HMA Pavement Construction,” NCHRP Report No. 626, Washington, DC, 133 p.

W. J. vdM. Steyn and E. Sadzik, Application of the portable pavement seismic analyzer (PSPA) for pavement analysis, Proceedings of the 26th Southern African Transport Conference (SATC), 2007.

Webster, S.L., Brown, R.W., and Porter, J.R., (1994) “Force Projection Site Evaluation Using the Electric Cone Penetrometerb and the Dynamic Cone Penetrometer,” Technical Report GL-94-17, U.S. Waterways Experimental Station, 172 pp.

Webster, S.L., Grau, R.H., and Williams, T.P., (1992) “Description and Application of Dual Mass Dynamic Cone Penetrometer,” Instruction Report GL-92-3, U.S. Waterways Experimental Station, 50 pp.

http://training.ce.washington.edu/WSDOT/Modules/07_construction/nuclear_gauge.htm.

Appendix A: On-Site Participant List

Last name	First name	Affiliation	Telephone	Email
		ICPF Project Team		
Chang	George	Transtec Group	C 512-659-1231	gkchang@thetranstecgroup.com
Horan	Bob	Asphalt Institute	C 804-539-3036	bhoran@AsphaltInstitute.org
Xu	Qinwu	Transtec Group, Inc.	C 512-709-4155	qinwu@thetranstecgroup.com
Michael	Larry	LLM-Asphalt Technology Consultant	C 301-331-6150	larry@larrylmichael.com
Gallivan	Lee	FHWA	317-226-7493	Victor.Gallivan@fhwa.dot.gov
		State DOT and etc.		
Arndorfer	Robert	WisDOT	608-246-7940	Robert.Arndorfer@dot.wi.gov
Paye	Barry	WisDOT	608-246-3855 C 920-321-8772	Barry.Paye@dot.wi.gov
Malaney	Mike	WisDOT (FWD coord.) Operator: Craig Vils	608-246-7956 C 414-750-0944	Michael.Malaney@dot.wi.gov
Schiro	Bob	WisDOT (Nuke)	C 608-516-6359	Robert.Schiro@dot.wi.gov
Steidl	Mark	WisDOT		Mark.Steidl@dot.wi.gov
Kircher	David	WisDOT		n/a
Stafford	Robin	WisDOT		robin.stafford@dot.wi.gov
Hess	Jeff	WisDOT		n/a
Alfaro	Frank	WisDOT		frank.alfaro@dot.wi.gov
Michalski	Jeff	WisDOT		Jeffrey.Michalski@dot.wi.gov
Hansley	Tim	WisDOT		Timothy.Hanley@dot.wi.gov
Garcia	Pete	FHWA – WI (NC/NW)	608-829-7513	Pete.Garcia@dot.gov
Spilak	Jason	FHWA – WI (ARRA)	608-829-7529	jason.spilak@dot.gov
Shemwell	Wesley	FHWA – WI	608-829-7521	wesley.shemwell@dot.gov
Graf	Greg	AECOM	C 715-498-7195	Greg.GRAF@aecom.com
		Roller/Components Vendors		
Mansell	Todd	Sakai America	C 770-324-6455	t-mansell@sakaiamerica.com
Hanes	Bruce	Trimble		bruce_hanes@trimble.com
Patrow	Adam	Fabco - tech support (Trimble)	C 608-235-1463	aap@fabco.com
Lingobardo	Brian	TopCon		blingobardo@topcon.com
Walrath	Tom	Positioning Solutions (TopCon)	C 414-379-2441	tomw@1psc.com
Behlendorf	Shane	Positioning Solutions	C 414-573-2374	behls23@yahoo.com
Kmiecik	Mike	Positioning Solutions	262-798-5252	mikek@1psc.com
		Paving Contractors		
Eslinger	Matt	Mathy	715-299-0245	meslinger@mathy.com
Dukatz	Ervin	Mathy		edukatz@mathy.com

www.IntelligentCompaction.com

Contact Information

Victor (Lee) Gallivan, P.E.
FHWA Indiana Division
575 N. Pennsylvania St.,
Indianapolis, IN 46204
(317) 226-7493,
victor.gallivan@fhwa.dot.gov

George Chang, P.E., PhD
The Transtec Group, Inc
6111 Balcones Dr. Austin, TX 78731
(512) 451-6233 Fax (512) 451-6234
gkchang@thetranstecgroup.com

Report Prepared by

George Chang, P.E., PhD
Qinwu Xu
The Transtec Group, Inc.

Bob Horan, P.E.
Asphalt Institute

Larry Michael
LLM Asphalt Consultant